

Øyvind Senneset

# A discussion of continental lithospheric stretching models and comparison with interpreted 2D seismic data of the Viking Graben of the northern North Sea

Master's thesis in Petroleum Geophysics

Supervisor: Ståle Emile Johansen

June 2019



Øyvind Senneset

# **A discussion of continental lithospheric stretching models and comparison with interpreted 2D seismic data of the Viking Graben of the northern North Sea**

Master's thesis in Petroleum Geophysics  
Supervisor: Ståle Emile Johansen  
June 2019

Norwegian University of Science and Technology  
Faculty of Engineering  
Department of Geoscience and Petroleum

 **NTNU**  
Norwegian University of  
Science and Technology



## I Abstract

Rifted margins mark the transition from a continent to an ocean and contain in their architecture a record of their rift history. However, not all rifts develop to the stage of crustal separation, but stop before this final stage, and become failed rifts. Scientists and professionals have tried to explain rifting processes, and commonalities and discrepancies between rifts with extensional models for over 40 years. In this thesis, I compare and discuss important and influential extensional models, to try and explain rifting processes on a general basis. This will then be put in the context of the development of the the failed rift the Viking Graben in the northern North Sea. The Viking Graben developed through multiple phases of rifting on a heterogeneous crust composed of structures inherited from the Caledonian orogeny and Devonian postorogenic extension. The inheritance and reactivation of basement structures are vital for the rift architecture of the rift that were to come.

A study regarding interpretation of regional seismic 2D lines from the northern North Sea has been carried out with the aim of constructing an understanding of the evolution of the Viking Graben. Features inferred from modelling has been observed and discussed with the goal of comparing the Viking Graben to theoretical extensional models. It has also been attempted to describe rift related unconformities, the role of basement structures during rifting and reactivation of pre-existing weaknesses.

It is clear that the entire rift can not be described by a single extensional model. The rifting process is influenced by the orientation of the basement grain and pre-existing structures of the highly heterogeneous crust. Although one model can not explain the entire development of the Viking Graben, individual components of the rift process can be explained through models. This include the post-rift thermal subsidence that can be described through a pure-shear McKenzie model, and that occasional observed asymmetry follow the theory of a simple shear model, but this can also be due to crustal inhomogeneities. It is concluded that a depth-dependent pure shear model is the best fitting model for the Viking Graben.

To expand on the discussion of application of rift models, more data is needed. Sub-crustal processes are active in the rift process, and not visible in the interpreted data in this thesis. For better and more detailed results deep seismic and gravimetric/magnetic data is required.

## II Sammendrag

Riftmarginer markerer overgangen fra et kontinent til hav, og inneholder en oversikt over dets rifthistorie i arkitekturen. Ikke alle rifter vil imidlertid utvikles til stadiet for skorpeseparering, men stanse før de når dette stadiet og bli en såkalt mislykket rift. I mer enn 40 år har forskere og fagmenn forsøkt å forklare riftprosesser, og fellestrekk og uoverensstemmelser mellom rifter med ekstensjonsmodeller. I denne masteroppgaven sammenligner og diskuterer jeg viktige og innflytelsesrike utvidelsesmodeller, for å forsøke å forklare riftprosesser på et generelt grunnlag. Dette vil så bli satt i en sammenheng med utviklingen av den mislykkede riften Vikinggraben i den nordlige Nordsjøen. Vikinggraben utviklet seg gjennom flere faser med rifting på en heterogen skorpe bestående av strukturer som stammer fra den kaledonske fjellkjeden og Devonsk post-orogensk ekstensjon. Arv og reaktivering av strukturer fra grunnfjellet er avgjørende for den kommende riften.

En studie angående tolkning av regionale seismiske 2D linjer fra den nordlige Nordsjøen, har blitt utført for å bygge en forståelse av utviklingen av Vikinggraben. Trekk beskrevet av modeller har blitt observert og diskutert med det formål å sammenligne Vikinggraben med teoretiske ekstensjonsmodeller. Det har også blitt forsøkt å beskrive ukonformiteter relatert til rifting, grunnfjellsstrukturers rolle under rifting, og reaktivering av allerede eksisterende svakheter.

Det er tydelig at hele riften ikke kan bli beskrevet av en enkelt ekstensjonsmodell. Riftprosessen er påvirket av orienteringen og reaktiveringen av strukturer i grunnfjellet og den svært heterogene skorpen. Selv om en modell ikke kan forklare hele utviklingen av Vikinggraben, kan enkelte komponenter i riftprosessen forklares ved hjelp av modeller. Dette inkluderer post-rift termal subduksjon som kan beskrives med en rent skjær McKenzie-modell, og tidvis observert asymmetri som følger teorien for en "simple" skjærmodell, men dette kan også være grunnet den inhomogene skorpen. Det konkluderes at en dybde-avhengig ren skjær modell er den mest passende modellen for å beskrive den generelle utviklingen av Vikinggraben

For å utvide diskusjonen om anvendelse av riftmodeller, er det behov for mer data. Prosesser som foregår under skorpen er aktive i riftprosessen, og ikke synlig i de tolkede dataene i denne oppgaven. For bedre og mer detaljerte resultater, er dyp seismikk og gravimetrisk/magnetisk data nødvendig.

### III Acknowledgement

This master thesis, delivered June 2019, is my final assignment for the Master of Petroleum Geophysics degree at the Norwegian University of Science and Technology (NTNU).

First, I would like to thank my main supervisor Ståle Emil Johansen of the Department of Geoscience and Petroleum at NTNU for guidance, advice and useful feedback throughout this and the previous semester. His presence and input has been greatly appreciated.

Secondly, I have to thank my co-supervisor Dicky Harishidayat for all the help regarding the data and software used in this thesis. As well as the other master students in the group meetings for interesting discussions and inspiration.

I want to acknowledge the NTNU- NPD-SCHLUMBERGER PETREL READY Database for the seismic and well data used in this thesis.

I also want to thank my friends and family for all the support throughout all my years of studying here at NTNU.

Finally, I want to thank my girlfriend for her patience and for always being supportive and giving me the motivation i needed.

# Contents

<b>Abstract</b>	<b>i</b>
<b>Sammendrag</b>	<b>ii</b>
<b>Acknowledgement</b>	<b>iii</b>
<b>List of Figures</b>	<b>vii</b>
<b>List of Tables</b>	<b>xi</b>
<b>Introduction</b>	<b>1</b>
1.1 Main goals of this thesis . . . . .	1
1.2 Lithospheric Stretching Models . . . . .	1
1.3 The Viking Graben . . . . .	1
1.4 Seismic Interpretation . . . . .	2
<b>The Earth's outer structure</b>	<b>3</b>
2.1 Continental versus oceanic lithosphere . . . . .	3
<b>Rifting Processes</b>	<b>3</b>
3.1 Intra-cratonic rifts . . . . .	4
3.1.1 Passive and active rifts . . . . .	4
3.1.2 Transition from passive to active rifting . . . . .	5
3.2 Lithospheric stretching models . . . . .	6
3.3 Pure shear . . . . .	6
3.3.1 Uniform stretching model . . . . .	6
3.3.2 Depth dependent models . . . . .	7
3.4 Lithospheric stretching models - Simple shear . . . . .	10
3.5 Combined simple and pure shear models . . . . .	11
3.6 Concept of lithospheric necking . . . . .	13
3.7 Applicability of rift models . . . . .	14
<b>The driving forces of rifting</b>	<b>15</b>
4.1 Weakening of the lithosphere . . . . .	16
4.2 The early stages of rifting . . . . .	16
4.3 Fault development, interaction and growth - the geometry of a rift . . . . .	17
4.3.1 Fault death . . . . .	18



4.3.2	Fault reactivation . . . . .	19
4.4	Rifting duration - Why does rifting cease? . . . . .	19
4.5	The width of the rift zone . . . . .	21
4.6	Controls on rift geometry . . . . .	22
4.7	Rift-related subduction . . . . .	22
<b>Extension along suture zones</b>		<b>23</b>
5.1	The Iapetus suture - a North Atlantic zone of weakness . . . . .	23
<b>Structural framework</b>		<b>24</b>
6.1	Caledonian collision . . . . .	25
6.2	Devonian crustal extension . . . . .	25
6.3	Permo-Triassic rifting . . . . .	25
6.4	Early to Middle Jurassic events . . . . .	27
6.5	Late Jurassic rifting . . . . .	28
6.6	Post-rift events . . . . .	29
6.7	Pre-Mesozoic influence on the basement of the Viking Graben . . . . .	30
<b>Stratigraphic framework</b>		<b>32</b>
7.1	Triassic deposits . . . . .	32
7.2	Jurassic deposits . . . . .	33
7.2.1	Statfjord Group . . . . .	33
7.2.2	Dunlin Group . . . . .	33
7.2.3	Brent Group . . . . .	33
7.2.4	Viking Group . . . . .	34
7.3	Cretaceous deposits . . . . .	34
7.3.1	Cromer Knoll Group . . . . .	34
7.3.2	Shetland Group . . . . .	34
7.4	Cenozoic deposits . . . . .	35
7.4.1	Rogaland Group . . . . .	35
7.4.2	Hordaland Group . . . . .	35
7.4.3	Nordland Group . . . . .	35
<b>The Petroleum System of the Northern North Sea</b>		<b>36</b>
8.1	Source rocks . . . . .	36
8.1.1	The Heather Fm. . . . .	36
8.1.2	The Draupne Fm. . . . .	36

---

8.2	Reservoir rocks . . . . .	37
8.3	Traps and seals . . . . .	37
<b>Methods</b>		<b>38</b>
9.1	Seismic data . . . . .	38
9.2	Seismic resolution and quality of data . . . . .	38
9.3	Polarity . . . . .	39
9.4	Well data and seismic-well tie . . . . .	40
9.5	Seismic analysis . . . . .	42
<b>Results</b>		<b>44</b>
<b>Interpretation</b>		<b>56</b>
11.1	Evolutionary interpretation . . . . .	61
11.2	Unconformities related to rifting . . . . .	65
11.2.1	The Base Cretaceous Unconformity . . . . .	65
11.3	Inherited basement structures of the northern North Sea . . . . .	71
11.4	Faults . . . . .	73
11.4.1	Øygarden Fault Zone . . . . .	75
<b>Discussion</b>		<b>76</b>
12.1	Application of models to the north Viking Graben . . . . .	76
12.1.1	Pure shear models . . . . .	76
12.1.2	Simple shear models . . . . .	78
12.1.3	Other models . . . . .	80
<b>Conclusions</b>		<b>81</b>
<b>References</b>		<b>82</b>

## List of Figures

1	A sketch of the lithosphere being extended . . . . .	2
2	Sketch showing the outer layering of the Earth . . . . .	3
3	Transition from active to passive rifting in the late synrift/post-rift. Doming and shallow asthenosphere volcanism are expected to occur in the late synrift/ early post-rift eventually associated with a second rift phase. From Huismans et al. (2001).	5
4	A simple comparison of the uniform and the non-uniform extension model: (a) Initial conditions show the lithosphere in thermal equilibrium before stretching. Decoupling is at a depth $y$ . (b) Showing the behaviour with the uniform extension model, where the entire lithosphere extends by $\beta$ and thins by $1/\beta$ . This results in an elevated, linear thermal gradient. (c) Showing the behaviour using the non-uniform depth-dependent model. The upper lithosphere is above the level $y$ , and extends by $\delta$ and thins by $1/\delta$ , and the lower lithosphere extends by $\beta$ and thins by $1/\beta$ . This results in a "two-legged" thermal gradient. From Royden and Keen (1980). . . . .	7
5	A sketch showing how a model regarding uniform extension and melt segregation produce oceanic crust and a smooth transition from unextended continental crust, to oceanic crust. The amount of melt that segregates is proportional to the amount of incoming undepleted asthenosphere. Modified from Beaumont et al. (1981) . . . . .	8
6	A sketch of a newly formed graben with uplifted flanks. The upward curving, dashed lines, represents the eventual total uplift of the original crustal boundaries that results from the surface erosion. The continuous line on the flanks represents the initial uplift. From Hellinger and Sclater (1983) . . . . .	9
7	Lithospheric stretching models. (a) is a simple sketch of the discontinuous, depth-dependent stretching model as described by Beaumont et al. (1981). (b) Sketch showing the initial geometry of continuous nonuniform stretching, including a polygonal region of the lithosphere. Modified from Ziegler (1990) . . . . .	10
8	A simple sketch displaying asymmetric lithospheric extension by simple shear. From Reston and Pérez-Gussinyé (2007) . . . . .	11
9	A simple sketch showing the combined shear model. The upper crust is deformed by simple shear forces, with an intra-crustal shear zone that soles out in the crust. The lower crust and mantle is deformed by pure shear forces. The uplift of the asthenosphere occurs under the zone of rifting, unlike the simple shear model. From (Ziegler, 1990). . . . .	12

10	A figure showing how extension takes place on planar faults in the upper crust, while deformation in the lower crust and mantle is achieved by pure shear. The lithospheric extension produces thinning and a flexural response of the lithosphere. From (Kusznir and Ziegler, 1992) . . . . .	13
11	The left side display kinematic rift models at different necking depths with different strength envelopes, while the right sides show the lithospheric response to the chosen depth of necking, (Ziegler and Cloething, 2003) . . . . .	14
12	A sketch from numerical modelling, showing the development and linkage a fault-segment, with abandoned faults outside the linked faults. From Gupta et al. (1998)	17
13	Sketch showing the progressive development of a blind fault. From Gawthorpe and Leedert (2000) . . . . .	18
14	Graph showing the duration of abortive and successful rifts. R = rift duration, D = periods of doming, stars = periods of main volcanic activity, S = duration of sea-floor spreading stage. All years are in My. Modified from Ziegler and Cloething (2003). . . . .	20
15	The main Late Paleozoic - Mosozoic rift axis are highlighted in red. The Iapetus suture is marked with green. Note how its exact location is unknown in the basins of the northern North Sea. Modified from Fazlikhani et al. (2017) . . . . .	23
16	Map showing the Viking Graben and the surrounding structures. From Færseth (1996). . . . .	24
17	The northern North Sea rift zone after Permo-Triassic and Jurassic extension. The rift margins are marked in yellow, while major intra-basinal highs are marked with blue. Most of the faults are of Permo-Triassic origin. Modified from Færseth (1996)	27
18	Interpreted deep seismic line and crustal transect depicting broad stratigraphy and structure across the northern Viking Graben. From (Faleide et al., 2010) . . . . .	29
19	Map showing the main fault trends and the location of shear zones (HFZ = Hardangerfjord Shear Zone; BASZ = Bergen Arcs Shear Zone; NSD = Nordfjord-Sogn Detachment; KSZ = Karmøy Shear Zone; RSZ = Røldal Shear Zone). From Fossen and Hurich (2005) . . . . .	31
20	Lithostratigraphic chart, showing many of the formations and groups of the northern Viking Graben. From Lundin . . . . .	32
21	Sea-bottom reflection from SG8043-101A. Left - wiggle trace; right - color display (bitmap). The positive amplitudes in the wiggle trace is displayed with red intensity in the color display, while the negative amplitudes are displayed with blue. . . . .	40
22	Sonic calibration window of well 30/11-2 . . . . .	41

23	Synthetic generation window of well 30/11-2 . . . . .	42
24	Seismic reflection configurations . . . . .	43
25	Different types of geological boundaries defining seismic sequences. From Catuneanu (2002) . . . . .	43
26	Map showing the interpreted lines used in this thesis. Most of the lines were interpreted to construct an overview of the architecture involving the Viking Graben, while some were interpreted with the purpose of describing specific structures or increase the confidence in the picked horizons . . . . .	44
27	Structural elements in the North Sea with major oil- and gas fields. (Halland et al., 2011) . . . . .	45
28	Stratigraphic column for a section of the Viking Graben, showing most the interpreted groups and formations, including the age and tectonic setting of the deposits. E = Era, P = Period. See Fig. 31 for location . . . . .	46
29	Line 1, NVGTI92-109 . . . . .	47
30	Line 2, NVGTI92-106 . . . . .	48
31	Line 3, NVGTI92-105 . . . . .	48
32	Line 4, NVGTI92-104 . . . . .	49
33	Line 5, NVGTI92-102 . . . . .	49
34	Line 6, NVGTI92-103 . . . . .	50
35	Line 7, NVGTI92-101 . . . . .	50
36	Line 8, NVGTI3-92-208 . . . . .	51
37	Line 9, NVGTI3-92-207 . . . . .	51
38	Line 10, NVGTI3-92-205 . . . . .	52
39	Line 11, NVGTI3-92-201 . . . . .	52
40	Line 12, SG8043-REP91-205D . . . . .	53
41	Line 13, SG8043-REP91-207A . . . . .	54
42	Line 14, SG8043-REP91-403A . . . . .	54
43	Line 15, NVGTI2-92-209 . . . . .	55
44	Line 16, NVGTI2-92-210 . . . . .	55
45	Line 17, NVGTI2-92-211 . . . . .	56
46	Model 1, based on interpretations of Line 2 (NVGTI92-106) in Fig. 30 . . . . .	57
47	Model 2, based on interpretations of Line 7 (NVGTI92-101) in Fig. 35. . . . .	58
48	Model 3, based on interpretations of Line 14 (SG8043-REP91-403A) in Fig. 42. . .	59
49	Uninterpreted line of Model 1 . . . . .	60
50	Uninterpreted line of Model 2 . . . . .	60

51	Uninterpreted line of Model 3 . . . . .	60
52	Some features described in this chapter . . . . .	64
53	Sketch showing different configurations of the BCU, (Kyrkjebø et al., 2003) . . . .	66
54	From Line 5 in the northern Viking Graben. Configuration of the BCU is relatively simple and geometric, represented by a continuous and clear reflection. Note the arrows representing onlap of post-rift strata at the basin margins. The green line represents the top Cretaceous. . . . .	66
55	From Line 2 in the Viking Graben north of the Snorre Field. The BCU is faulted over the rotated fault block showing local angular unconformities, while being continuous on the side marked by onlaps on each side. . . . .	67
56	From Line 1 in the northernmost North Sea between the Magnus and Møre Basins. Configuration of the BCU being offset by faults with large vertical displacement. . .	68
57	From Line 6 between the Viking Graben and the northwest of the Horda Platform, showing faults with minor throw. The blue line represents the Top Rogaland Group	68
58	From Line 3, crossing the Vega Field in the northern North Sea. Highly faulted blocks underlay the uneven BCU at this location . . . . .	69
59	From Line 3, in the western margins of the northern Viking Graben, crossing the Statfjord Field. Showing a large part of the rotated fault block eroded and sediments deposited in the hangingwall low . . . . .	69
60	From line 6, on the Horda Platform east of the Troll Field. The BCU is in this location developed rather as a disconformity, with large offsets from faults . . . . .	70
61	From line 7, close to the Norwegian coastline. Affected by a non-rotated horst-graben complex with significant relief, where several unconformities merge into one that lack Cretaceous and Tertiary sediments . . . . .	71
62	From Line 1. Showing well 32/4-1 penetrating the strata down to the basement on the Horda Platform . . . . .	72
63	A fault model in a multiphase rift showing how faults (red) from rift phase 1 (RP1) is being reactivated, and crosscut and interacting with new faults (blue) from rift phase 2 (RP2). Some new faults are being retarded and isolated by the pre-existing faults. From Duffy et al. (2015) . . . . .	74
64	The domino-style normal faults seen in rectangle 1, has a striking resemblance to the faults on the western side of the graben axis in Model 2 (from the Gullfaks South and westwards). Whereas the type of faults in ellipse 2 under the simple shear model is not observed. (Modified from Unternehr et al. (2010) . . . . .	79

**List of Tables**

1 Table showing color legend of horizons interpreted . . . . . 47

# 1 Introduction

## 1.1 Main goals of this thesis

The objectives of this thesis are:

- (i) To create an overview of important lithospheric stretching models and how our understanding of the development and behaviour of rifts have changed. As well as understanding how rift-related faulting occur.
- (ii) To use regional 2D seismic data and well data from the northern North Sea to map the Viking Graben.
- (iii) To discuss features observed on the seismic data in a discussion to determine if the development of the Viking Graben can be explained partially or fully, by any of the lithospheric extensional models

## 1.2 Lithospheric Stretching Models

Lithospheric stretching models are theoretical models that aim to explain how rifts and passive margins developed. There are largely two main models to consider, the McKenzie model (1978), and the Wernicke model (1985). The McKenzie model incorporates pure shear, while the Wernicke model is based upon a simple shear regime. They both suggest a quite different development and architecture. Throughout the years, they have been modified and further developed to provide explanations for properties observed in rifts and passive margins, such as uplift of the flanks, melt segregation and multiphase rifting. For a rift model to be applicable and survive outside of the laboratory, it needs to be tested against real-life examples. This will involve being applied to largely different crustal settings that will influence the behaviour of the rift-forming processes.

## 1.3 The Viking Graben

The Viking Graben is one of the dominating structures of the northern North Sea. An approximately 300 km long north-south graben structure, created by episodes of rifting and the corresponding thermal subsidence. The Viking Graben is located roughly between 59°00' and 62°00'N in axial direction, and 2°00' and 4°00'E orthogonal to the axis. The Viking Graben connects to the Central Graben in the south and the Sogn Graben in the north, and the graben proper is flanked by the East Shetland Basin and East Shetland Platform to the west and the Utsira Basin and Horda Platform to the east. The present day structure and appearance of the northern North Sea are a



result of periods of rifting in the late Permian to early Triassic, as well as in the late Jurassic, and following thermal subsidence.

## 1.4 Seismic Interpretation

Interpretation of seismic data is crucial to the discovery and production of hydrocarbons. After processing the raw seismic data, information of the subsurface can be acquired through interpretation techniques. This involves picking continuous lateral reflectors and faults to generate an image of the geological subsurface conditions. To correctly do this it is required to have a good understanding of how subsurface formations may affect wave reception.

To confidently choose the correct horizons when interpreting, well data is very useful. Wells contain important geological information, that is used to identify the horizons. The seismic data is received with the y-axis being in the time-domain. The well data is in metrical depth. To correlate them, one can either depth-migrate the seismic data, by knowing the velocity of the seismic waves through the layers it propagates through, or perform a seismic-to-well tie through seismic check-shot data. The latter has been done in this thesis.

[https://en.wikipedia.org/wiki/Sedimentary\\_basin](https://en.wikipedia.org/wiki/Sedimentary_basin)

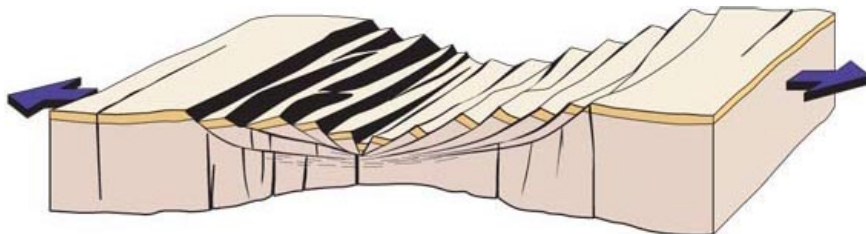


Figure 1: A sketch of the lithosphere being extended

## 2 The Earth's outer structure

The lithosphere and asthenosphere make up the outer structure of the earth. Whereas the lithosphere consists of the upper, elastic portion of the mantle and the brittle crust, the asthenosphere is composed of the highly viscous, mechanically weak and ductilely deforming region of the mantle below the lithosphere. The thickness of the crust is depended on it being oceanic or continental, and will influence the underlying elastic and ductile layers (Fig. 2). Within the lithosphere is the Moho, a boundary between the crust and the lithosphere. All parts of the Earth's outer structure are active in processes involving extension and rifting.

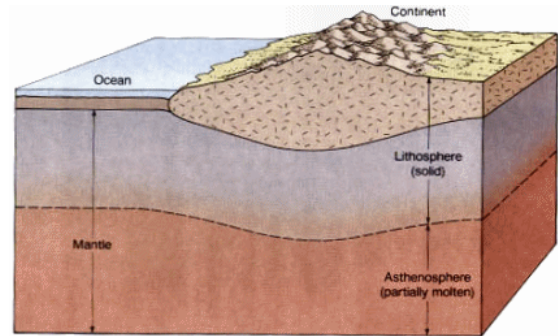


Figure 2: Sketch showing the outer layering of the Earth

### 2.1 Continental versus oceanic lithosphere

The strength of continental and oceanic lithosphere is differently dependent. The strength of continental lithosphere is controlled by its depth-dependent rheological structure, while the strength of the oceanic lithosphere depends on its thermal regime, which controls its essentially age-dependent thickness. Comparing the continental and oceanic lithosphere, the oceanic has a more homogeneous composition and simpler rheological structure.

Generally, the oceanic lithosphere is considerably stronger than the continental. This suggests that extensional stresses in oceanic lithosphere can be large enough to cause deformation of the proximal continental lithosphere without causing deformation of the oceanic lithosphere at the same time (e.g. the Permian separation of Cimmerian terranes from Africa-Arabia (Ziegler et al., 1998)). In this thesis, rifting of the continental lithosphere will be considered.

## 3 Rifting Processes

Rifts and rift-related passive-margin basins play an important role among the sedimentary basins that developed through time in the domains of the North Atlantic. During the Late Palaeozoic to Cenozoic age, several cycles of rifting are recognized in which the subsidence of graben-shaped basins took place under different large scale tectonic settings.

A distinction is made between rifting that led to the break-up of cratonic areas and the opening of major oceans, and back-arc rifting that is related to either decreased convergence rates of a continental and an oceanic plate or to the decay of a subduction system.

The development of pull-apart features that are associated with major wrench faulting represents a special category of rapidly subsiding grabens. The development of this type of basin can be associated with both types of rifting.

Another type of small-scale graben formation can be associated with subsidence of foredeep basins in response to tectonic loading of the foreland crust by advancing thrustsheets and nappes (Ziegler, 1990).

### **3.1 Intra-cratonic rifts**

Continental or intra-cratonic rifts are long and narrow features bounded on one or both sides by normal faults, where several kilometers of displacement have occurred, resulting in deep rift valleys that form sedimentary basins (Allen and Allen, 1990). Passive margins are rifts that have proceeded to the final stage of a successful rift, where extrusion of magma initiates oceanic crustal accretion of a stretched lithosphere. To understand the driving forces of intra-cratonic rifts and passive margins, numerous models have been proposed. They can essentially be subdivided into two groups, whereas the first consider the mechanical behaviour and deformation patterns at upper and lower crustal levels and sub-crustal lithospheric levels, with the emphasis on mechanical stretching of the lithosphere (passive rifts). The other group deals with the thermally induced upward displacement of the asthenosphere/lithosphere boundary in response to upwelling, advecting asthenosphere currents (active rifts).

#### **3.1.1 Passive and active rifts**

The first rifting idealization is the concept of passive rifting, which essentially are rifts generated in response to far-field tectonic forces. Here, tensional stresses in the continental lithosphere cause it to fail, allowing hot mantle rocks to penetrate the lithosphere. Crustal doming and volcanic activity are simply secondary processes.

Active rifting is associated with thermal upwelling of sub-lithospheric mantle. Conductive heating from the mantle plume, heat transfer from magma generation, or convective heating may cause the lithosphere to thin. If heat fluxes out of the asthenosphere are large enough, relatively rapid thinning of the continental lithosphere causes isostatic uplift. Tensional stresses generated by the uplift may then promote rifting.

### 3.1.2 Transition from passive to active rifting

The idealized modes of rifting are now believed to be end-member concepts of a continuous spectrum resulting from the evolution of several main rift forces, and that there may be a temporal transition from passive to active rifting within a single rift system.

A two-dimensional numerical model by Huisman et al. (2001) was created to examine the interplay of passive extension and active convective thinning of the mantle lithosphere, investigating the relative importance of thermal buoyancy forces associated with asthenospheric doming and far-field intraplate stresses on the style of rifting. The authors propose that passive intraplate driven extension provides an efficient mechanism for destabilizing the lower lithosphere, making it susceptible for rifting. This is in disagreement with other authors, that have suggested that thickening of the mantle could lead to an unstable lithosphere (Houseman et al., 1981). They conclude that in the late synrift to early post-rift stage, the stresses caused by active upwelling of the asthenosphere may start to compete with the far-field intraplate stresses. At this stage, domal forces may start to dominate and thus, drive the system to change from passive to active rifting. In this scenario, the model predicts (1) drastic increase of subcrustal thinning beneath the rift zone, (2) lower crustal flow towards the rift flanks, (3) middle crustal flow towards the rift center, (4) coeval occurrence of tensional stresses within and compressive stresses around the upwelling region, and (5) possible surface uplift. They propose yet a change of the dominant forces, as the thermal cooling in the post-rift stage suppresses the thermal buoyancy forces, the far-field forces will yet again dominate the stress state, and the lithosphere becomes more sensitive to small changes in the intraplate stresses. Active and passive rifting is shown in Fig. 3. The figure also shows the related topography.

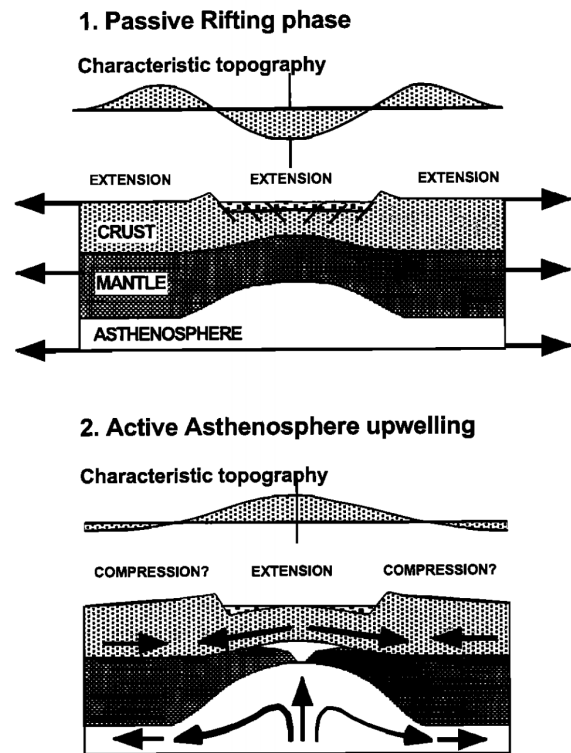


Figure 3: Transition from active to passive rifting in the late synrift/post-rift. Doming and shallow asthenosphere volcanism are expected to occur in the late synrift/ early post-rift eventually associated with a second rift phase. From Huisman et al. (2001).

## 3.2 Lithospheric stretching models

While the concept of active and passive rifting explores the degree of importance of the upwelling asthenosphere currents, there are conceptual models that try to explain the distribution and type of shear. These models can also be divided into two main groups, pure and simple shear models.

## 3.3 Pure shear

### 3.3.1 Uniform stretching model

One of the earliest and most important models that try to explain rifting is the uniform stretching, or *pure shear model*, also known as the *McKenzie model*, where the author propose a simple, but influential model for the development and evolution of sedimentary basins (McKenzie, 1978). Two events are explained, where the first consists of a instantaneous initial stretching of the lithosphere by far field forces, which in turn produces thinning and passive upwelling of hot asthenosphere. This stage is associated with block faulting and subsidence. Following this, the lithosphere thickens by heat conduction to the surface, and further slow subsidence occurs due to the increased density. This subsidence is not associated with faulting. The heat flow and slow subsidence is only dependent on the amount of stretching, which can be estimated from change in thickness of the crust caused by the extension. It is proposed that the best method for determining the extension is from the crustal thickness obtained from seismic refraction. The initial thickness found at the margins of the basin, a point which did not experienced thinning, divided with the thickness of a point that did experience thinning, will yield a stretching factor called  $\beta$ . Higher  $\beta$  means greater stretching and therefore also greater thinning. The stretching factor can be measured in other ways, commonly by measuring fault heaves to estimate extension, or by subsidence analysis where an unthinned marginal rift area is compared with basinal areas affected by the stretching. It is therefore important to be careful when comparing stretching values.

By assuming that the stretching is uniform, meaning that the stretching is constant with depth, it neglects the role that basement faults play during lithospheric stretching. While the rifting continue, the crust will become thinner and the heat flux will increase. As the extension eventually cease, the decrease in heat flux will cause the crust to cool, contract and eventually collapse. Essentially, the space available for sediment and water loads depends on the thermal history, and the thickness of the elastic layer of the lithosphere.

### 3.3.2 Depth dependent models

The uniform stretching model has later been modified to discontinuous depth-dependent stretching models, where the amount of extension is unevenly distributed at crustal and subcrustal lithospheric levels. Royden and Keen (1980) argue the fact that rheological properties vary continuously with temperature and pressure, and therefore will the lithosphere not deform homogeneously under stress. The deformation of the crust happens through brittle failure, whereas the lower lithosphere is expected to extend by ductile flow. In the model for non-uniform extension it is assumed that the upper and lower lithosphere can be decoupled at a depth  $y$ , to allow for an inhomogeneous behavior of stress. Above  $y$ , the lithosphere extends by a factor  $\delta$ , and below by a factor  $\beta$ . Only when  $\delta = \beta$  is the extension uniform. As with the uniform extension model, there is an initial change in elevation in response to the extension, which depends on the initial crustal thickness, the decoupling depth  $y$ , and the relative magnitudes of  $\delta$  and  $\beta$ .

A simple comparison of the uniform and the non-uniform model is seen in Fig. 4.

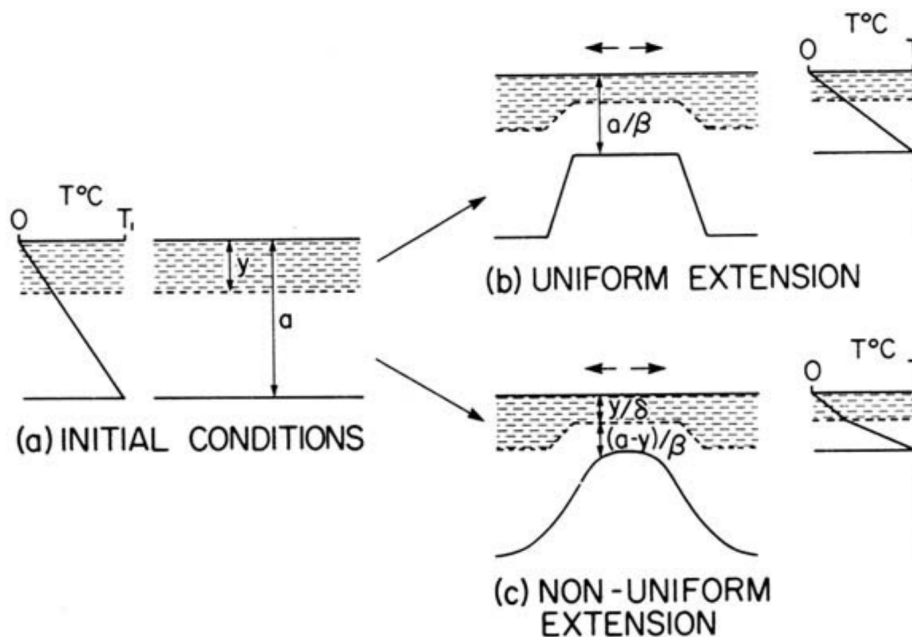


Figure 4: A simple comparison of the uniform and the non-uniform extension model: (a) Initial conditions show the lithosphere in thermal equilibrium before stretching. Decoupling is at a depth  $y$ . (b) Showing the behaviour with the uniform extension model, where the entire lithosphere extends by  $\beta$  and thins by  $1/\beta$ . This results in an elevated, linear thermal gradient. (c) Showing the behaviour using the non-uniform depth-dependent model. The upper lithosphere is above the level  $y$ , and extends by  $\delta$  and thins by  $1/\delta$ , and the lower lithosphere extends by  $\beta$  and thins by  $1/\beta$ . This results in a "two-legged" thermal gradient. From Royden and Keen (1980).

Further modifications of the uniform model include the consideration of melt segregation (Beaumont et al., 1981). It is similar to the uniform extension model, but also provides an explanation for the properties of the extended continental crust and its transition to oceanic crust by postulating that basaltic melt segregates from the asthenosphere and migrates to the crust. This model was postulated because the uniform extension model does not address problems of the formation of oceanic crust and the nature of the continental to oceanic crustal transition. If  $\beta \rightarrow \infty$ , the continental lithosphere will be completely replaced by asthenosphere. The uniform extension and melt segregation model assume that the crust and lithosphere are uniformly extended by  $\beta$ , but in addition a fraction of basaltic melt segregates from the asthenosphere brought in to replace the extended lithosphere (Fig. 5). Where  $\beta \rightarrow \infty$ , the melt will form the oceanic crust, elsewhere it will pass through the stretched lithosphere, due to its low density, and can be considered to underplate the crust or to intrude it.

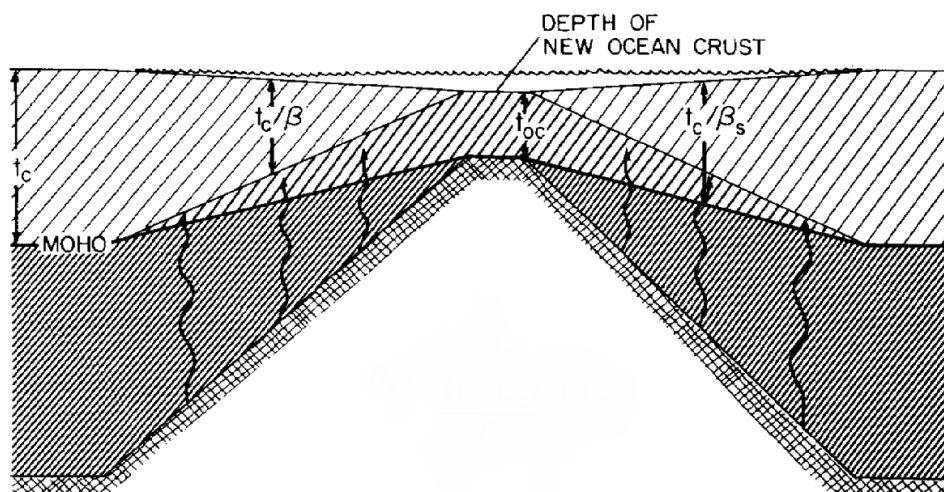


Figure 5: A sketch showing how a model regarding uniform extension and melt segregation produce oceanic crust and a smooth transition from unextended continental crust, to oceanic crust.

The amount of melt that segregates is proportional to the amount of incoming undepleted asthenosphere. Modified from Beaumont et al. (1981)

Another modification to the non-uniform stretching model is made by Hellinger and Sclater (1983). They argue that the rifting process in intracratonic rift basins is irregular and not continuous, and that if there is only one period of extension and it lasts for less than 15-20 My, then the uniform extension model is probably adequate. For multiple-stage rifting and single stages of longer duration a numerical model is needed. The authors argue that extension and subsidence within the rift during a tectonic phase is commonly accompanied by uplift and erosion of the rift

flanks, and that subcrustal heat input during rifting occur over an area much broader than the rift proper. To explain the uplift of the flanks, the authors consider two mechanisms: subcrustal thinning by extension below the flanks and tilted major normal faults in the crust between graben and flanks. The uplift of the flanks is said to be a result of upward forces working due to the existence of a nonvertical fault and the upward forces due to the thermal anomaly associated with the distributed extension. The uplifted flanks will then proceed to be eroded, which leads to further uplift of the crust and an eventual balance of forces. Because of the added effect of the subcrustal extension, the erosion will be greater and the crust will eventually subside below sea level, after the extension is over. A sketch of the model at the end of the extensional phase is shown in Fig. 6.

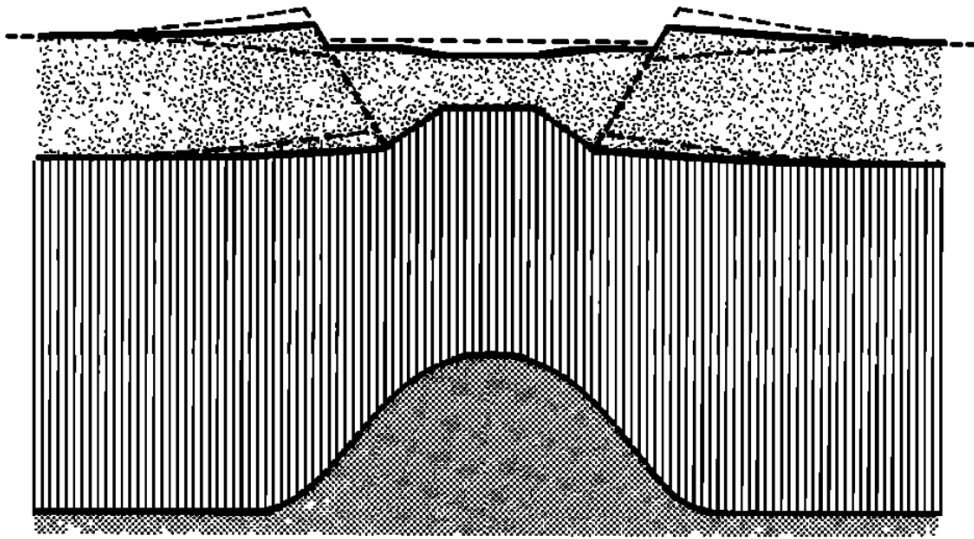


Figure 6: A sketch of a newly formed graben with uplifted flanks. The upward curving, dashed lines, represents the eventual total uplift of the original crustal boundaries that results from the surface erosion. The continuous line on the flanks represents the initial uplift. From Hellinger and Sclater (1983)

The final modification that will be considered, is by Rowley and Sahagian (1986). Their continuous, depth-dependent stretching concept assumes an equal amount of extension at upper and lower lithospheric levels, whereby extensional strain is diffused at deeper levels over a wider area than at shallower levels. Like the model by Hellinger and Sclater (1983), they are both depth-dependent and attempt to account for the broad symmetrical shoulder uplift that is often associated with active rifts. Essentially, the model involves continuous nonuniform stretching within a polygon region bounded by symmetrical, outward-sloping boundaries within the mantle (Fig. 7). This geometry results in thinning of the lithosphere below crustal regions that are less stretched or unstretched. Crustal uplift results from asthenospheric upwelling below these regions. This in turn, results in stretching factors for the mantle that are less than those for the crust.



The models introduced have been continuously improved. They are all related and have multiple things in common. One thing that is characteristic for all of them, is the lack of a thoroughgoing lithospheric shear zone, which was introduced in simple shear models.

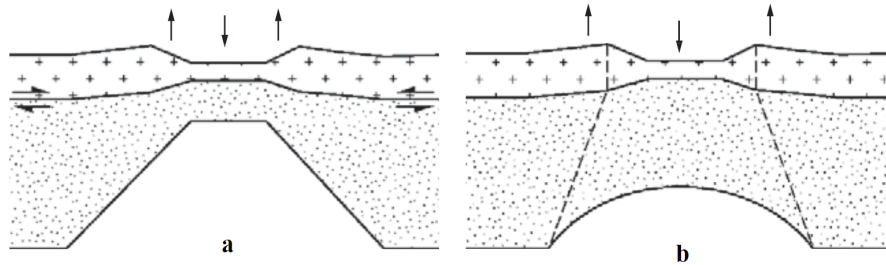


Figure 7: Lithospheric stretching models. (a) is a simple sketch of the discontinuous, depth-dependent stretching model as described by Beaumont et al. (1981). (b) Sketch showing the initial geometry of continuous nonuniform stretching, including a polygonal region of the lithosphere. Modified from Ziegler (1990)

### 3.4 Lithospheric stretching models - Simple shear

A *simple-shear model* was proposed by Wernicke (1981, 1985) and unlike the pure-shear models, it involve the development of an intra-crustal shear zone that dips laterally through lower crustal and upper mantle levels to, and even through, the base of the lithosphere (Wernicke, 1985). In this model, the zones of upper and lower crustal and sub-crustal lithospheric attenuation are laterally offset, thus introducing asymmetry in the thermal evolution, compared with the pure shear, uniform-stretching models. This means that the zone of upwelled asthenosphere does not lie beneath the main zone of crustal extension (Coward, 1986). Wernicke (1985) argues for there being three main zones in an extensional shear zone: (i) the zone where the upper crust has thinned and there are abundant faults above the detachment zone, (ii) the discrepant zone where the lower crust has thinned while there is negligible thinning in the upper crust, and (iii) the zone where the shear zone extends through the lithospheric mantle (Fig. 8).

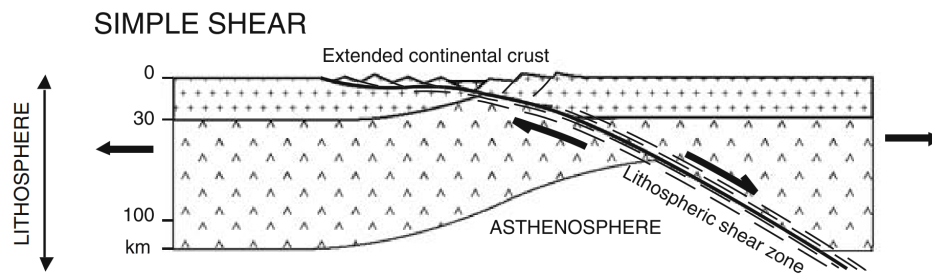


Figure 8: A simple sketch displaying asymmetric lithospheric extension by simple shear. From Reston and Pérez-Gussinyé (2007)

The simple shear model satisfies many of the geometric relationships evident on reflection seismic data at upper and middle crustal levels and may explain the absence of post-rift subsidence of marginal grabens (Ziegler, 1990). By introducing asymmetry, the transfer of tensional strain to one side of the rift system would require an asymmetric uplift of the rift shoulders. In extreme cases of the simple shear model, the zone of lower crustal and sub-crustal lithospheric attenuation could lie entirely outside the zone of upper crustal stretching. During the rift stage, the area of non-attenuated upper crust would become progressively uplifted by attenuation of the subcrustal lithosphere, and would develop during the post-rift stage into a thermal-sag basin. This concept has led to the development of the "linked tectonics" model. Which is a model that emphasizes the linked nature of faults in a way that is analogous to that developed for thrust regimes. A linked fault system requires three components; ramps, flats and sidewalls or transfers (Gibbs, 1990).

### 3.5 Combined simple and pure shear models

Barbier et al. (1986) modified the simple shear model by assuming that the intra-crustal shear zone, into which faulting at upper crustal levels soles out, coincides with the transition from brittle to ductile deformation. This *combined simple and pure shear model* suggests, like the continuous depth-dependent stretching models, that tensional strain is dissipated at lower crustal and subcrustal lithospheric levels over a wide area that extends beyond the zone of upper crustal extension. As such, this model accounts for the broad, symmetrical doming of rift flanks. In a combined simple shear/pure shear model, the lower crust and mantle deforms by pure shear, while the upper crust is deformed by simple shear forces (Fig. 9).

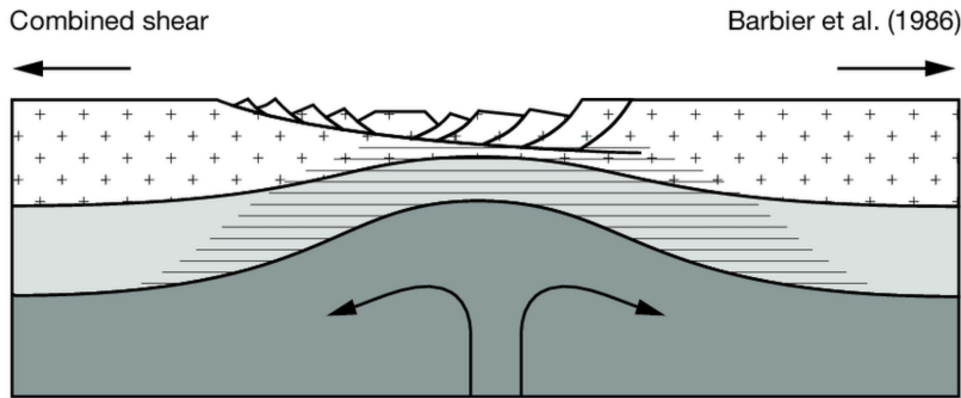


Figure 9: A simple sketch showing the combined shear model. The upper crust is deformed by simple shear forces, with an intra-crustal shear zone that soles out in the crust. The lower crust and mantle is deformed by pure shear forces. The uplift of the asthenosphere occurs under the zone of rifting, unlike the simple shear model. From (Ziegler, 1990).

Kusznir et al. (1987) further investigated the importance of detachments controlling extensional sedimentary basin formation using a coupled simple shear/pure shear model of continental extension. The authors explain that the main consequence of involving detachments during extension is to allow for lateral separation of the rift and thermal subsidence basins, and that total extension, detachment depth and relative position of pure and simple shear deformation are major factors in controlling the basin geometry. Kusznir et al. (1987) argue against the assumption of Airy isostasy (flexural rigidity equal to zero), which is the common assumption in uniform stretching models. They propose that a significant lithosphere flexural rigidity must exist during the rifting phase and post-rift thermal subsidence phase.

This was further explored by Kusznir et al. (1991) and Kusznir and Ziegler (1992), where they use the concept of detached simple and pure shear forces, and a significant flexural rigid lithosphere, to propose a *simple-shear/pure-shear flexural cantilever model*. The model describes the geometric, thermal and flexural isostatic response of the lithosphere to extension by planar faulting of the upper crust and plastic faulting distributed deformation in the lower crust and mantle. During faulting, the upper crustal footwall and hanging-wall blocks behave as two mutually self supporting flexural cantilevers (Fig. 10). Hanging wall collapse and footwall uplift are generated through their response to isostatic forces induced by extension. It is also considered how extension on multiple faults will generate block rotation through the interaction of hanging wall and footwall blocks. The general crustal structure and basin geometry for faults are predicted and dependent on fault spacing, horizontal displacement, polarity, and the amount of extension, as well as erosion of footwall uplift (Kusznir and Ziegler, 1992).

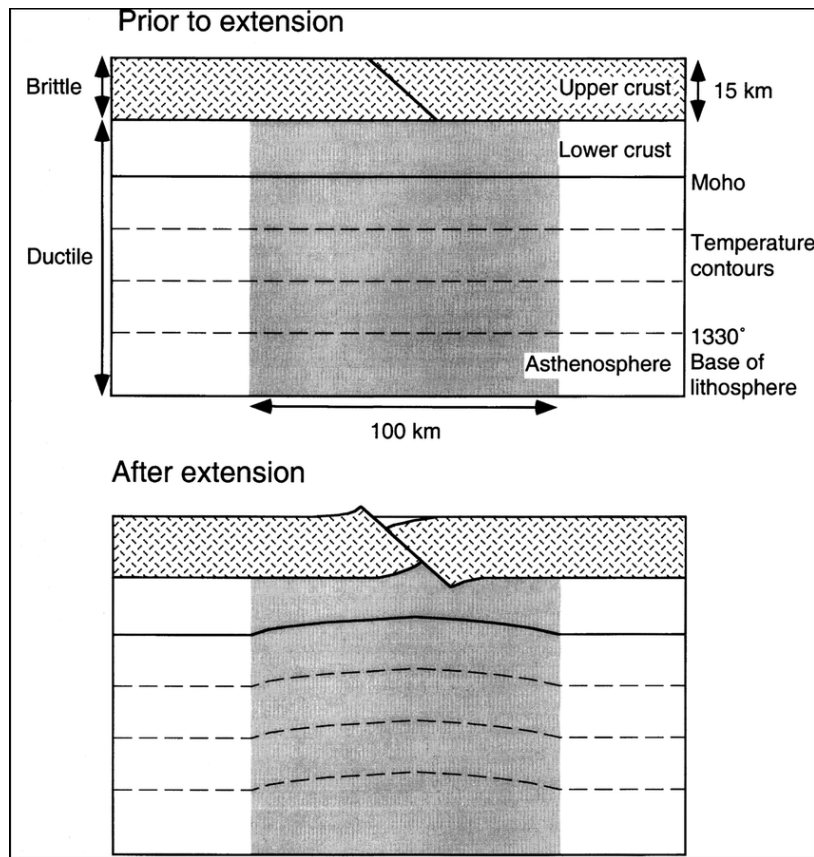


Figure 10: A figure showing how extension takes place on planar faults in the upper crust, while deformation in the lower crust and mantle is achieved by pure shear. The lithospheric extension produces thinning and a flexural response of the lithosphere. From (Kusznir and Ziegler, 1992)

### 3.6 Concept of lithospheric necking

The necking depth is the level where crustal thinning takes place, and determines the ratio between thinning of the crust and the lower lithosphere. In the absence of isostatic forces, the necking depth remains horizontal. In other words, the level of necking is defined as the level of no vertical movement in the absence of isostatic forces (Braun and Ceaumont, 1989). Under pure-shear conditions, the necking depth is determined by the rheological properties of the lithosphere (Fjeldskaar et al., 2004). This is an important concept when developing extensional stretching models as the lithospheric response is different for different necking depths. A chosen necking depth of less than 15 km causes downward flexing of the rift zone and no shoulder uplift will occur. However if the necking depth is more than 15-20 km and even as deep as to the Moho, it will cause upward flexure of the rift zone and an uplift of the rift shoulders. As seen in Fig. 11, the depth of necking chosen in the upper figure leads to upward flexure of the lithosphere and thus uplift of the flanks, while the choice of necking depth in the lower figure leads to downward flexure and no uplift.

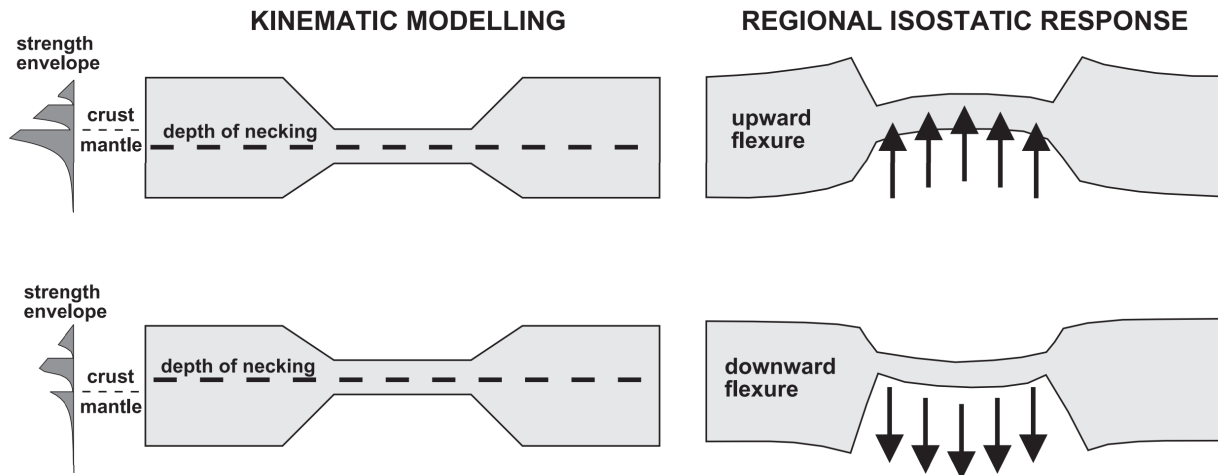


Figure 11: The left side display kinematic rift models at different necking depths with different strength envelopes, while the right sides show the lithospheric response to the chosen depth of necking, (Ziegler and Cloething, 2003)

### 3.7 Applicability of rift models

For the rift models to be valid and applicable, they need to be tested against examples of real world rift system where significant amount of geophysical data sets are available. The data sets need to be of sufficient quality and coverage that the crustal configuration of the rifts, the stretching factors at upper and lower crustal levels, the reflectivity of the upper and lower crust, as well as the definition of potential intra-crustal detachment and/or shear zones can be determined. When applying a model, the heat-flow data, distribution of eventual rift-related igneous activity and the configuration and evolution of the lithosphere-asthenosphere boundary, must also be taken into consideration.

The models introduced in this chapter are early models that invoked one or two phases of relatively simple symmetric (pure shear) or asymmetric (simple shear), or a combination thereof, of extensional deformation to explain first-order patterns of normal faulting, crustal thinning and sedimentary records. Geophysical data acquired frequently over the past 30 years, have revealed a structural complexity that challenges these simple models regarding the occurrence of rifting through multiple phases and a varied characterization of structural, sedimentary and magmatic processes.

However, even though rifts differ from each other in many details, there is possible to account for numerous first-order similarities in a common set of evolutionary phases (Naliboff et al., 2017). *The stretching phase* is the earliest phase representing the onset of continental extension. It is

characterized by distributed faulting in the upper crust, and relatively uniform lithospheric thinning accommodating small amounts of total extension. In the following phase, *the thinning phase*, significant thinning and lithospheric necking occurs when ductile layers thin sufficiently so the brittle crust couple with the upper mantle. Accompanying this is accelerated strain localization onto detachment faults with large offsets. The third phase, *the hypertension and exhumation phase*, occurs when deformation migrates oceanward and further localizes onto concave detachment faults cutting through the entire lithosphere. This phase can be associated with hyperextension of the crust leading to mantle exhumation and magmatism, which directly proceed break-up and mid-ocean ridge spreading.

However, these phases are only enough to account for the similarities observed in rifts, but cannot explain important differences, such as variations in margin width, asymmetry, rift abandonment and distal domain faulting patterns. To account for this, it is difficult to set up a series of phases or rules that a rift follows as it can be influenced by the initial and evolving rheology of the lithosphere, the velocity of the extension, structural inheritance and periods of tectonic quiescence (Naliboff et al., 2017).

## 4 The driving forces of rifting

The driving mechanism for lithospheric extension has been variably attributed to plate-boundary forces, to hot-spots and to the gradual development of upwelling asthenospheric convective systems under continents. Most of the Triassic-Early Jurassic rift systems of West- and Central-Europe and of the North Atlantic and Tethys domain were non-volcanic and crustal doming only played a very subordinate role. This speaks against the development of these rifts in response to hotspots. It is also doubtful whether subduction processes along the distant margins of Pangea played a major role in the development of the Permo-Triassic Gondwana rifts and those of the Arctic-North Atlantic and Tethys domains. More likely, the early Mesozoic graben systems developed in response to frictional forces that were exerted on the lithosphere by slowly developing upwelling convection systems that were located beneath the central parts of the Pangea. These systems gradually asserted themselves and caused during the Middle Jurassic the development of the Tethys-Central Atlantic sea-floor spreading systems, and during the Cretaceous and Paleogene the development of the North Atlantic and Norwegian-Greenland Sea spreading axis (Ziegler, 1990).

## 4.1 Weakening of the lithosphere

Both oceanic and continental lithosphere can be considerably weakened by transform faults and thermal effects caused by thick sedimentary layers. This, in addition to spatial variations in the rheological structure of the lithosphere play an important role in areas around future zones of crustal separation that can be deformed tensionally during rifting. The presence of such lithospheric discontinuities can reduce the strength of the lithosphere, and the orientation of the discontinuities plays an important role in terms of reactivation potential. It can be shown that the location of most of the major Mesozoic and Cenozoic rift systems appears to be controlled by the distribution of orogens where the lithosphere is characterized by deep-reaching crustal shear zones and lithological discontinuities, and possible upper mantle reflectors related to subducted crustal material (Ziegler and Cloething, 2003).

Rift systems superimposed on former orogeny and that follow their strike are generally strongly influenced by the pre-existing basement fabric and can possibly be reactivated at stress levels considerably below the bulk yield strength of homogeneous crust. Such zones are areas where concentration of strain is possible, even up to several 100 km to one or both sides of the zones of mantle-lithosphere stretching. Linkage of such weakness zones and decoupling of the upper crust from the mantle-lithosphere at the level of the ductile lower crust can give rise to simple-shear extensional deformation as proposed in the Wernicke model (Wernicke, 1981, 1985).

On the other hand, in areas where a rift cross-cuts the orogenic fabric of the crust, pre-existing crustal and mantle-lithosphere discontinuities cannot be reactivated under the prevailing stress field. This will cause the development of new faults and the deformation is likely to be caused by pure shear, similar to what described in the McKenzie model (McKenzie, 1978).

## 4.2 The early stages of rifting

According to Ziegler and Cloething (2003), can simple-shear deformation of the entire lithosphere play an important role in the early stages of rifting, while being confined to the upper crustal levels in the advanced stages. During initial rifting stages, reactivation of pre-existing crustal discontinuities can lead to the subsidence of isolated graben and half-grabens that are linked by shear zones.

### 4.3 Fault development, interaction and growth - the geometry of a rift

When considering the growth of individual faults, it is generally referred to two models. The first is the isolated fault model, that describes how individual faults within an array of faults can be initiated as kinematically isolated structures at random locations, eventually coalescing to form a large fault by incidental interaction and linkage. The other type is coherent fault models, where fault segments initiate as elements within a larger structure. It is possible to distinguish between faults that developed according to the isolated and coherent fault models based on finite displacement distributions (Childs et al., 2017)

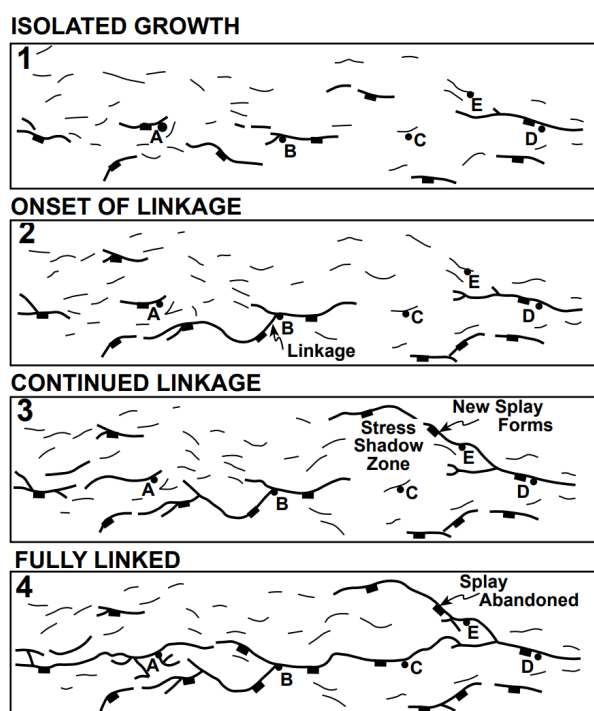


Figure 12: A sketch from numerical modelling, showing the development and linkage a fault-segment, with abandoned faults outside the linked faults. From Gupta et al. (1998)

The basin architecture of extensional rift basins are largely characterized by the development of fault zones. The development of and growth of a fault can be described through 3 stages: (i) The fault initiation stage, where a large number of scattered small-displacement faults define isolated depocentres. (ii) The interaction and linkage stage, where several of the scattered faults start to link together and grow due to stress feedback between the faults. The deformation starts to become localized along major fault zones. (iii) The final stage is the "through-going fault zone stage". This is when the fault zone is fully developed through the linkage of several smaller faults. Commonly, the faults positioned between other faults, experience the largest displacement rate by being frequently loaded by laterally adjacent segments (Fig. 12). The faults not linked in this through-going fault zone, risk abandonment and becoming inactive

due to being located in stress shadows of the dominating fault zone. At this stage, major half graben and graben depocentres may develop (Gawthorpe and Leedert, 2000). The development from many small faults with small displacements, to fewer and fewer, but longer faults with larger displacement and higher displacement rates, can be seen in the basin record, since the early basins should be numerous, isolated and bounded by small faults that show evidence for progressive abandonment. The basins should show low subsidence rates and be widely preserved across the hangingwall



basement of later developed basins.

One model of fault growth is the progressively development and linkage of more and more faults. Another is where most of the fault growth occurs at depth, from the base of the brittle upper crust upwards. In this scenario, the linkage and abandonment of faults takes place in the subsurface. Eventually, a fully formed major fault will break through the surface and very rapidly propagate laterally to reach its equilibrium length, which will be approximately the length of the strata above the upper crust. It will be the sole fault that reaches the surface to transfer crustal extensional strain, and is characterized by a growth monocline and the presence of high-angle to locally reverse secondary faults and fractures in the hanging wall (Fig. 13).

It is indicated from observations of a variety of rift basins that folding plays an important role in the development of fault zones. Transverse folds are commonly associated with along-strike displacement gradients. In the hangingwall of normal faults, transverse synclines define displacement maxima, whereas transverse anticlines are associated with displacement minima at segment boundaries (Gawthorpe and Leedert, 2000).

#### 4.3.1 Fault death

Dead faults are faults that are not currently active. The permanency of abandonment of faults are often unclear, as it can be permanently, temporary or episodic abandoned. Fault death is a common occurrence in the evolutionary span of a rifted basin. Spatial and temporal change in regions of active faults can change quite rapidly (in less than 1 Ma) and can have major implications for the dynamics of crustal extension. One obvious reason for fault abandonment is that the fault rotates with time, in a direction that makes it unfavourable oriented for further movement. This rotation can happen around both vertical and horizontal axes, and can be locked in a position that is disadvantageous compared to more favourable fault directions. Another cause of fault inactivity could be that the interaction with other faults put it at a disadvantage. Slip on one fault can trigger

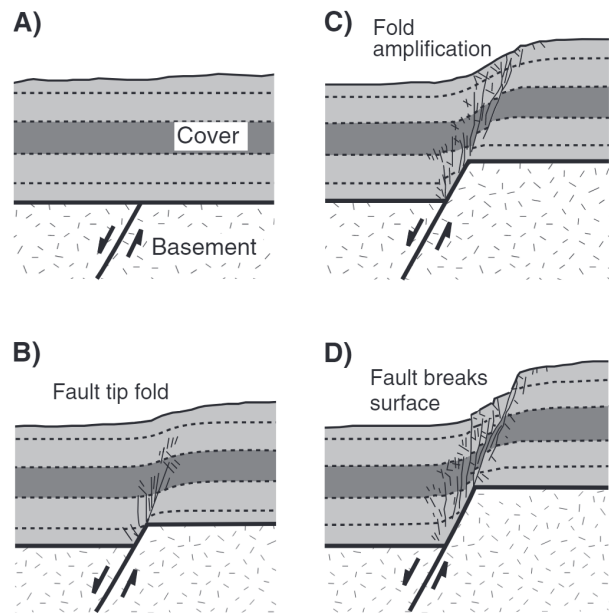


Figure 13: Sketch showing the progressive development of a blind fault. From Gawthorpe and Leedert (2000)

or inhibit slip on another. This will influence the further behaviour of closely bound groups of sub-parallel normal faults, and is very likely very important for small faults. But if this interaction can hinder the growth and permanently deactivate larger faults is unclear. Deformation patterns over large distances may be more influenced by flow in the ductile part of the lithosphere, than the stress transmitted through the brittle part (Jackson, 1998).

### 4.3.2 Fault reactivation

Tensional reactivation of thrust faults plays an important role in the extension of orogenically destabilized lithosphere (Ziegler and Cloething, 2003). Theoretical analyses of fault reactivation show that one of the principal parameters controlling fault reactivation is the contrast in cohesive and frictional strengths between intact and previously faulted rocks (Etheridge, 1986). The likelihood of fault reactivation depends on the dip of the existing fault plane. Low-angle faults are more favourable as the resolved shear stress on the plane is higher. When a listric fault, which decreases in dip downwards, reactivates, the uppermost part of the fault may be too steep and new reverse faults typically develop in the footwall of the existing fault. In these cases, where only the deeper parts of the fault are reactivated, the shortening is accommodated over a much broader area in the shallow part of the section. Multiple previous experiments have shown that the amount of reactivation is strongly dependent on lithology, cohesiveness and the steepness of the previously active faults (Etheridge, 1986; Koopman et al., 1987; Mandl, 2000). Inversion is when a fault is reactivated in the opposite direction to its original movement. During inversion, the layers filling rift structures undergo lateral compression and can be pushed up and outwards, thus creating local extension near the surface (Konstantinovskaya et al., 2007).

## 4.4 Rifting duration - Why does rifting cease?

Figure 14 show a selection of rifts, both abortive and successful, some experienced doming, and others experienced periods of volcanic activity. It is obvious that there is a wide range of duration rifting, ranging from just 7.5 My to 280 My. Ziegler (1990) suggest that the variations in the duration of the rifting stage of successful rifts is a function of the time required for the evolution of upwelling asthenosphere to the point where the currents are able to drive apart major continents.

There is not shown any correlation between the duration of the rifting stage of rifts, which are superimposed on orogenic belts and those that developed within stabilized cratonic lithosphere. This suggests that the availability of crustal discontinuities that can be tensionally reactivated, does not play a major role in the time it takes to achieve crustal separation. However, such discontinuities

can play a significant role in the localization and distribution of strain, by weakening the crust. In this way, they contribute to the preferential tensional reactivation of young as well as old orogenic belts (Ziegler and Cloething, 2003).

Failed, or aborted rifts are rifts that does not progress to the stage of crustal separation and becomes passive margins. To become a successful rift, the rifting activity must concentrate on a limited zone, that eventually will become the zone of crustal separation. This mean that if there are other surrounding rift systems that experience rift activity, they may be aborted when rifting activity concentrates away from them. This is similar to the processes that can cause fault death of individual faults. Plate interactions play a major role in the evolutionary history of rifts, particularly in the duration of the rifting stage and whether or not the rift becomes aborted (Ziegler, 1990). Modifications in the drift-pattern and interaction of lithospheric plates can cause alterations of the stress regime in the rift, and result in a transition from orthogonal to oblique extension, causing partial inversion of rifts. Essentially, the duration of the rifting stage is a function of the persistence of the controlling stress regime governing its evolution. This again can depend on extensional strain concentration to the future zone of crustal separation, of crustal separation occurring in genetically related rift systems, or on fundamental changes in plate motions and interaction. The time it takes to achieve crustal separation is largely a function of constraints on lateral movements of the diverging blocks, and thus, of plate interaction (Ziegler and Cloething, 2003).

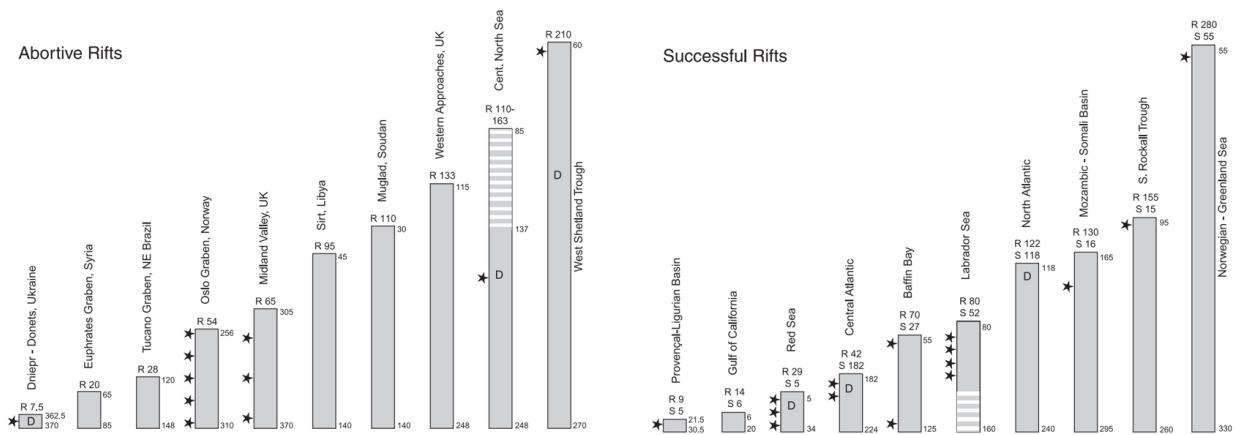


Figure 14: Graph showing the duration of abortive and successful rifts. R = rift duration, D = periods of doming, stars = periods of main volcanic activity, S = duration of sea-floor spreading stage. All years are in My. Modified from Ziegler and Cloething (2003).

## 4.5 The width of the rift zone

Variations in the width of continental rifts from narrow to wide are classically explained in terms of the temperature and strength of the lithosphere undergoing tensional stress. It is indicated through model experiments where conjugate faults meet at the base of the brittle crust, that the width of a rift zone is dependent on the thickness of the crust and the depth at which the brittle/ductile zone is located at the onset of lithospheric extension (Allemand and Brun, 1989). This explanation does not take into account the possible existence of low-angle detachment faults at lithospheric scale as described by Wernicke (1985).

The style of rifts, as defined at upper crustal and syn-rift sedimentary levels, is influenced by the thickness and thermal state of the crust and subcrustal lithosphere at the onset of rifting, by the amount of crustal extension and the width over which it is distributed, as well as whether the mode of crustal extension is orthogonal or oblique (Ziegler, 1990; Færseth, 1996).

Through time, crustal strain will concentrate on the more intensely thermally weakened parts of a rift, generally the axis, and thus cause a narrowing of the rift. The transition from wide to narrow rifts require lowering of the geothermal gradient. However, in cases with slow strain rates, lateral rift systems can be abandoned and the rift activity can shift to less extended areas (Ziegler and Cloething, 2003).

At lithospheric scale, the strength of the mechanically strong upper part of the mantle–lithosphere, which depends on its thermal state and the thickness of the crust, plays an important role in the localization of rift zones. Moreover, lateral thickness heterogeneities of the lithosphere appear to play an important role in the localization of rifts. At crustal scale, its composition, the thickness of its mechanically strong upper part and the availability of pre-existing crustal discontinuities, which can be tensionally reactivated, play a dominant role in the width and deformation mode of an evolving rift (Ziegler and Cloething, 2003).

Through the length of a rift, the width can change. The explanation for this can be the influence of pre-existing crustal structures from past tectonic events or that it develops as a result of the interaction of an active mantle plume with a continental lithosphere that is initially laterally homogeneous (Koptev et al., 2018). A mantle plume located over the central part of a rift, will cause increased uplift and a thermally warmer region, leading to a more narrow part of the rift than areas away from the center, where the influence of the plume decreases.

## 4.6 Controls on rift geometry

Most rifts consist of a series of separate, but linked segments that together form the linear zone characteristic of rifts. The length of the segments vary depended on the elastic thickness of the lithosphere. Areas of warm, thin lithosphere will consist of longer segment lengths than areas of colder, thicker lithosphere. Extended continental lithosphere is bounded on one or both sides by normal faults, but the dimensions and internal structure of the basins vary along the length of the rift systems, as well as between different rift systems. Half graben morphology is seen in the majority of rift basins, with most of the strain accommodated along the master fault bounding the deep side of the basin. Displacement decreases towards the tips of master faults, which is normally the longest faults with the greatest displacement. Shorter smaller offset faults are often seen in the hanging wall of the border faults. The rheology of the upper continental lithosphere exerts a strong control on rift-basin geometry, as the length and width of rifts is seen to decrease width decreasing effective elastic thickness.

## 4.7 Rift-related subduction

An initial tectonic subsidence occur when the lithosphere undergoes horizontal extension and faulting of the crust that causes stretching and decreasing thickness of the extended region. This thinner crust will subside relative to thicker, undeformed crust.

The thermal subsidence of passive continental margins are controlled by lithospheric thermal contraction and sediment loading of the crust. Similar mechanisms dominate the subsidence of tectonic inactive rifts. The amount of tectonic post-rift subsidence is caused by the cooling and contraction of the lithosphere and. The return of the lithosphere to thermal equilibrium is controlled by the magnitude of the thermal anomaly that was induced during the stage of crustal attenuation. Thermal anomalies induced during rifting that did not lead to crustal separation are relatively smaller than those where it lead to a successful rift. Their magnitude largely depends on the degree of displacement of the lithosphere/asthenosphere boundary during rifting, and whether asthenospheric material rose up diapirically to upper mantle or to the moho. The thickness of the sediment column developing in basins above inactive rifts are, in addition to the thermal anomaly, dependent on the degree of crustal attenuation that was achieved in them during the rifting stage, the water depth and the density of the sediments (Ziegler, 1990).

## 5 Extension along suture zones

A fundamental concept in plate tectonics is the Wilson Cycle theory where oceans close and reopen along former sutures. There can be several reasons for why a rift would develop at or near a former suture, such as (i) the former orogen being thermally weaker compared to the surroundings due to long-term thermal heating and in that way, be an area of localization of the rift, (ii) inherited thrust faults can weaken margins and cause reactivation of structures and localization of deformation, and (iii) initiation of extension because of gravity-driven flow of thickened crust by the previous mountain-building phase (Buiter and Torsvik, 2014). However, it is not always the case that extension follow former sutures. One possible explanation for this, is that collisions lead to a large region of deformation (200-500 km), where several zones of weakness can be susceptible for strain localization, thus developing a different zone of rifting than the previous suture. Additionally, the Earth's mantle play an active role in aiding rifting and break-up.

### 5.1 The Iapetus suture - a North Atlantic zone of weakness

The Iapetus Ocean closed in the Silurian ca. 430-420 Ma ago. This later produced a suture zone between (among others) present day Norway and Greenland, known as the Iapetus suture. The Caledonian orogeny was the result of this closure bringing Baltica and Laurentia together. The Caledonian collision resulted in a highly heterogeneous crust with brittle thrusts and normal faults. Rift basins generally develop on structurally and mechanically heterogeneous crust involved in prerifting deformation events. The formation of the Caledonian orogeny was followed by extensional collapse and formation of Devonian sedimentary basins on the margins. The North Atlantic Ocean opened after 200-300 Ma of extension, when the straub was finally localized enough to cause break-up.

The exact location of the Iapetus suture is still not know and has not been identified on the mid-Norwegian margin due to the strong extensional overprint of Caledonian structures (Fig. 15).

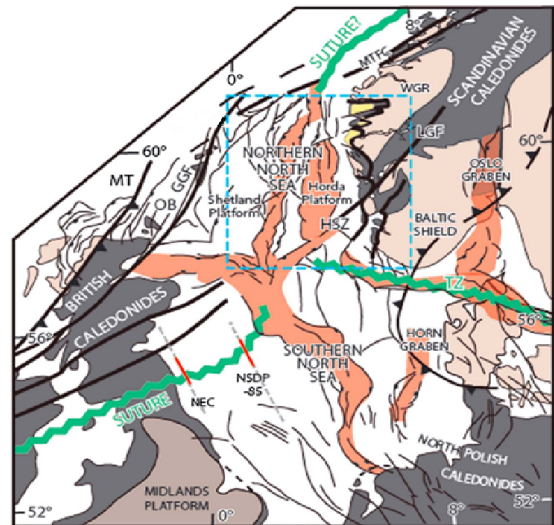


Figure 15: The main Late Paleozoic - Mesozoic rift axis are highlighted in red. The Iapetus suture is marked with green. Note how its exact location is unknown in the basins of the northern North Sea. Modified from Fazlikhani et al. (2017)

Modified from Fazlikhani et al. (2017)

The exact location of the Iapetus suture is still not know and has not been identified on the mid-Norwegian margin due to the strong extensional overprint of Caledonian structures (Fig. 15).

However, even though the exact location of the suture zone is not positively identified, it is thought that the Central and Viking Graben were controlled by the location of the Iapetus suture and that the suture is more or less parallel to the trend of the Viking/Sogn Graben (Lyngsle and Thybo, 2006). Fichler and Hospers (1989) suggests, from interpretation of deep seismic data, that the Iapetus suture is located beneath the East Shetland Platform. Furthermore, on a broad scale, it seems clear that the separation of Greenland and Norway represents a slightly modified reopening along the Caledonian suture zone, following the theory of the Wilson Cycle (Doré et al., 1997).

## 6 Structural framework

The North Sea rifts are examples of intracratonic basins, meaning they are positioned on continental crust. It is vital for the formation of sedimentary basins on continental crust that the lithosphere is thinned, resulting in subsidence to maintain isostatic equilibrium. The North Sea has been subjected to several periods of stretching/thinning and subsidence that affected the basin formation, and the geometric shape of the basins are influenced by the structure of the underlying rocks and by the thickness of the crust.

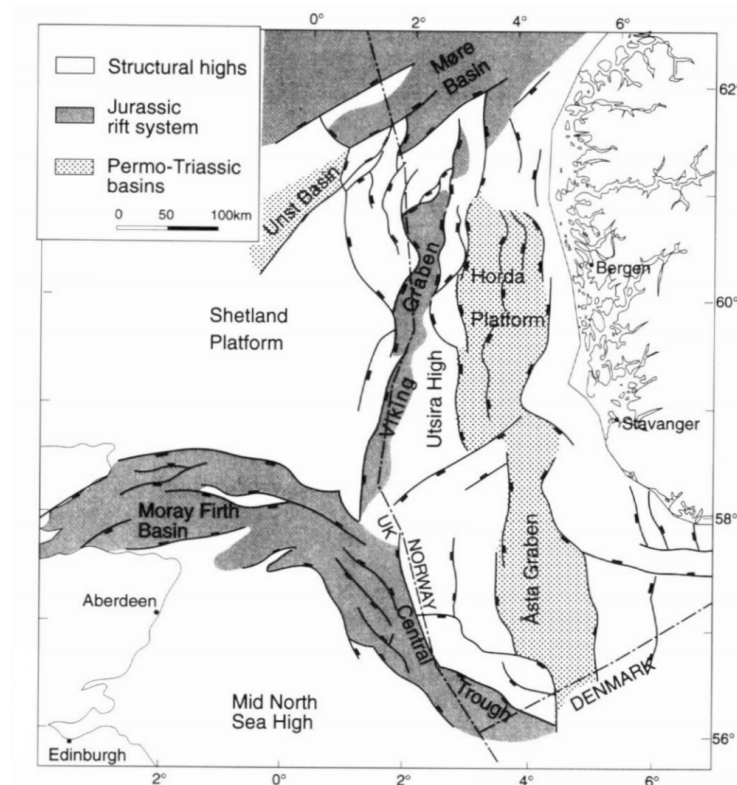


Figure 16: Map showing the Viking Graben and the surrounding structures. From Færseth (1996).

## 6.1 Caledonian collision

The Scandian phase of the Caledonian orogeny lasted from about 425 to 400 million years ago, and was caused by the collision of the continents Laurentia and Baltica, closing the Iapetus Ocean. The collision resulted in a highly heterogeneous crust with a structural imprint expressed in the form of lithological layering, mylonitic fabrics, shear zones and thrusts in the lower and middle Caledonian crust, as well as brittle thrusts and normal faults in the, now mostly removed, upper Caledonian crusts. Such a crust is likely to respond to later extensional deformation by a certain amount of reactivation, depending on geometry, dip, orientation relative to the extension direction and relative strength. However, the high degree of heterogeneity, makes it difficult to explain the current basin in terms of control exerted on it by a 'Caledonian grain' in a specific direction (Færseth, 1996).

## 6.2 Devonian crustal extension

The extensional history of the North Sea rift started with Devonian extension of thickened Caledonian crust as the northwestern Europe underwent extension to form sedimentary basins. It is believed that the Devonian stretching involved reactivation of Caledonian thrusts, most notably as low-angle extensional shear. Devonian basins developed in association with these shear zones, and many are preserved along the western coast of Norway. Intracontinental stretching followed in the Permo-Triassic and Jurassic that produced the North Sea rift system (Færseth et al., 1995). The basins are the results of these rifting episodes and the original crustal framework being reworked by the rifting. These events of multiple periods of stretching and subsidence, with related sediment-distribution gives the North Sea a complex history, which is one of the reasons why the North Sea is so prosperous in regards to hydrocarbons. During the Devonian, the Old Red Sandstone was deposited in response to the extensional collapse of the Caledonides. The Devonian sediments are only found in a few wells in the northern North Sea

## 6.3 Permo-Triassic rifting

The structure of the northern Viking Graben was generated in the late Permian/early Triassic by the activation of major north-south faults, through the accelerated opening of the Norwegian-Greenland Seas. Caledonian thrusts were also reactivated (Ramberg et al., 2013a). This Permo-Triassic episode was the first of two major rifting phases in the northern North Sea (Færseth, 1996). The Permo-Triassic is mainly restricted to a N-trending depression approximately 170-180 km wide. Most of the fault-related structures seen on seismic data is from the later rifting episode in the Late



Jurassic. Despite of this, clear evidence from this early rifting episode can be found east and west of the Viking Graben, where it has not been affected by the strong Jurassic overprint (Badley et al., 1988). It is believed that in these areas, instead of the Jurassic rifting overprinting the structures, the major Permo-Triassic structures were reactivated (Marsden et al., 1991). The Horda Platform to the east of the Viking Graben is proven to contain syn-rift units of Permian to middle Triassic age. The Unst Basin, on the opposite side of the Viking Graben, contain a few kilometer thick beds of red sandstones from the Permo-Triassic (Marsden et al., 1991).

It has been estimated that the magnitude of extension during the Permo-Triassic was approximately 1.4-1.5 (Marsden et al., 1991), and that the extension occurred as far west as to the West Shetland basin. The Alwyn-Ninion-Hutton alignment (green lines in Fig. 17) acts as the limit of thick Triassic sediments to the west. It is delineated by the Hutton Fault to the north. The throw of the alignment decreases to the south and is eventually shifted eastwards to major faults which bound the Hilds fault block to the east and southeast (purple lines). The eastern margin is represented by the Øygården Fault Zone (red lines). In this area the top basement is vertically displaced 3-5 km across normal faults. North of the Øygården Fault Complex, the structural pattern is controlled by the easterly-dipping Sogn Graben fault. The structures and distribution of faults can be seen in Fig. 17.

The most active faults were along the eastern margin, making the structure of the Permo-Triassic basin asymmetric. North of the Horda Platform an array of westerly-tilted half graben are bounded by east-facing faults which offset the top basement. This tectonic style has the characteristics of domino-style tilting.

In addition to producing the general structure upon which the later Jurassic rifting acted, the Permo-Triassic rifting was important in the sense that the basin system had yet to reach thermal equilibrium at the onset of the Jurassic stretching some 70 Ma after the first rifting episode (Nøttvedt et al., 1995). This suggests that the North Sea was a hybrid basin affected by both subsidence and active stretching simultaneously.

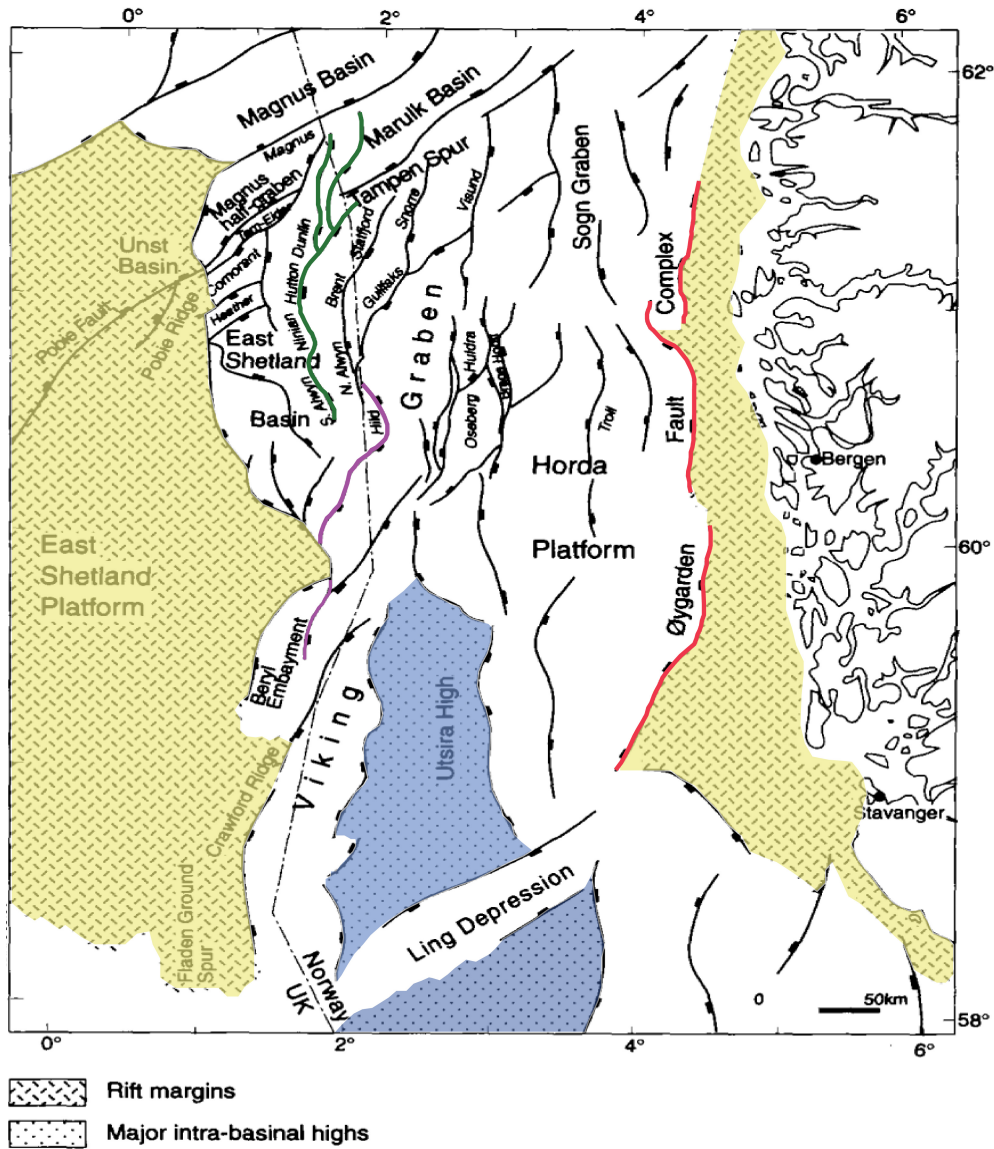


Figure 17: The northern North Sea rift zone after Permo-Triassic and Jurassic extension. The rift margins are marked in yellow, while major intra-basinal highs are marked with blue. Most of the faults are of Permo-Triassic origin. Modified from Færseth (1996)

#### 6.4 Early to Middle Jurassic events

The transition from Triassic to Jurassic coincides with a change from continental to shallow marine depositional environments, due to a transgression accredited to post-rift subsidence following the Permo-Triassic rifting (Faleide et al., 2010). The transgression resulted in shallow water with poor vertical circulation due to the uneven underlying land surfaces, which again led to the accumulation of black shales over large parts of NW Europe. In the northern North Sea fluvial and partly marine sandstone deposits of Lower Jurassic age are important reservoir rocks in the Viking Graben. The most intense subsidence occurred in the areas that experienced the most intense thinning (highest

$\beta$ ). This was naturally along the graben axis of the Permo-Triassic rifting, and consequently where the thickest sequences of post-rift sediments were deposited.

Whereas the Viking Graben continued to subside during the Aalenian and Bajocian times, the axial parts of the Central Graben became thermally uplifted and subjected to erosion. This elevated structure consisted of little consolidated Early Jurassic and Triassic sediments, which were rapidly eroded and deposited towards the north. The mainly recycled Triassic sandstones were deposited in the continuously subsidence basins in major deltaic complexes, such as the Brent Group in the Viking Graben (Ziegler, 1990). The uplift of the Central Graben was accompanied by the development of a major volcanic complex at the triple junction between Viking Graben, Central Graben and the Moray Firth Graben.

## 6.5 Late Jurassic rifting

The second major rifting episode was initiated in the latest Middle Jurassic. According to Badley et al. (1988) it is estimated that the mantle lithosphere had regained about 90% of its original thickness by isothermal adjustment at this point. During this phase, block tilting was associated with the rifting in much higher degree than in the Permo-Triassic phase. Many of the Permo-Triassic faults were reactivated, and only a few new large faults were generated in the Late Jurassic rifting. Additionally, several smaller fault blocks were generated, which represents the main hydrocarbon-trapping style in the northern North Sea (Færseth, 1996). Normal faulting led to the rotation of basement blocks and their overlying sediments, this caused local erosion of Lower-Middle Jurassic and even Upper Triassic strata (Faleide et al., 2010). During the rifting The Heather and Draupne Formations were deposited, the two main source rocks of the northern North Sea. They show the typical wedge-shape with internal layering in the half graben structures.

The onset of rifting was not synchronous throughout the whole area, and it appears that tilting and listric normal faulting did not occur on the Horda Platform until later in the Jurassic. At the rifting onset, the area was at or near-sea level, evident from the fact that the deltaic deposits of the Brent Group are generally the youngest pre-rift sediments.

This extensional phase was more localized than the previous, and mainly concentrated along the axis of the Sogn and Viking Graben. Thus, it is assumed that the margins generally retains its pre-rift thickness (Ramberg et al., 2013b). The East Shetland Platform represents the western boundary for the Jurassic basin, and to the north the East Shetland Basin is located between the platform and the Viking Graben proper. There was a slight change in extension direction from the Permo-Triassic to the Late Jurassic. While the Permo-Triassic rifting followed a N-S trend, the

Jurassic extension had a NW/SE extension.

The period of active rifting lasted throughout the Late Jurassic and ceased more or less synchronous over the area in the Early Cretaceous (Badley et al., 1988). Fig. 18 shows a transect of the northern Viking Graben, showing the distribution of pre-rift, syn-rift and post-rift sediments, respectively.

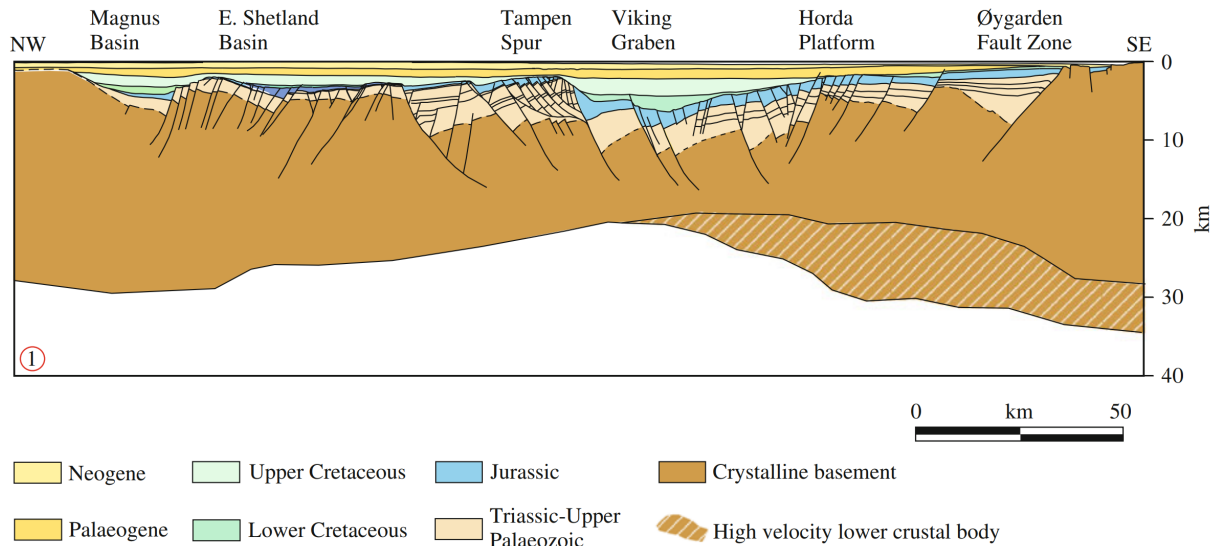


Figure 18: Interpreted deep seismic line and crustal transect depicting broad stratigraphy and structure across the northern Viking Graben. From (Faleide et al., 2010)

## 6.6 Post-rift events

The Late Jurassic rifting was the last phase of major rifting in the Viking Graben. Between the Jurassic and Cretaceous there is a major unconformity due to a major transgression in the Early Cretaceous. This Base Cretaceous Unconformity (BCU) can be found throughout large parts of the northern North Sea. The thermal subsidence, which was accompanied by faulting, resulted in the deposition of thick early Cretaceous sediments. The major structural features inherited from the syn-rift had a major impact on the sediment distribution and basin configuration. The deposition of thick Cretaceous strata continued following the regional subsidence, and the rift basin became gradually drowned by sediments. The sediment supply outpaced or balanced the subsidence and the subsidence pattern were determined by the crustal thinning profile, reliant on the thermal contraction and the isostatic/elastic response to sediment loading (Faleide et al., 2010). The post-rift structure eventually evolved into a saucer-shaped basin that were unaffected by the syn-rift structures. When the basin achieved thermal equilibrium in the early Cenozoic, the subsidence ceased, and the pattern of basin filling became more dependent on extra-basinal processes.

The Viking Graben was influenced by the early Cenozoic rifting and break-up in the NE Atlantic,

by differential vertical movements causing major uplift of the basin margins. The sedimentary architecture are related to tectonic uplift of surrounding clastic source areas. In the Palaeocene, tectonic subsidence accelerated throughout the basin and outpaced sedimentation rates along the basin axis. The subsidence was accommodated by progressive basin-marginward movement of planar normal faulting (Badley et al., 1988). In general, the present day structural basin shape was further generated through regional subsidence.

### 6.7 Pre-Mesozoic influence on the basement of the Viking Graben

A series of large normal faults with predominant N, NE and NW orientations characterize the northern North Sea. The eastern margin of the Viking Graben is dominated by the Øygarden Fault Zone. It originated in the Permo-Triassic and stretches north for over 300 km. It contrasts the western boundary, between the Viking Graben and the East Shetland Platform, which are primarily represented by normal faults of Jurassic origin (Færseth, 1996). In the graben proper there are faults which binds half graben structures with several kilometer throws. The half grabens are the fundamental elements of the rifted area.

The large faults in the northern North Sea are basement-involved, and probably cut the whole brittle upper crust. The general structure of these faults are planar, however, there is generally a change of dip from 25-35° where the faults cut down into the basement to 40-50° at higher levels. Major faults with low-angle or listric geometries occur along the western margin of the Viking Graben. They developed during Jurassic rifting and are particularly related to the eastern Tampen Spur, the Beryl Embayment and the Fladen Ground Spur, i.e. uplifted footwalls flanking asymmetric graben segments.

Figure 19 shows the main fault trends in the North Sea. The main zones that can be recognized in the northern North Sea are the Hardangerfjord Fault Zone, the Nordfjord-Sogn Detachment as well as the Øygården Fault Zone. They all originate from before the Late Jurassic rifting and is believed to exert a control on the development of the Viking Graben. The Hardangerfjord Shear Zone is assumed to be a Proterozoic shear zone, reactivated during Devonian extension. The Nordfjord-Sogn Detachment is a major extensional shear zone up to 6 km thick. It is similar to those seen in the Basin and Range that are the basis of the Wernicke model. The detachment formed towards the end of the Caledonian orogeny and cross-cuts the Caledonian nappes. It was mainly active during the Devonian, but was reactivated during Triassic and may have influenced the development of fault structures in the North Sea rift basin (Norton, 1987). The Øygarden Fault Zone occur immediately offshore west coast of Norway and reflect the presence of a deep, basement-involved zone of weakness. The orientation of this extensive N-S structure is discordant with the

Caledonian grain typical of mainland Norway. It marks a sharp thickness change from onshore Norway to the Horda Platform. It is believed to represent a site of a linear N-S discontinuity representing a Precambrian Zone of crustal weakness that exerted the main structural control during the Permo-Triassic rifting (Færseth et al., 1995).

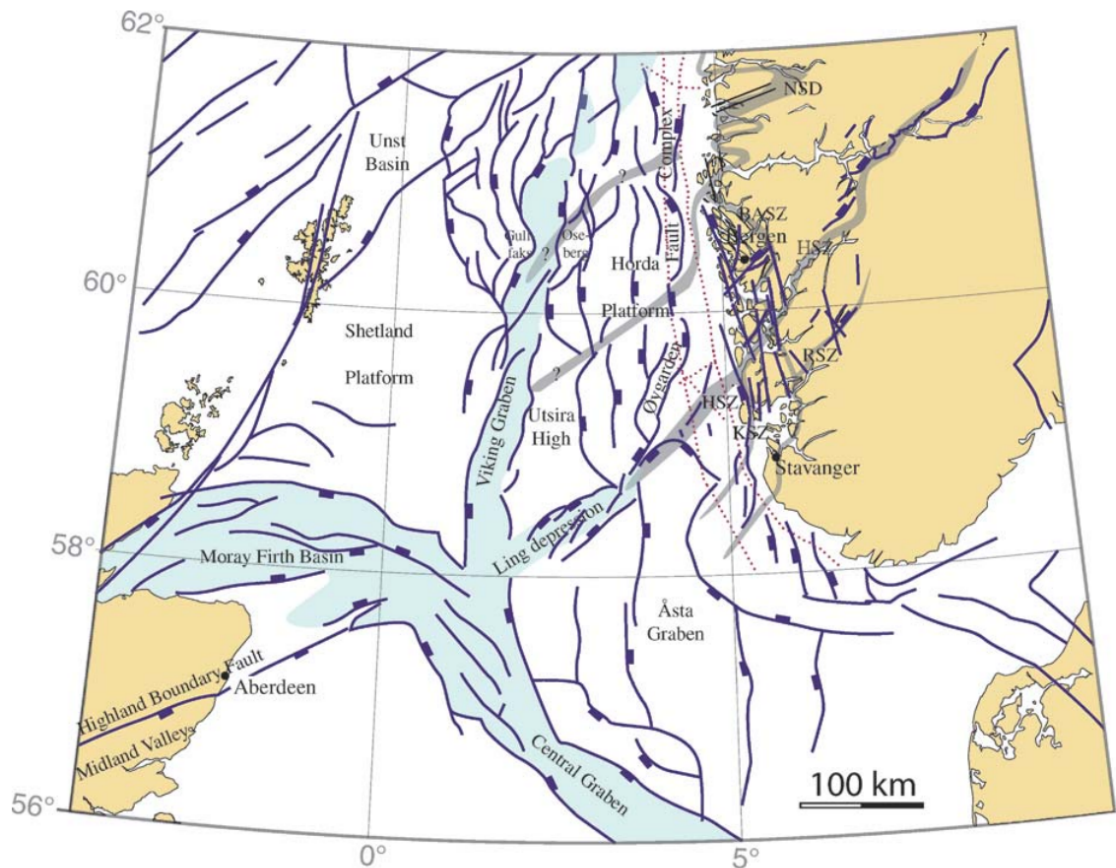


Figure 19: Map showing the main fault trends and the location of shear zones (HFZ = Hardangerfjord Shear Zone; BASZ = Bergen Arcs Shear Zone; NSD = Nordfjord-Sogn Detachment; KSZ = Karmøy Shear Zone; RSZ = Røldal Shear Zone). From Fossen and Hurich (2005)

## 7 Stratigraphic framework

The factpages of the Norwegian Petroleum Directorate (NPD) provides an extensive rundown of the stratigraphy of the Norwegian continental shelf. This chapter is intended as an overview of the most important groups and formations, making up the sedimentological structure of the Viking Graben. Note that not all formations described in this chapter are interpreted in the results of Chapter 10. Figure 20 show the deposits in the northern Viking Graben from Triassic through Eocene age. The Triassic deposits are generally the lowermost deposits above the basement and the deepest sediments found in the seismic, thus a natural starting place in this overview.

### 7.1 Triassic deposits

During the Triassic with its major N-S rifting, thick and coarse fluvial sediments was deposited along the rift margins. Towards the basin center it grades into finer-grained river and lake deposits. The lithography is mainly intervals of interbedded sandstone, reddish claystones and mudstones and shales. The grain size varies from very fine to very coarse. In the Viking Graben, the main stratigraphic group is the Hegre Group. More than 2 km of Triassic sediments have been found in the east, where the group is thickest. There is also significantly thick Triassic deposits on the East Shetland Platform. In the northernmost part of the North Sea, the group thins towards the west. The transition to the

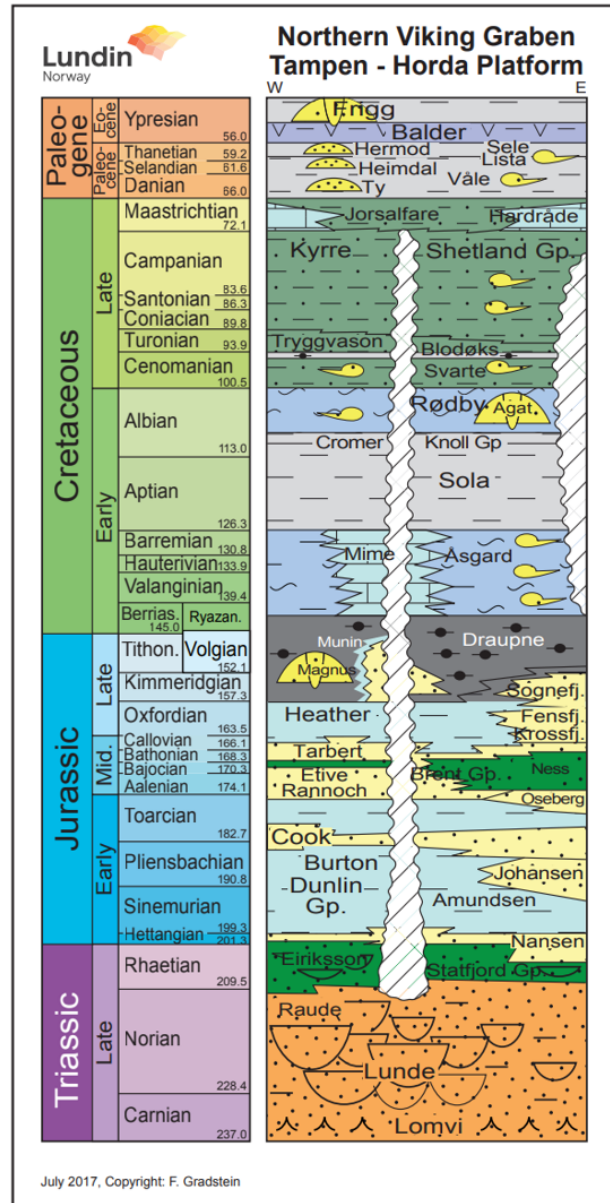


Figure 20: Lithostratigraphic chart, showing many of the formations and groups of the northern Viking Graben. From Lundin

Jurassic is marked by a widespread marine transgression for north and south (Halland et al., 2011).

## 7.2 Jurassic deposits

Whereas the Triassic sediments were deposited in a continental environment, the Lower Jurassic sediments were mainly deposited in a shallow marine setting. Due to a warm and humid climate during the early Jurassic, larger amounts of older sediments and bedrock on land, were eroded. Huge amounts of gravel, sand and mud was transported out to the sediment basins on the shelf, leading to the lower and middle Jurassic consisting of primarily marine sandstone and mudstone. There was a widespread transgression that drowned large parts of northwestern Europe and accumulated black shales.

### 7.2.1 Statfjord Group

The Statfjord Group is overlapping from Triassic to Jurassic deposits, and it exhibits the continental to shallow marine transition, consisting of shale, interbedded with thin siltstones, sandstones and limestones. Above, there are massive sandstone bodies, interbedded with shales, overlain by thick sandstones. It is thickest in the central part of the Viking Graben.

### 7.2.2 Dunlin Group

The Statfjord Group is succeeded by the Dunlin Group, which consists mainly of dark marine sediments. At the margins of the basin there are well developed white to light grey, very fine to medium grained marine sandstones that extend into the basin. Although the Dunlin Group is primarily made up of dark marine shales, it is normally without enough organic content to become a significant source rock. As with the Statfjord Group, the Dunlin Group is thickest in the Viking Graben, east of the Statfjord and Brent fields. It is more widespread than the Statfjord Group and can be recognized over the East Shetland Basin and the Horda Platform.

### 7.2.3 Brent Group

Overlying the Dunlin Group is the important Brent Group, named by its formations: Broom, Rannoch, Etive, Næss and Tarbert. The group was deposited in the Middle Jurassic as a delta sequence and consists of grey to brown sandstones, siltstones and shales with subordinate coal beds and conglomerates. The Brent delta covered the whole northern North Sea basin and created the



most important reservoir rock in the North Sea. The Brent delta was drowned at the onset of the rifting period that would take place in the Late Jurassic (Ramberg et al., 2013b).

#### **7.2.4 Viking Group**

The Upper Jurassic sediments were deposited during the rifting, making them syn-rift deposits. The Brent Group is overlain by the Viking Group, named after the Viking Graben, where it was mainly deposited. The Viking Group is often represented at a basal level by the widely distributed Heather formation shales. The deposition of the Heather formation occurred during the Late-Jurassic transgression. It was deposited in an open marine environment that developed due to this transgression. The Draupne Formation consists of dark brown to black shales and was deposited in a restricted, deep marine environment. It is commonly the uppermost formation of the Jurassic deposits of the northern North Sea

The three final formations of the Viking Group are more restricted and less important for the northern North Sea petroleum system and is the Krossfjord, Fensfjord and Sognefjord formations. They are all coastal to shallow marine sands that interfinger the Heather formation, mainly on the Horda Platform, as they developed as a response to eustatic sea-level changes or basin-wide changes in sediment supply.

### **7.3 Cretaceous deposits**

The upper boundary of the Viking Group is an unconformity, normally overlain by higher velocity and lower radioactivity Cretaceous sediments. In the Cretaceous the main depository environment changed from a restricted, shallow marine to more open marine conditions.

#### **7.3.1 Cromer Knoll Group**

The group overlying the Cretaceous unconformity is the Cromer Knoll Group, consisting mainly of fine-grained marine sediments with varying content of calcareous sediments. In the half-graben structures of the Viking Graben it is often more than 600m, gradually thinning towards the basin margins. The group thickens towards the north to the Sogn Graben, where it is at its thickest.

#### **7.3.2 Shetland Group**

Above the Cromer Knoll Group we find the thick Shetland Group. In the North Sea, it is normally between 1000 and 2000 m, thinning towards the basin margins. It consists of marine sediments,

mainly claystones, siltstones and marlstones with varying content of calcareous material. The group is present throughout most of the North Sea, absent only on local highs and a few salt diapirs.

## **7.4 Cenozoic deposits**

The Cenozoic deposits are influenced by the post-rift thermal subsidence which caused basin-wide sediment-draping of the rift-systems.

### **7.4.1 Rogaland Group**

The lowest group of the Cenozoic in the northern North Sea is the Rogaland Group. The lithology is varying with sandstones interbedded with shales in the west, that pass laterally into shales eastwards. Towards the top of the group the content of tuff in the shales increase. The group thins towards east and is commonly a few hundred meters in the North Sea. The upper boundary is marked by a change from tuffaceous laminated shales to more irregularly bedded sediments of the Hordaland Group.

### **7.4.2 Hordaland Group**

The Hordaland Group reaches only a few hundred meters in the northern Viking Graben, but has an average thickness of around 1100-1200 m in the Central Graben and the southern Viking Graben. The thickness also decreases towards the basin margins. It consists of deep marine claystones with minor sandstones, mainly deposited in deep water. The upper boundary is placed at the contact with claystones of the Nordland Group or sandstones of the Utsira Formation. A boundary with the Utsira Formation is normal in the Viking Graben.

### **7.4.3 Nordland Group**

Overlying the Hordaland is the final group, the Nordland Group. In the Viking Graben area its thickness is approximately 1000 m. The dominating lithology is marine claystones, however the sandy Utsira Formation occurs in the lower part of the group in the Viking Graben area and is commonly a few hundred meter thick. The upper boundary of the Nordland Group is the sea bed.

## 8 The Petroleum System of the Northern North Sea

There are essentially 5 things needed to have a functional petroleum system. (i) A source rock where hydrocarbons can be produced under the appropriate conditions, (ii) a reservoir rock where the hydrocarbons can be stored, (iii) a migrational pathway from the source rock to the reservoir rock, (iv) a seal that hinder the hydrocarbons from flowing through the reservoir rock and into the overburden and (v) a trap that laterally enclose the hydrocarbons.

### 8.1 Source rocks

Hydrocarbon source rocks are rocks capable of generating and expelling significant amounts of oil or gas. They contain quantities of organic material, that will be buried, which causes pressure and consequently temperature to increase. This will cause the source rock to be matured and generate oil, gas or both.

In the north Viking Graben, Upper Jurassic marine shales, deposited during the major rifting stage, are the main hydrocarbon source (Barnard and Bastow, 1991). The Draupne and Heather Fm. have been identified as the primary source rocks, but there are other sources, such as the coals of the Brent Group and Statfjord Fm., as well as shales of the Dunlin Group, however, their source potential and volume is geographically restricted and minor compared to the Upper Jurassic sources.

#### 8.1.1 The Heather Fm.

The Heather Formation is Bathonian to latest Oxfordian of age. This marine mudstone covered much of the northern North Sea and in the graben areas attains a thickness of up to 1000 meters. It consists mainly of fine-grained grey silty mudstone with thin streaks of limestone and localized bodies of sandstone. Although it is commonly perceived as representing shelf facies, it also includes mass-flow sandstone of slope or basin association (Johnson et al., 2005).

#### 8.1.2 The Draupne Fm.

The Draupne Formation formed a several hundred meters thick rich source rock which is the prime source rock in the North Sea (Faleide et al., 2010). It was deposited in a marine environment with restricted bottom circulation and often with anaerobic conditions. The formation consists of moderately to highly organic-rich, marine mudstone with local bodies of mass-flow sandstone. The main characteristic of the Draupne Formation is its very high radioactivity (often more than

100 API units), indicating its high content of organic carbon. The average value of total organic carbon of the Draupne Formation are generally between 5% and 10% (Johnson et al., 2005). It has anomalously low velocity, density and high resistivity, making it easy to recognize on well logs. It was deposited as the rifting intensity reached its maximum during the Late Jurassic to Early Cretaceous and ranging from Oxfordian to Ryazanian in age. It can also be found in the East Shetland Basin and over the Horda Platform and accumulated widely throughout the rift basins, locally exceeding 3000 meters in sediment thickness (Gautier, 2005).

## 8.2 Reservoir rocks

The most prominent group of reservoir rocks of the northern North Sea is the deltaic Brent Group of the Middle Jurassic. The initial porosity is believed to have been 35% to 50%, but have been reduced through compaction and cementation during burial (Johnson et al., 2005). The Brent Group is stratigraphically underlying the Late Jurassic source rocks, but through displacement by faulting, it is locally positioned above the source rocks, thus making the migration of hydrocarbons from source to reservoir possible. Other prominent reservoir rocks include Triassic rocks, Late Jurassic syn-depositional submarine fan complexes and submarine fan and channel sandstones of Paleogene age.

## 8.3 Traps and seals

The Viking Graben is generally blanketed by fine-grained marine mudstones of Tertiary age that deeply bury most traps and provide an effective regional seal. The majority of hydrocarbon traps of the Early and Middle Jurassic are formed by tilted fault blocks, where the traps vary considerably in both size and complexity. The structure of the trapping faults are determined by the Late Jurassic rifting. There are also post-rift traps present, such as structural traps of the Paleogene age, trapping hydrocarbons sourcing from syn-rift deposits of the Late Jurassic.

## 9 Methods

### 9.1 Seismic data

In this thesis, regional seismic in the northern North Sea has been interpreted with the purpose of obtaining a depiction of the Viking Graben, and its basin-controlling structures. The seismic lines interpreted are shown in map view in Fig. 26 and cover much of the Viking Graben and its eastern margin. The (close to) vertical line in the map represents the boarder between the Norwegian and British marine territories. The horizontal line in the north represents the boarder between the North Sea and the Norwegian Sea.

The interpreted data are seismic 2D lines from the data-sets: NVGTI-92, NVGTI-2-92, NVGTI-3-92 and SG8043-REP91. Together, the data-sets cover most of the northern North Sea. The interpreted lines were chosen as they were believed to give the best information about the Viking Graben. Most of the interpreted lines are crossing the graben axis, while 3 follow the axis and cross the other lines more or less orthogonally. Some lines are chosen to support or confirm the interpretation of other lines, or to better describe specific structures. All the lines reach a depth of approximately 7s TWT. No time to depth conversion has been performed, all lines have been interpreted in the time domain. To obtain the correct age and formation name, and thus, lithology, well-to-seismic ties have been performed when deemed necessary.

For the interpretation, the Schlumberger Petrel Software has been used. Petrel is very commonly used in the petroleum industry as a tool for handling seismic data interpretation. The tools used were primarily the "Seeded 2D autotracking" option on horizons that showed good continuity and quality. It will track the chosen horizon until it comes to a discontinuity and no longer fulfil the constraints of the autotracking parameters. Also, "Guided autotracking" and "Manual interpretation" were used on horizons of lesser quality and continuity.

The high-resolution drawing program Adobe Illustrator CS6 has been used to create many of the figures presented, by modifying and editing the interpretations made with Petrel.

### 9.2 Seismic resolution and quality of data

Seismic reflections are generated as a response to density and velocity changes in the subsurface. These changes happen at unconformities and at bedding surfaces that separate rocks of different physical properties, lithology, textures and structural behavior.

The resolution of seismic data controls the level of details visible on the seismic records. The

vertical resolution is limited to  $\lambda/4$ , where  $\lambda$  is the seismic wavelength. If a bed within a medium of different properties has a thickness of  $\lambda/4$ , the bottom and top of the bed will be displayed as one strong reflection. This means that the recorded seismic event might represent the average of several thin bedding surfaces phased together. A bed thickness less than the seismic wavelength can result in very large amplitudes, while thick beds can have small amplitudes due to the top and base of the reflections being completely separated (Boggs, 2010). The resolution will also be poorer with increasing depth due to a decrease in the frequency as the velocity and wavelength increases. The increased compression of the rocks at depth will increase the velocity.

The horizontal resolution is controlled by the Fresnel Zone, which is the part of a reflector, which the seismic signal covers at a certain depth. The radius of the Fresnel Zone will increase with depth, increased velocity and lower frequency, which again will decrease the horizontal resolution.

It is important as a geophysicist to be able to distinguish between good and bad data. With a bad data set it is possible to interpret features that is related to noise as real geological features. The data used in this thesis is of generally good quality. The 2D-lines from the NVGTI data-sets are better than those from the SG8043 (compare for example Fig. 31 and 41). This is acceptable, because it is the NVGTI-lines that have mainly been used in the interpretation. Another point is that the quality is generally decreasing below the interpreted Top Triassic horizon. The quality of the data post-Jurassic is good.

### 9.3 Polarity

The determination of polarity must be resolved before interpreting seismic reflections. There are currently two international standards of polarity of seismic data, the American and the European standard. The American gives positive amplitudes (peaks) when there is an increase in impedance, this is commonly displayed with a red color. The European standard is that an increase in impedance leads to negative amplitudes (troughs), commonly displayed as a blue horizon (Simm and White, 2002). The determination of polarity can be resolved by analyzing the seismic data, more specifically, the transition from seawater to the sea-bottom.

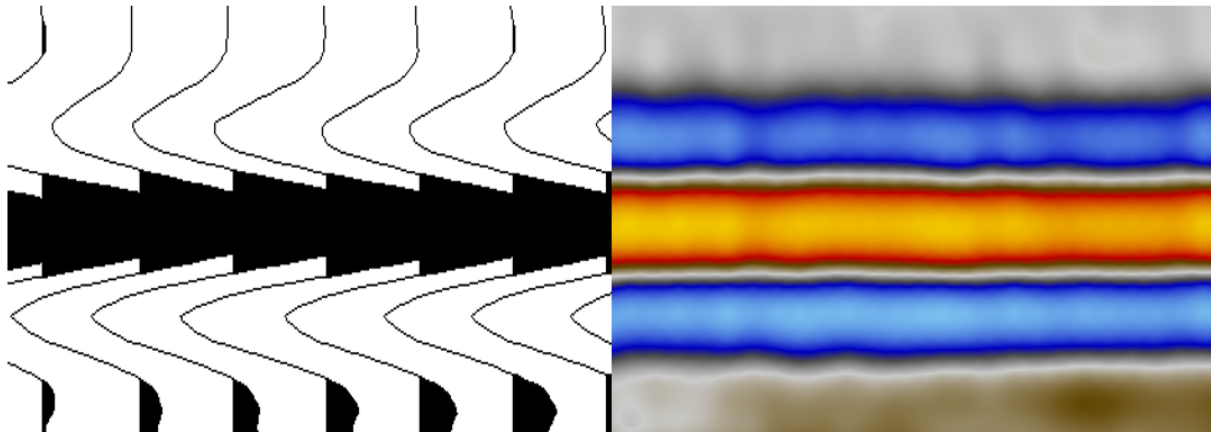


Figure 21: Sea-bottom reflection from SG8043-101A. Left - wiggle trace; right - color display (bitmap). The positive amplitudes in the wiggle trace is displayed with red intensity in the color display, while the negative amplitudes are displayed with blue.

From Fig. 21 it is clear that increasing acoustic impedance results in a positive amplitude (red), and the two blue, negative amplitudes are interpreted as sidelobes. The positive is interpreted as the sea-bottom, and concluding that the data set has American polarity which is important to know when choosing which reflections to interpret.

#### 9.4 Well data and seismic-well tie

Information extracted from wells are very important when interpreting seismic data as wells contain important geological information. The seismic data is solely in the time domain, while well data is measured in units of depth. It is therefore necessary to correlate them. This is done through seismic-to-well tie, that establish a time-depth relationship. The seismic well-tie was performed by generating a synthetic seismogram (Fig. 23), by correlating sonic and density logs together with borehole seismic data, called check-shot data. The synthetic seismogram is then compared with the seismic data surrounding the well location. Bad logs can cause mistakes in calculations which will affect the time-depth relationship.

The first step after uploading the logs and checkshot data is the *sonic calibration*. In this step, the seismic times from the checkshot and integrated sonic times for the chosen well is matched (Fig. 22).

Following the sonic calibration, a synthetic seismogram can be generated. The purpose is to create the connection between geological and geophysical information, with the purpose of tying geological markers to seismic horizons and generate accurate time-depth relationships. In this step it is useful

to perform a synthetic seismogram shift, where the original synthetic seismogram is shifted in the time domain, in order to get a good fit with the seismic.

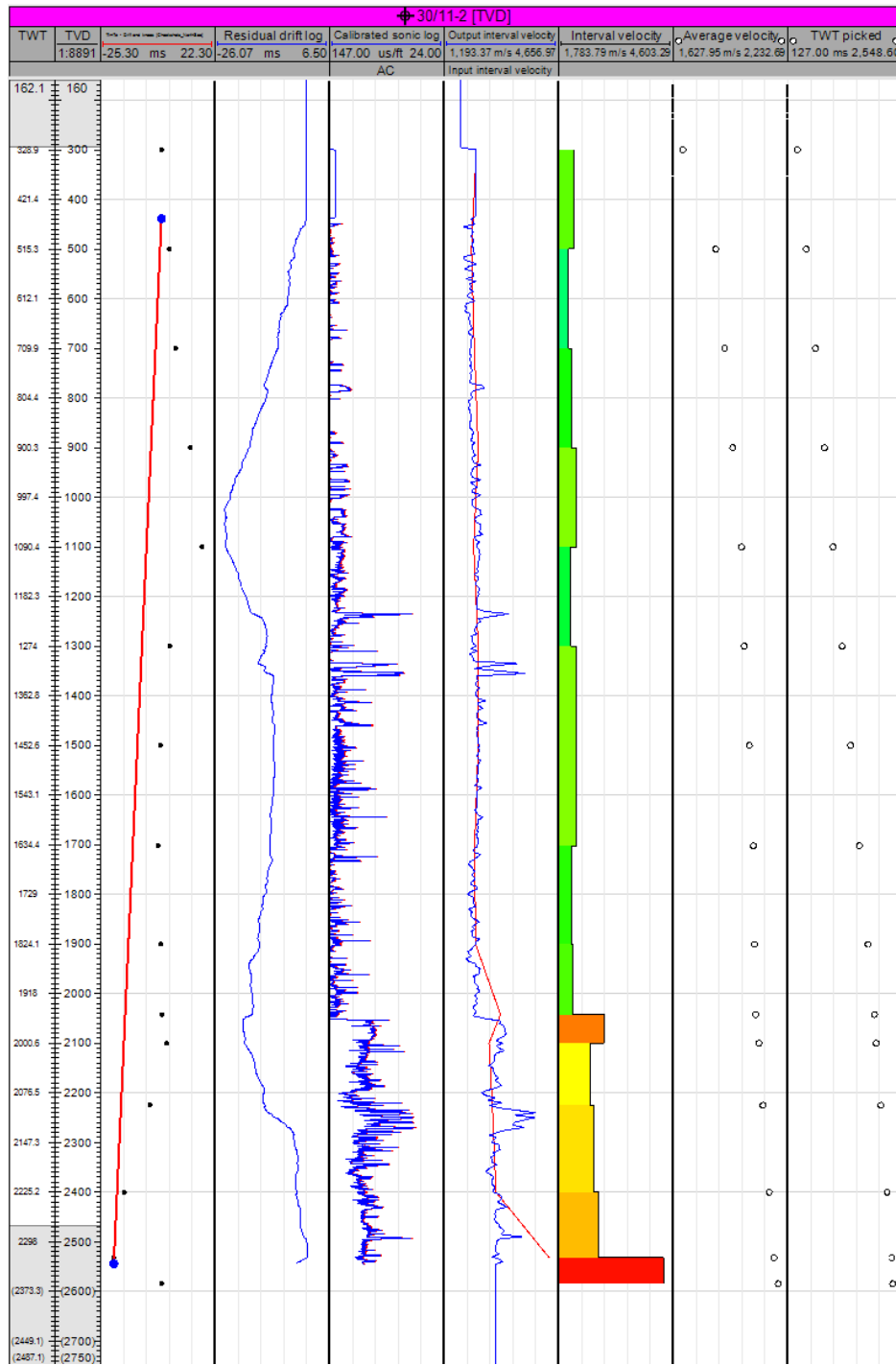


Figure 22: Sonic calibration window of well 30/11-2

In Fig. 23 well 30/11-2 is correlated with the seismic line NVGTI-2-92-210. The synthetic is seen in the position of the well with the seismic from the line on both sides. It has been slightly shifted to make the synthetic fit with the seismic.



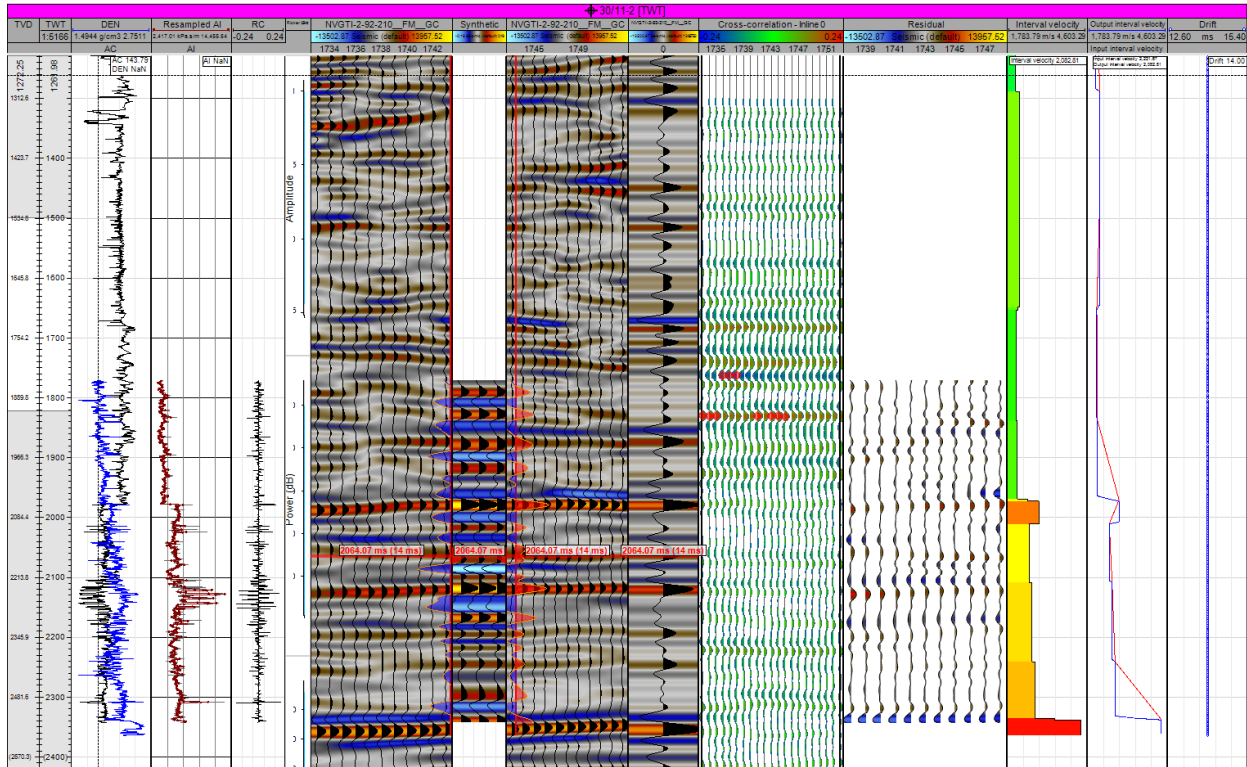


Figure 23: Synthetic generation window of well 30/11-2

### 9.5 Seismic analysis

Seismic facies are mappable, three dimensional seismic units composed of groups of reflections whose parameters differ from those of adjacent facies units (Mitchum et al., 1977). Seismic facies can be analysed based on configuration, continuity, amplitude, frequency and interval velocity. The seismic reflection configurations can provide information on depositional processes and stratification. The continuity of reflectors are commonly dependent on the lateral extension of the deposits. The amplitude is related to the acoustic impedance contrast and can give information about the sediment type. The frequency can give information about the bed thickness and fluid content. Finally, the interval velocity can give lithofacies estimations, porosity estimations and information about fluid content.

Fig. 24 displays some reflection configuration patterns. They are all commonly interpreted as representing uniquely different events and lithology. Such as reflection free is commonly interpreted to be salt or igneous rock, parallel as deposits with a uniform rate of deposition and divergent configuration as deposits with laterally varying deposition rate or surface tilting during deposition. Knowing how to make these connections are important when interpreting seismic facies for the evolutionary history of a basin.

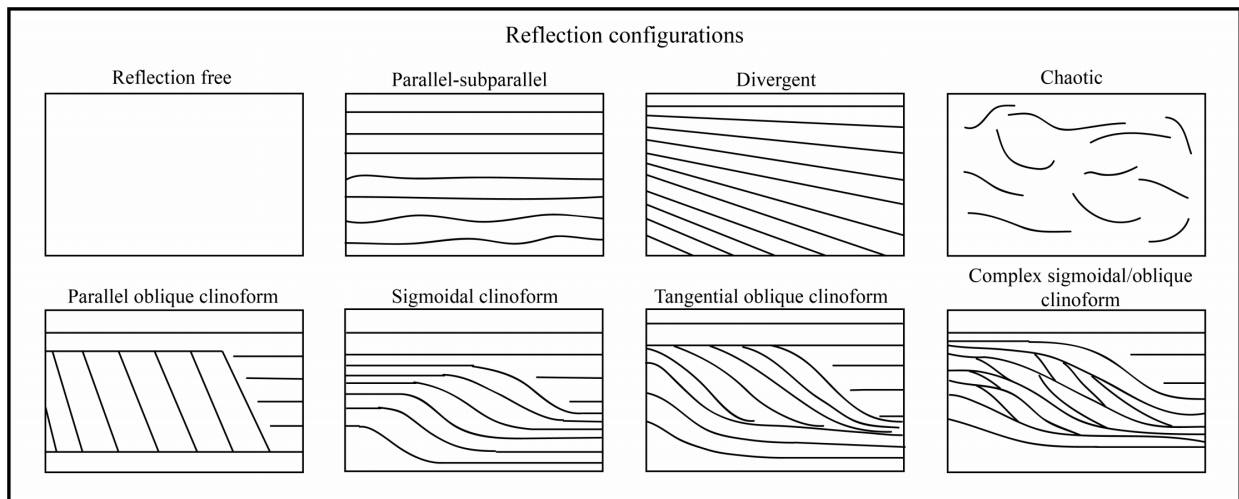


Figure 24: Seismic reflection configurations

In the analysis, the seismic facies has been separated by surfaces corresponding to tops of formations or groups. These surfaces represent time lines and are chosen based on amplitude, continuity, internal facies characteristics and reflection termination patterns. Reflection termination patterns include onlap, toplap, offlap, downlap and erosional truncation (Fig. 25).

**Onlap** is the base-discordant relation in which initially horizontal strata terminate progressively against an originally inclined surface, or in which initially inclined strata terminate progressively updip against a surface of greater inclination.

**Downlap** is a base-discordant relation in which initially inclined strata terminate downdip against an initially horizontal or inclined surface.

**Offlap** is a term used for reflection patterns generated from strata prograding into the deep water and terminating in the deeper basin.

**Toplap** is the termination of strata against an overlying surface mainly as a result of non-deposition with perhaps only minor erosion.

**Truncation** means the termination of strata along an unconformity surface due to post-depositional erosional or structural effects

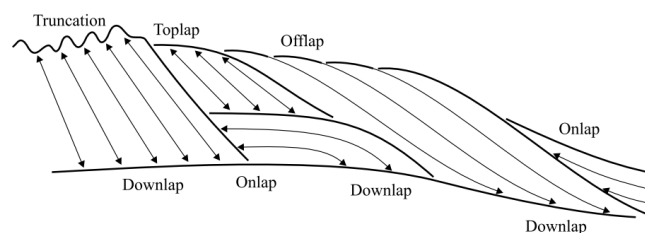


Figure 25: Different types of geological boundaries defining seismic sequences. From Catuneanu (2002)

## 10 Results

In this chapter, all the interpreted 2D lines will be presented. In some lines, individual horizons have been excluded, when they could not be interpreted with confidence or were of significant importance. The Tertiary and Cretaceous units are relatively well defined, but the pre-Cretaceous units are more equivocal. The results are used to understand the basin architecture, with the aim of discussing it in the context lithospheric stretching models. The line numerations are referring to the map in Fig. 26, and the colors of the horizons are explained in table 1. All lines are from east to west (or south to north) in map view.

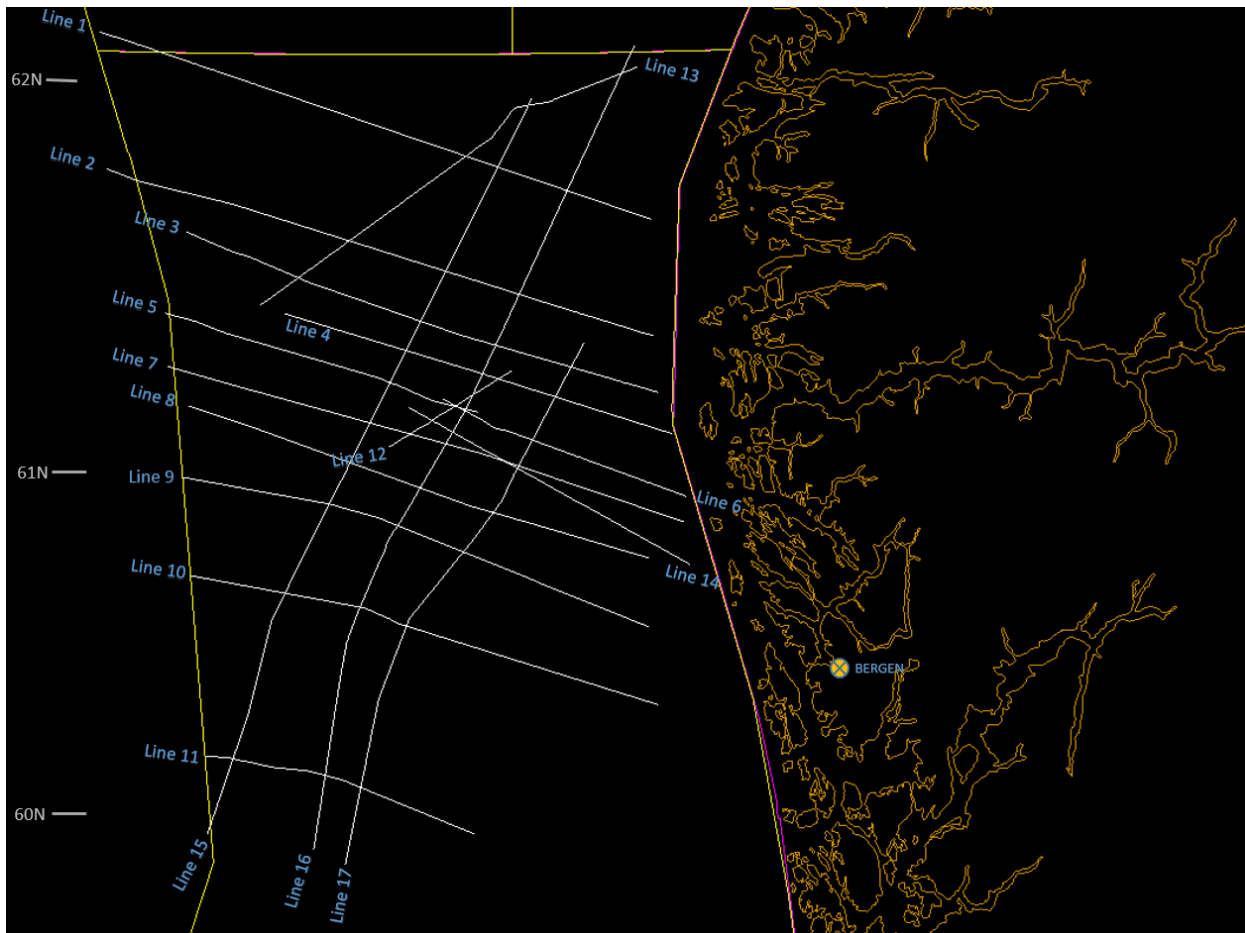


Figure 26: Map showing the interpreted lines used in this thesis. Most of the lines were interpreted to construct an overview of the architecture involving the Viking Graben, while some were interpreted with the purpose of describing specific structures or increase the confidence in the picked horizons

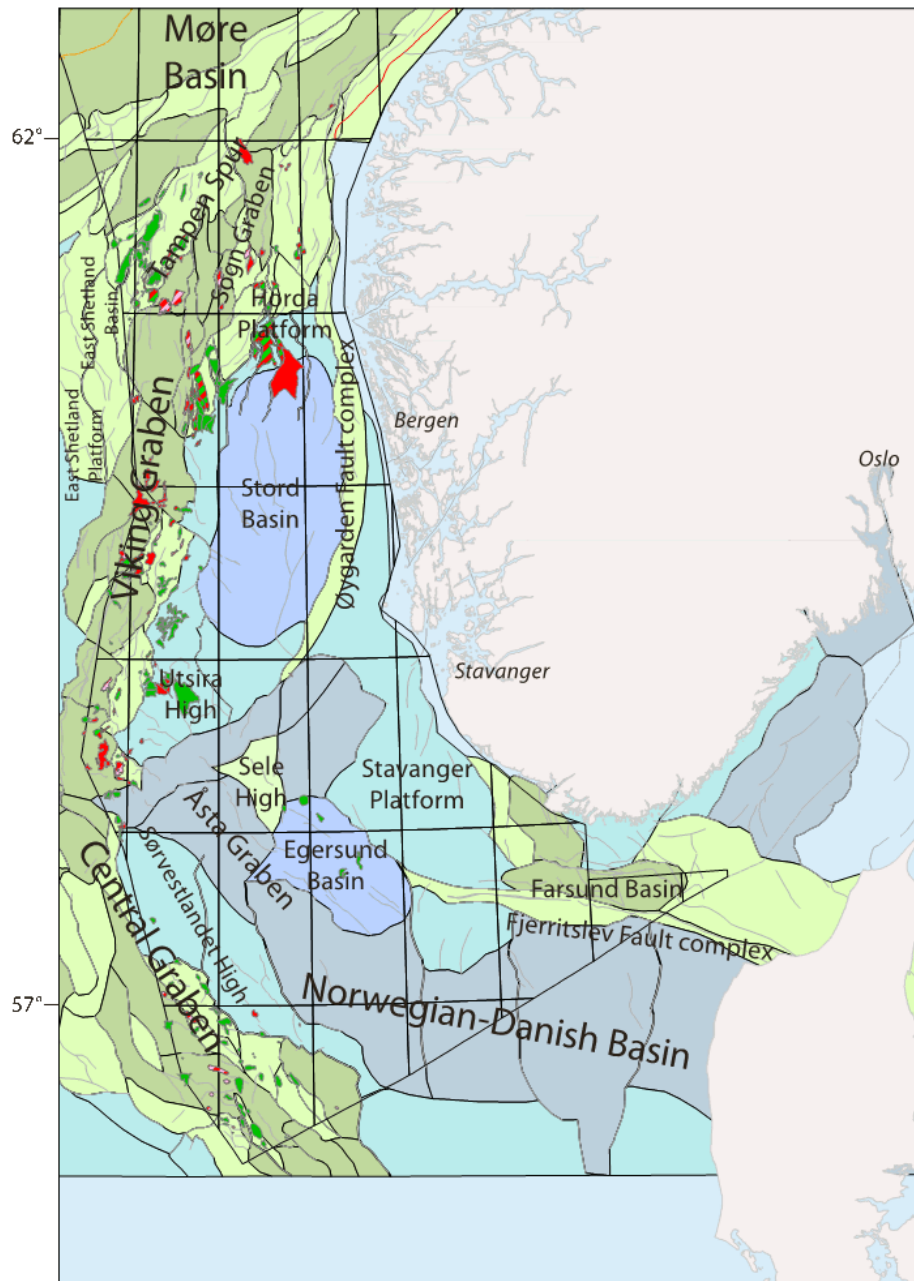


Figure 27: Structural elements in the North Sea with major oil- and gas fields. (Halland et al., 2011)

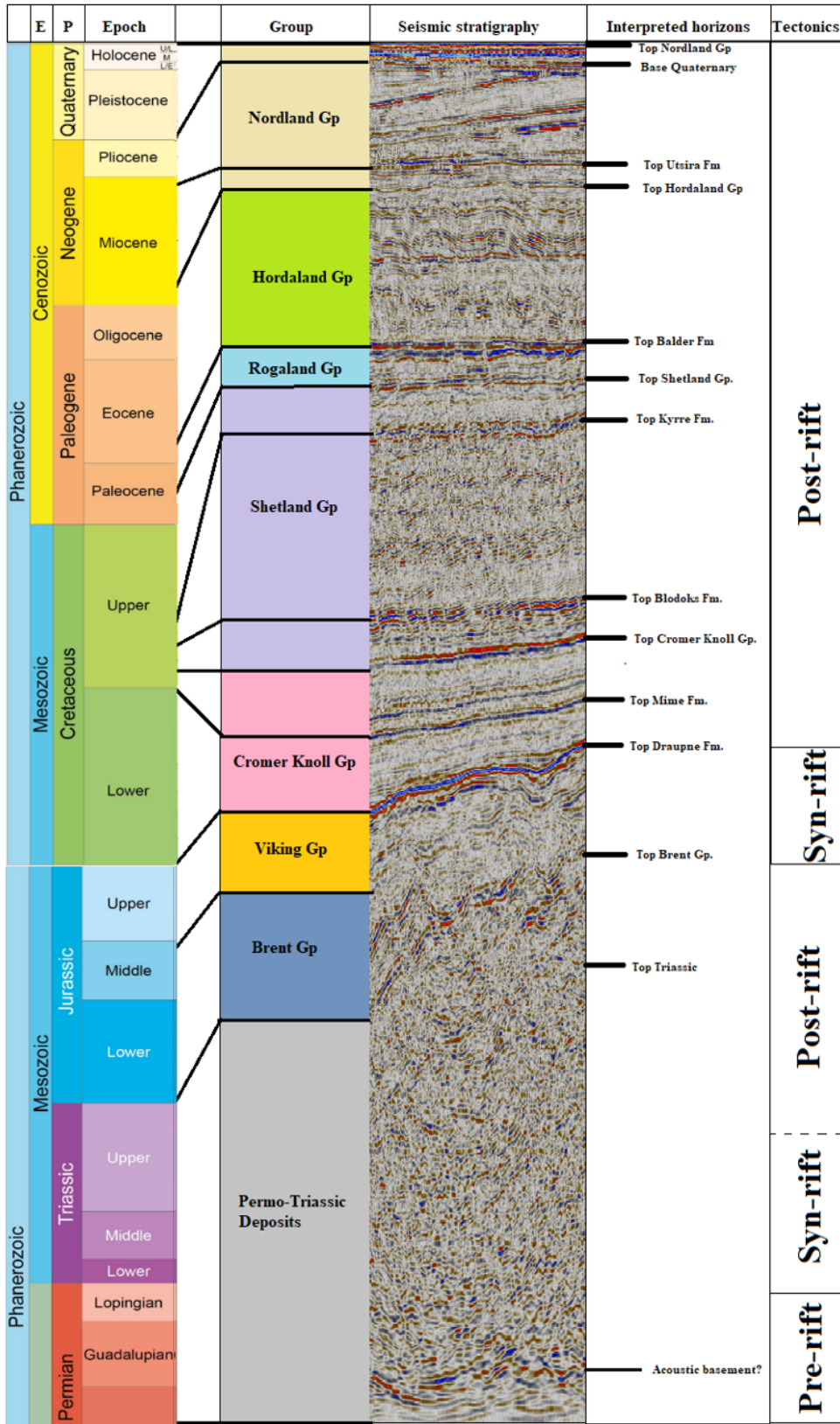


Figure 28: Stratigraphic column for a section of the Viking Graben, showing most the interpreted groups and formations, including the age and tectonic setting of the deposits. E = Era, P = Period. See Fig. 31 for location

Color legend		
Color	Name of Formation/Group	Notes
Black	Top Nordland Group	Coincides with the seabed
Blue	Base Quaternary Unconformity	
Purple	Top Utsira Formation	Miocene deposits of the Nordland Group
White	Top Hordaland Group	Often demanding to interpret
Cyan	Top Balder Formation	
Light Green	Top Shetland Group	
Green	Top Kyrre Formation	
Light Blue	Top Blodøks Formation	Combined with the Tryggvason Formation
Orange	Top Cromer Knoll Group	
Red	Top Mime Formation	Not included in all lines
Magenta	Top Draupne Formation	Represents the Base Cretaceous Unconformity
Dark Blue	Top Brent Group	Latest pre-rift deposits
Yellow	Top Triassic	Pre-rift and syn rift deposits
Dark Green	Basement	Included when it can be positively determined with the help of basement-penetrating wells

Table 1: Table showing color legend of horizons interpreted

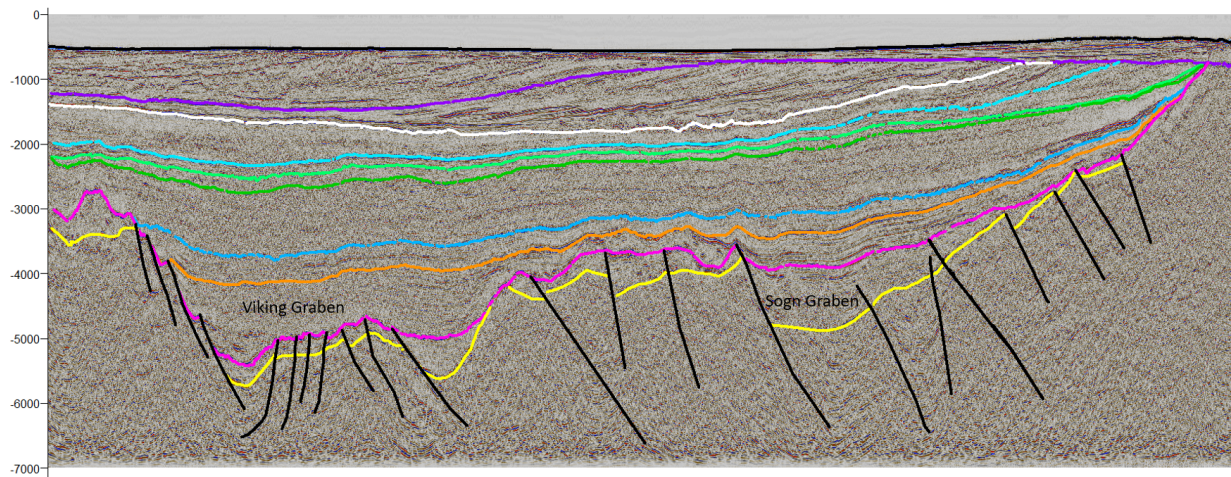


Figure 29: Line 1, NVGTI92-109

Line 1 is the northernmost interpreted line, located in the very north of the North Sea. There are two deeper areas, separated by a high, coinciding with the southern end of the Sogn Graben and the northern end of the Viking Graben. The western side contains 4 faults with major detachments. The faults are generally very steep, with some variations in polarity. There is only one well drilled through it, found on the western end.

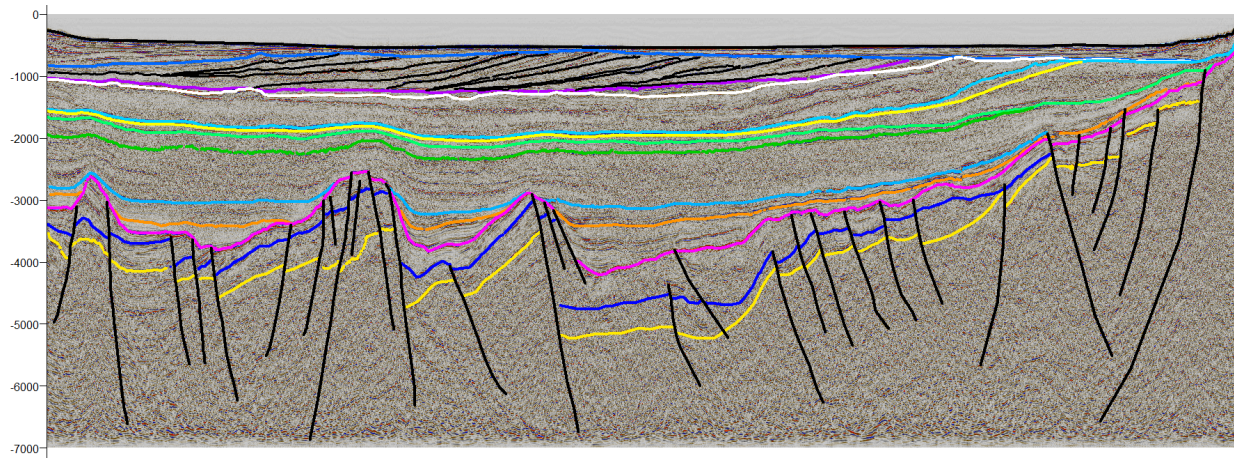


Figure 30: Line 2, NVGTI92-106

Line 2 shows a section consisting of several structural lows. The direction of the faults change often and the thickness of the sediments increase towards the middle of the basins. Note that the yellow line representing the Sele Formation below Top Balder Formation is only interpreted for this line. There are wells both on the eastern and western side of the line. This line is the basis for model 1 (Fig. 46)

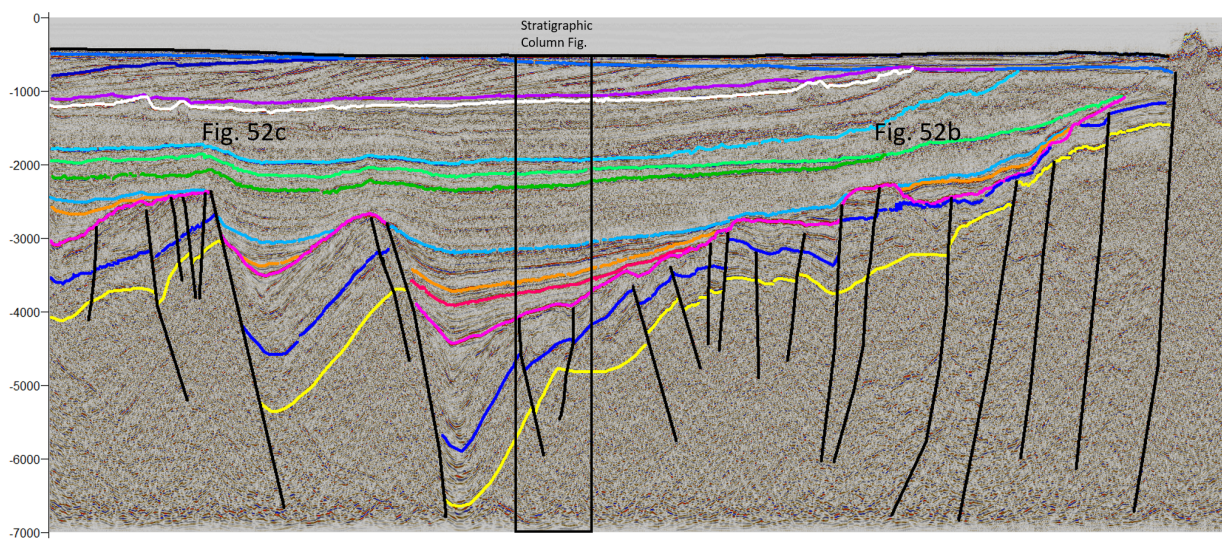


Figure 31: Line 3, NVGTI92-105

Line 3 is a line with large offsets of the syn and pre-rift deposits. There are two considerable faults on the western side. The sedimentary thicknesses are thinning on the highs and towards the eastern margin which is characterized by several deep faults. There are multiple wells intersecting this line.

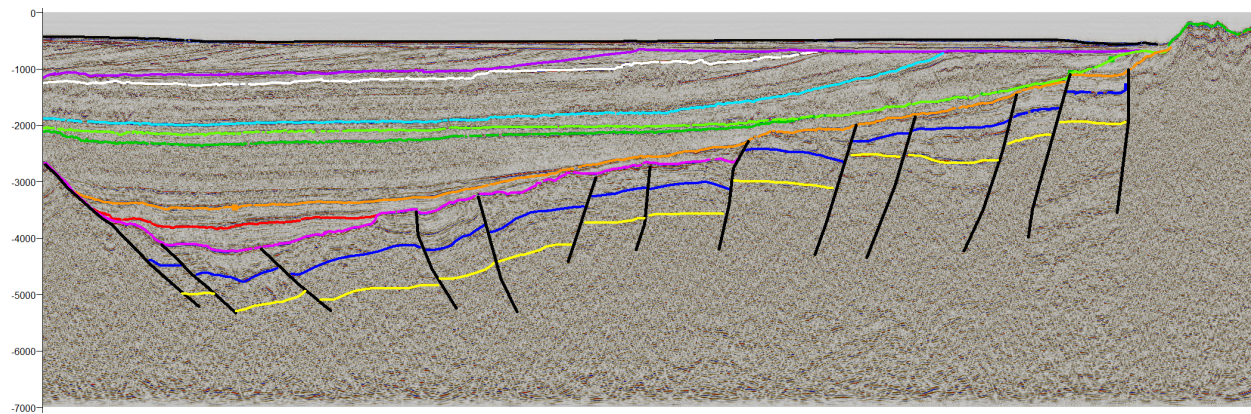


Figure 32: Line 4, NVGTI92-104

Line 4 does not reach as far west as the previously described lines. A large fault is cut off at the western side, and the sediments thicken towards this fault. The fault pattern is generally symmetric, dipping towards the east on the western part, and towards west on the eastern part. Basement is interpreted to reach the surface on the eastern margin. The line is intersected by three wells.

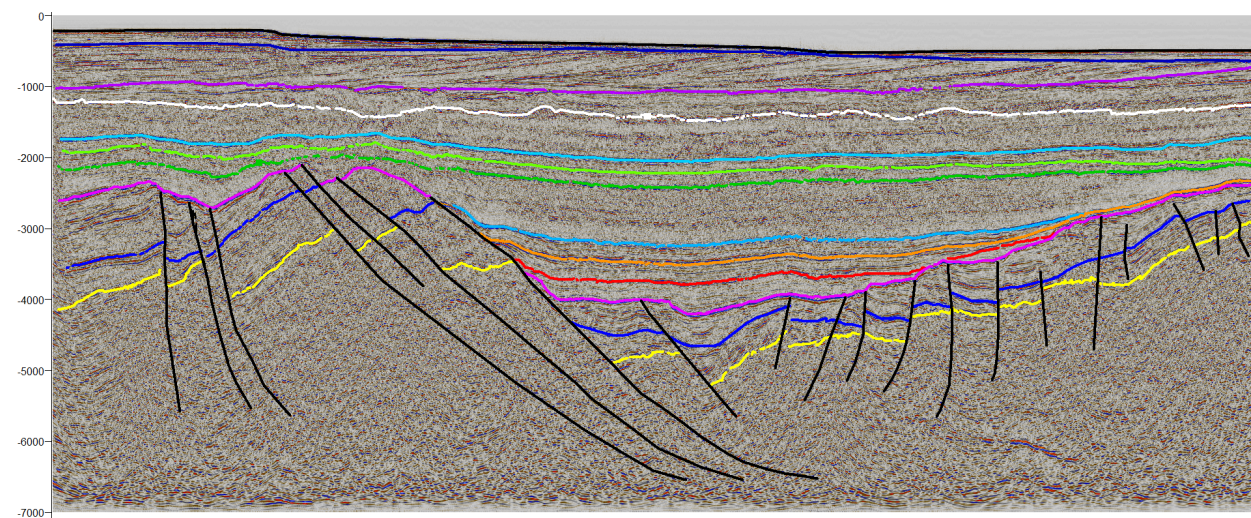


Figure 33: Line 5, NVGTI92-102

Line 5 runs across the Statfjord, Tordis and Gimle fields. The western side of the line consists of steep east-ward dipping faults, with large offsets towards the graben axis. In the deepest part of the basin there is a change in polarity of the faults through a full-graben, and from this on, the faults are dipping in a westerly direction, with significantly lesser throw. The line is only intersected by one well, but there are a significant number of wells nearby.



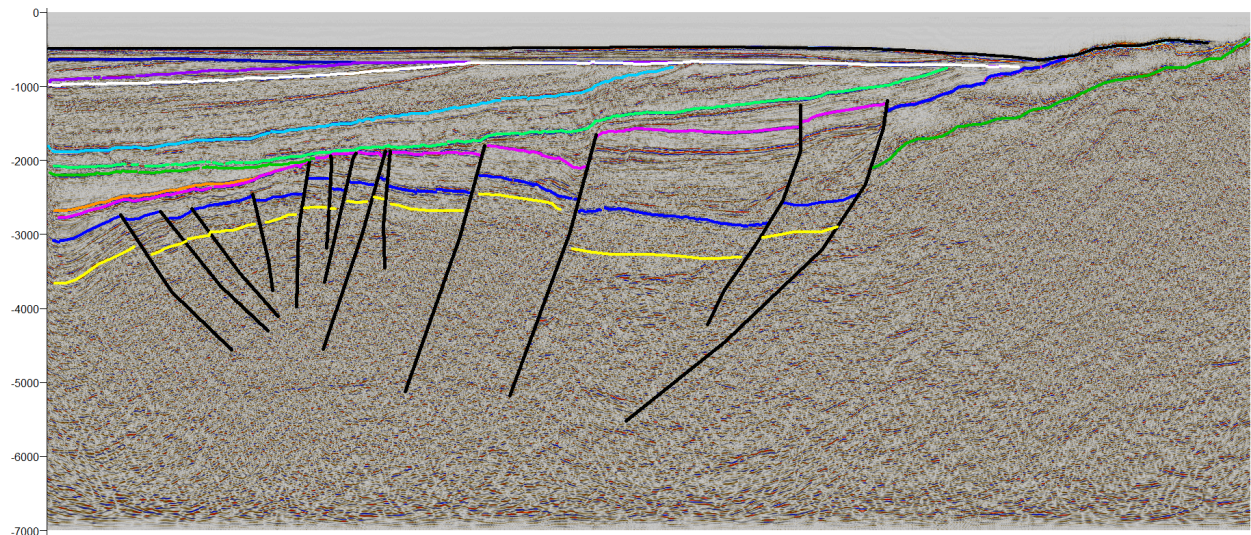


Figure 34: Line 6, NVGTI92-103

Line 6 intersects the end of Line 5 and continues further east and on to the Horda Platform. The line shows the gradual transition onto a platform environment and is intersected by two wells. The picked Brent Group and Top Triassic is of low confidence in the eastern end. This can also coincide with the basement. There are no wells here to confirm this.

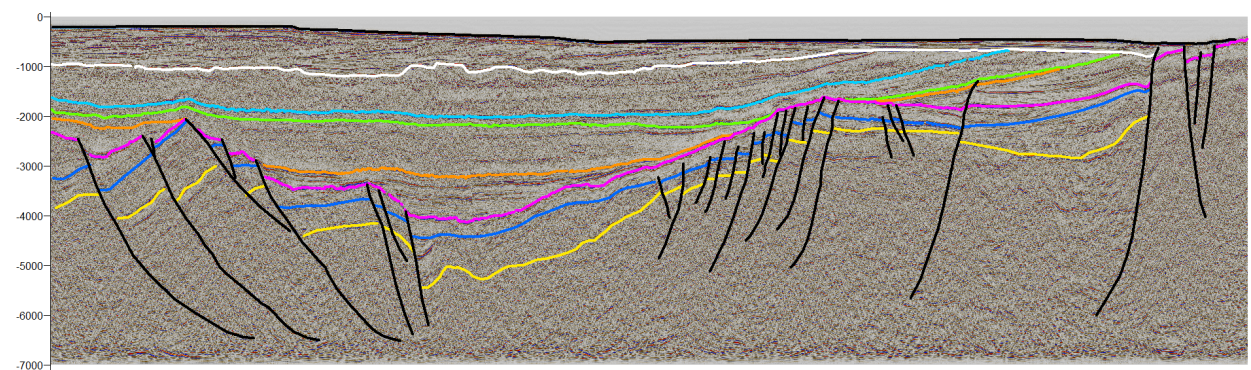


Figure 35: Line 7, NVGTI92-101

This is the second line that is found as a model in the interpretation chapter (Fig. 47). It crosses the Gullfaks South Field on the western side, and the northern part of Troll Field on the eastern. The faults in the Gullfaks area is characterized by domino faulting pattern with smaller antithetic faults. The faults on the eastern side are numerous before transition in to a platform type area. There are two wells intersecting the line.

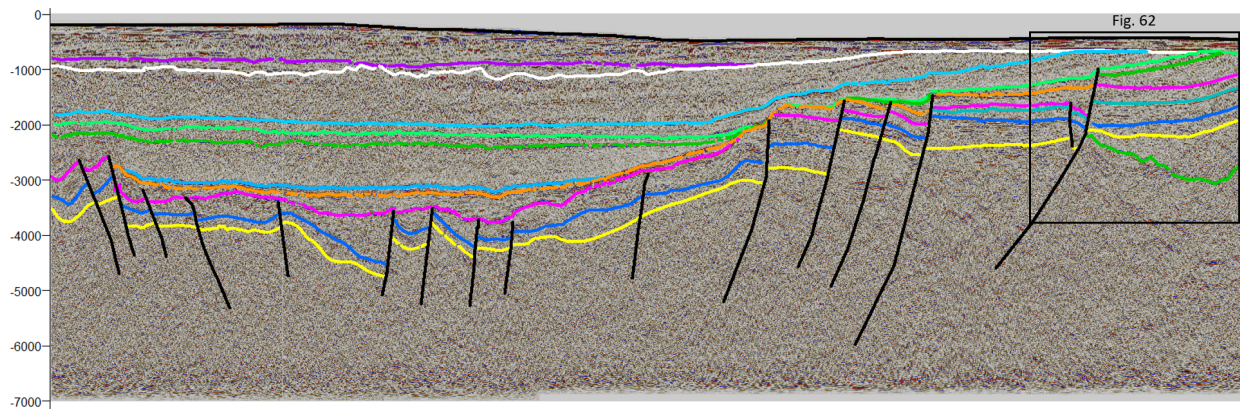


Figure 36: Line 8, NVGTI3-92-208

Line 8 is intersected by several wells, one of which penetrates the basement on the eastern side (outlined), making it possible to interpret. It shows thick packages of post-rift sediments, especially over the graben axis. The easterly dipping faults on the western side, show generally small displacements. The polarity of the faults change across the graben axis and have larger displacements on the eastern sub-platform.

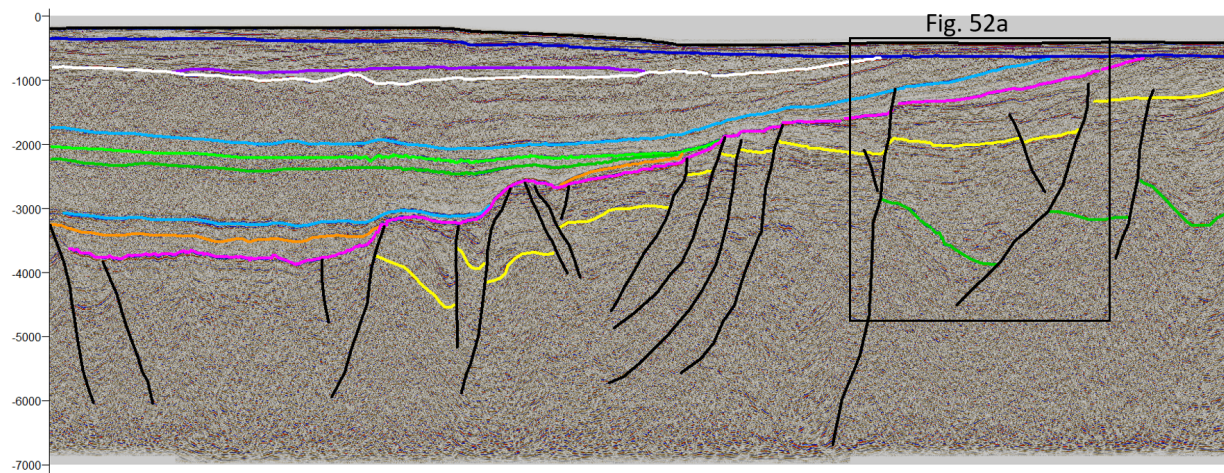


Figure 37: Line 9, NVGTI3-92-207

Line 9 intersects the Huldra Field, Veslefrikk and the southern part of Troll. The fault pattern is chaotic, with wells only on the eastern side. There is one basement-penetrating well, thus the basement is interpreted in this area. Any pre-rift deposits are difficult in the area around the graben axis.

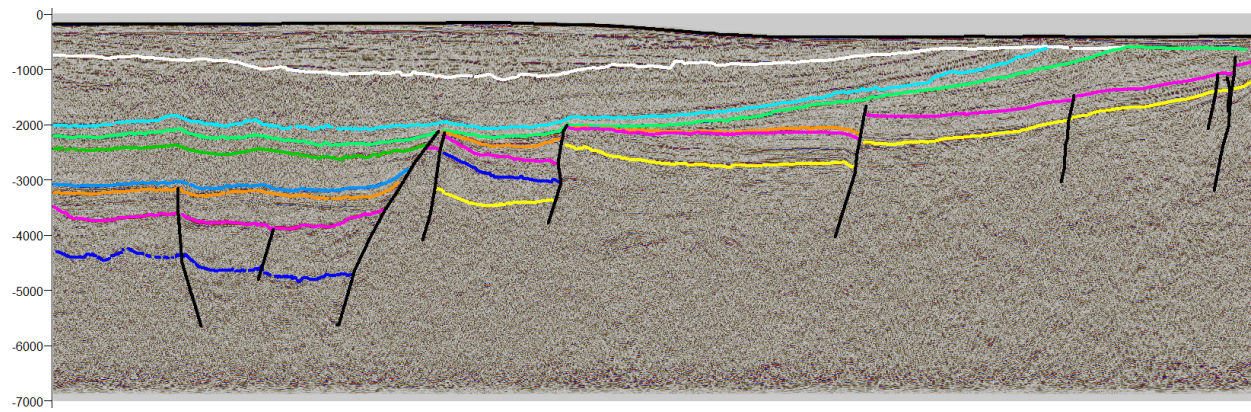


Figure 38: Line 10, NVGTI3-92-205

Line 10 intersect the northern part of the Oseberg Field, and the southern part of the Brage Field. There are large displacements on the fault that separates the graben axis from the platform areas. The deposits from the thermal subsidence phase show the typical saucer shape. There are few wells intersecting this line.

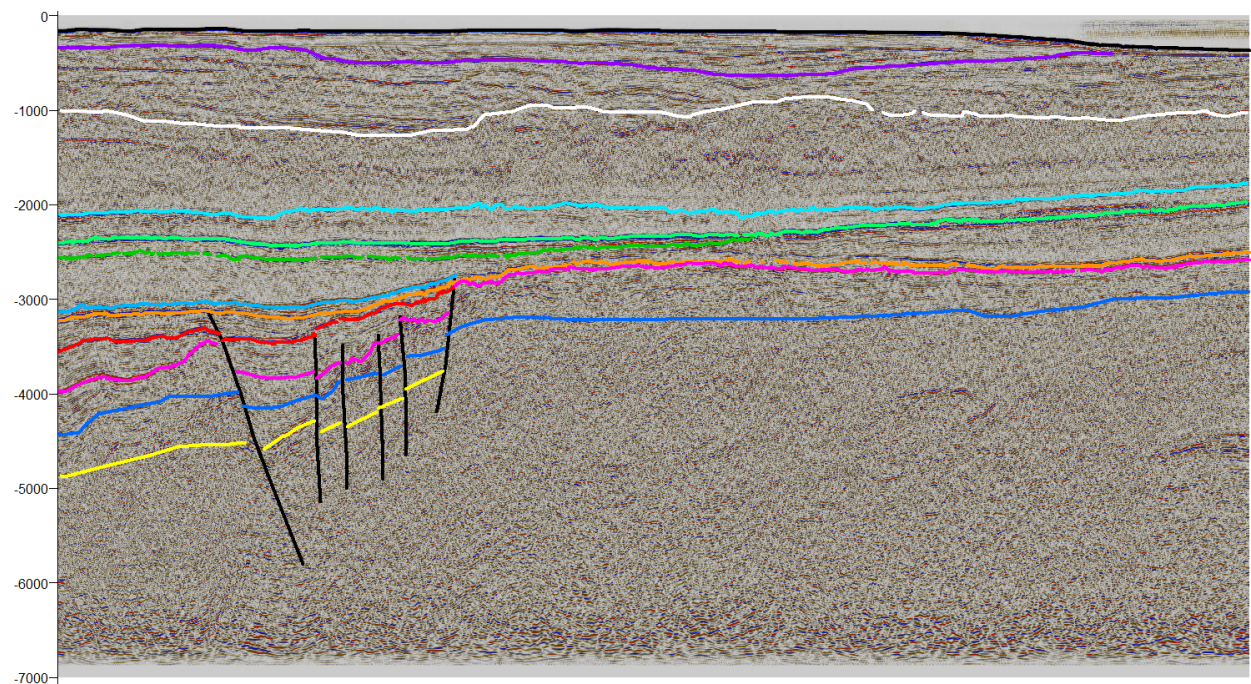


Figure 39: Line 11, NVGTI3-92-201

Line 11 is located between the Oseberg Sør and Frigg fields. It is the southernmost interpreted E-W line. It shows little faulting on the eastern side, before transitioning into a series of high angle faults. The sediment sequences thicken towards the faults. Symmetry is difficult to determine, as the western side of the graben is not included.

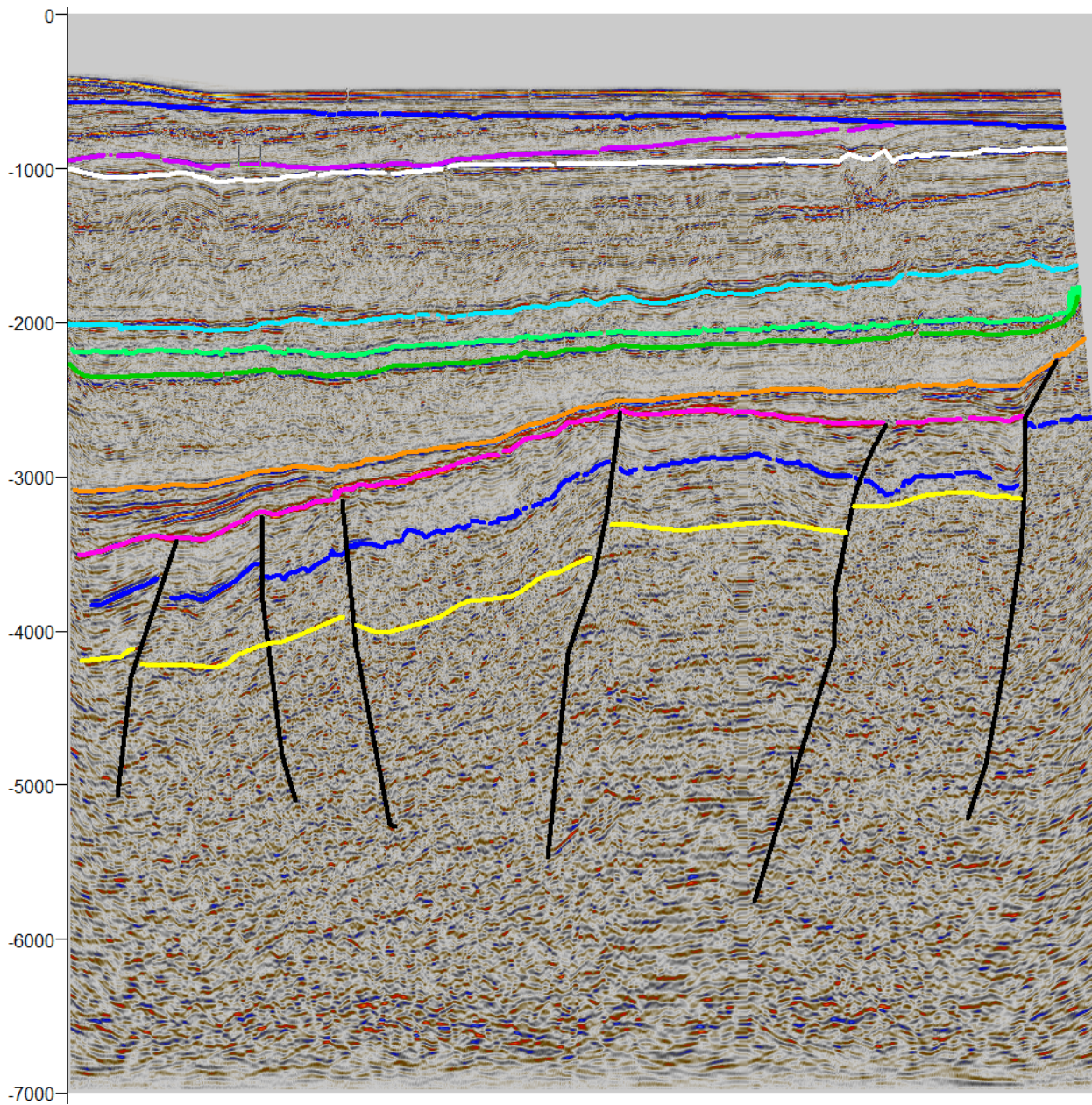


Figure 40: Line 12, SG8043-REP91-205D

Line 12 cross several of the lines that are interpreted. It was chosen to determine consistency between the interpreted lines, rather than to contribute to the interpretation of the graben. The left side of the line intersects the more central part of the graben, while the right side is at the transition to the platform areas.

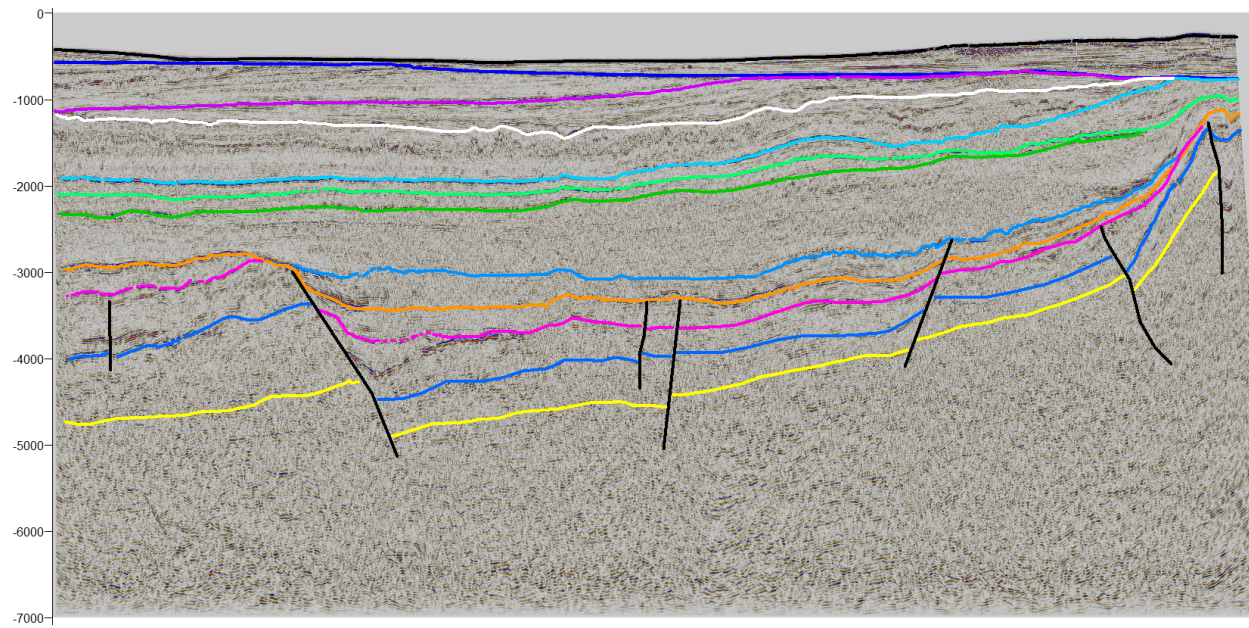


Figure 41: Line 13, SG8043-REP91-207A

Line 13 is of lesser quality than the previously interpreted lines. It stretches from between the Vigdis and Visund Fields (the left side of the line) to the boarder between the North Sea and the Norwegian Sea near the coast of Norway. It intersect many of the previously interpreted lines, and was also used to increase confidence in the chosen horizons.

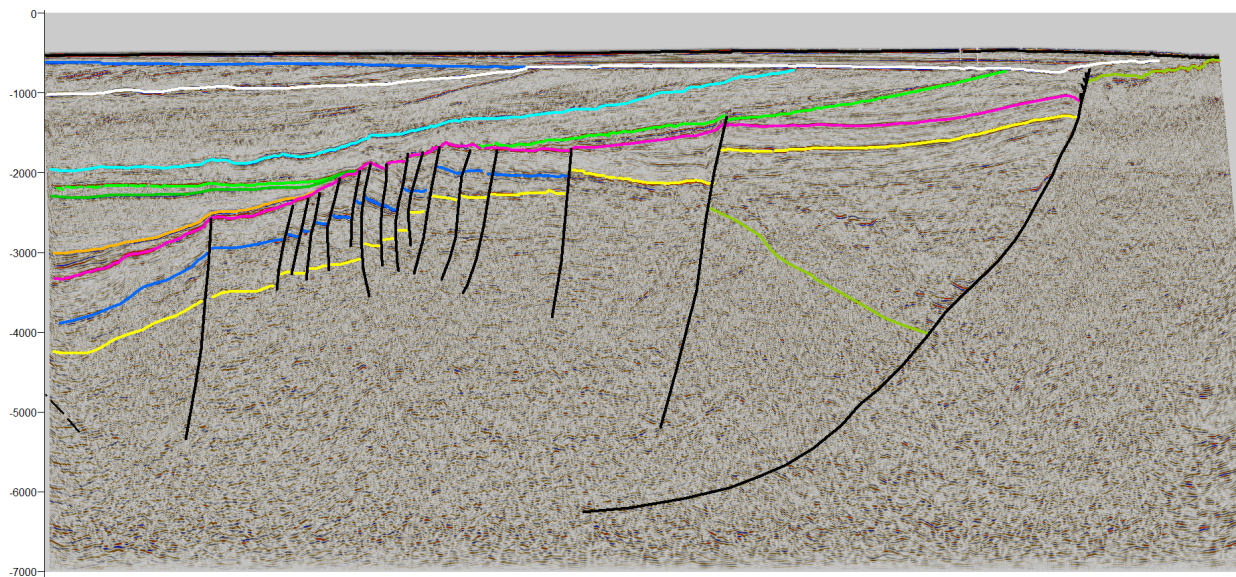


Figure 42: Line 14, SG8043-REP91-403A

Line 14 is the third and last line that is made as a model in the interpretation chapter (Fig. 48). It shows basement on the eastern side, and a highly faulted transition from the graben axis, just outside the line, to the lesser faulted platform area. It shows late faulting of the Cretaceous deposits,

indicating faulting lasting longer than in the axial areas. The Øygarden Fault is a dominating feature in this line.

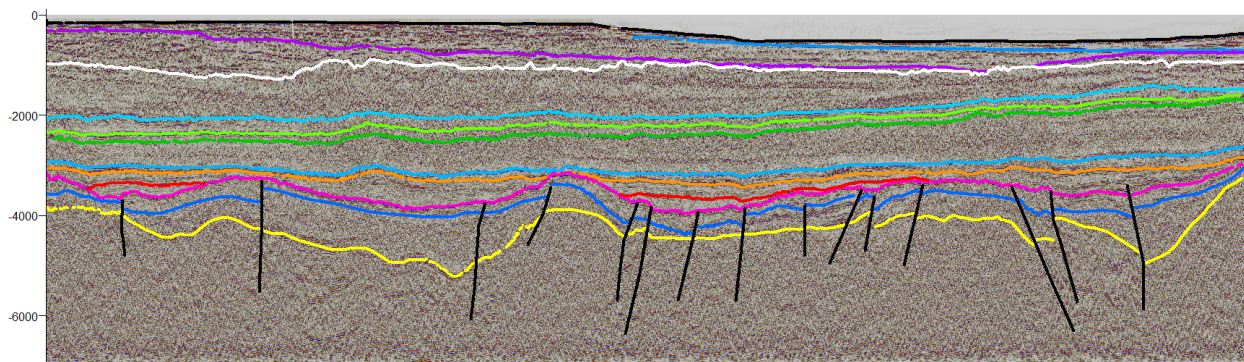


Figure 43: Line 15, NVGTI2-92-209

Line 15 is a N-S line that cross most of the previously interpreted lines. It is more or less going over the graben axis, thus making it difficult to interpret the pre-rift deposits. The interpretation of this line is largely based on the intersecting lines.

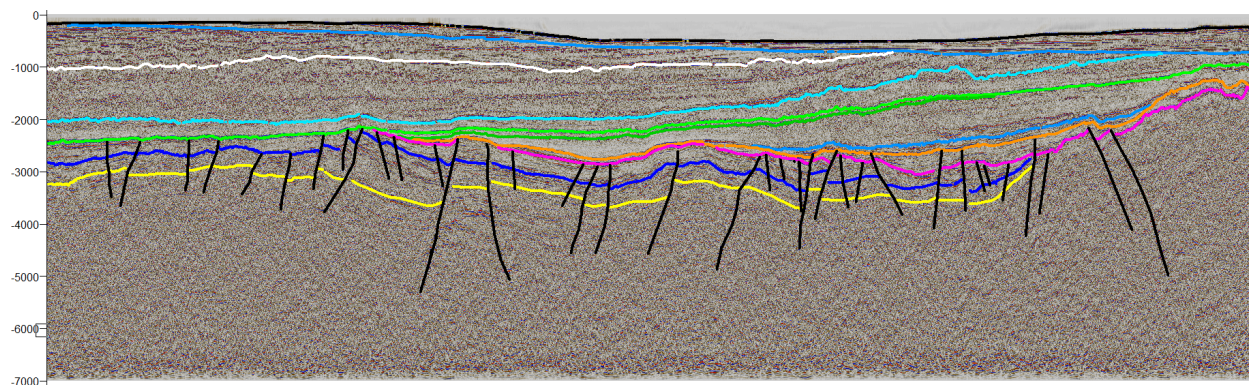


Figure 44: Line 16, NVGTI2-92-210

Also a N-S line, but crossing further east than line 15. It reach from the East Frigg Field in the south, to the boarder to the Norwegian Sea in the north. Line 16 cross most of the Oseberg Field and more wells than line 15. The interpretation of the Top Triassic is of higher confidence than the previous line. The lines representing the Triassic and Middle Jurassic deposits stop at the northern (right) part of the line. This is due to a basement-penetrating well, confirming that Late Jurassic deposits are found to be directly overlying the basement in the northern part.

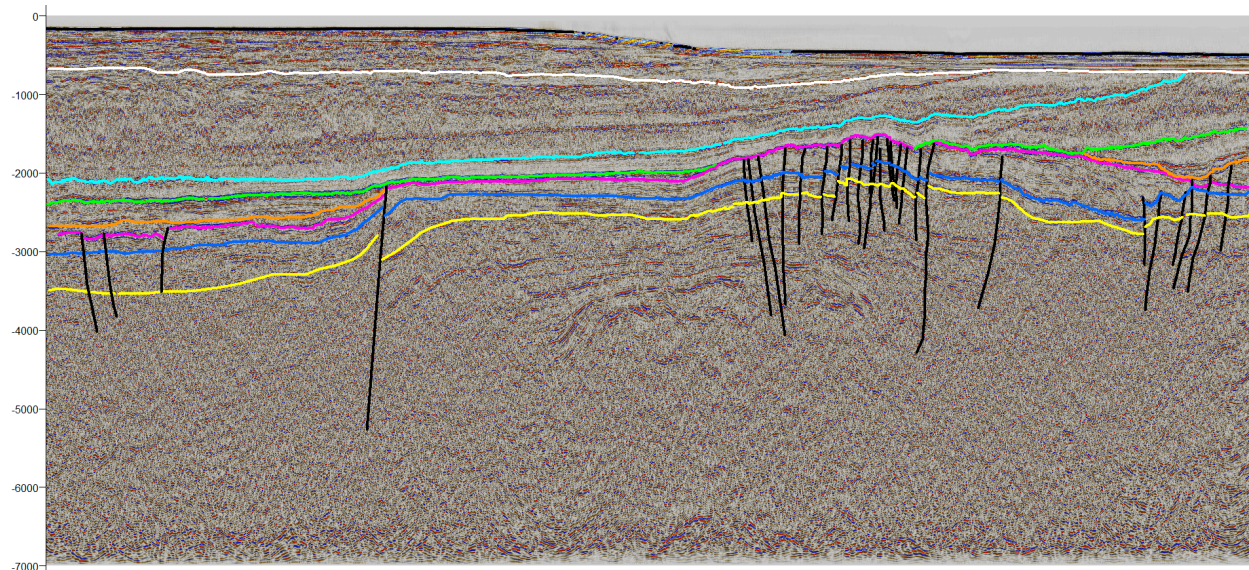


Figure 45: Line 17, NVGTI2-92-211

Line 17 is the easternmost N-S line interpreted, and is positioned to the east of the graben axis. It is little faulted in the southern before transitioning into the Troll Field, where faults dominate. In this area there are many wells. This line does not reach as far north as the two previous lines, but stop right after intersecting line 3. The position of the basement is not interpreted in this line

## 11 Interpretation

This chapter include an evolutionary interpretation of the development of the Viking Graben based on the results presented in the previous chapter. There has been made models that better show the age-distribution of sediments and will be heavily involved in the interpretation. The three models are based on Line 2, Line 7 and Line 14, respectively. Wells are included in the models. The uninterpreted lines of the three models will be included below. There is also included a more detailed interpretation of the Base Cretaceous Unconformity, which marked the transition from syn-rift to post-rift dominance. Following this, a discussion of basement structures of the northern North Sea and its importance on the rifting, is included. This is largely based on previous literature and studies made of the basement.

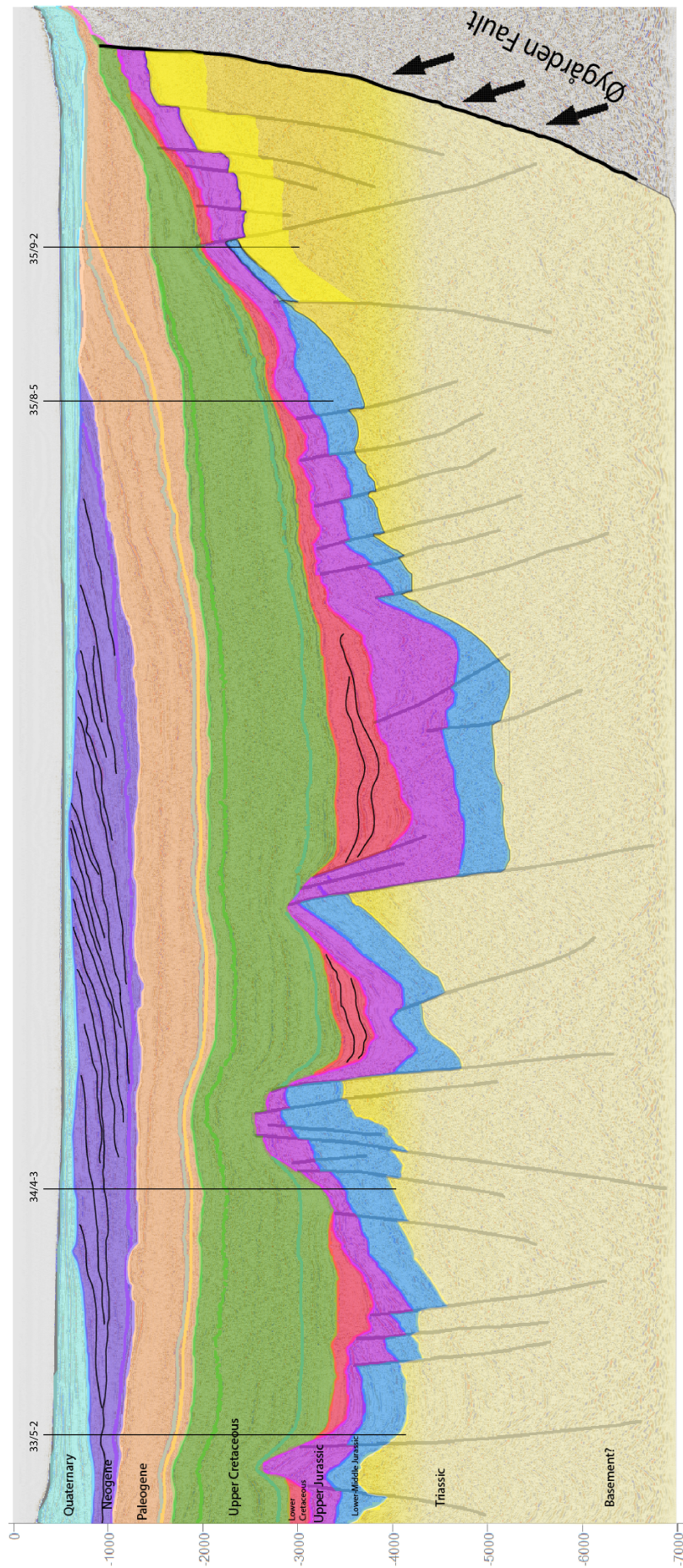


Figure 46: Model 1, based on interpretations of Line 2 (NVGTI92-106) in Fig. 30



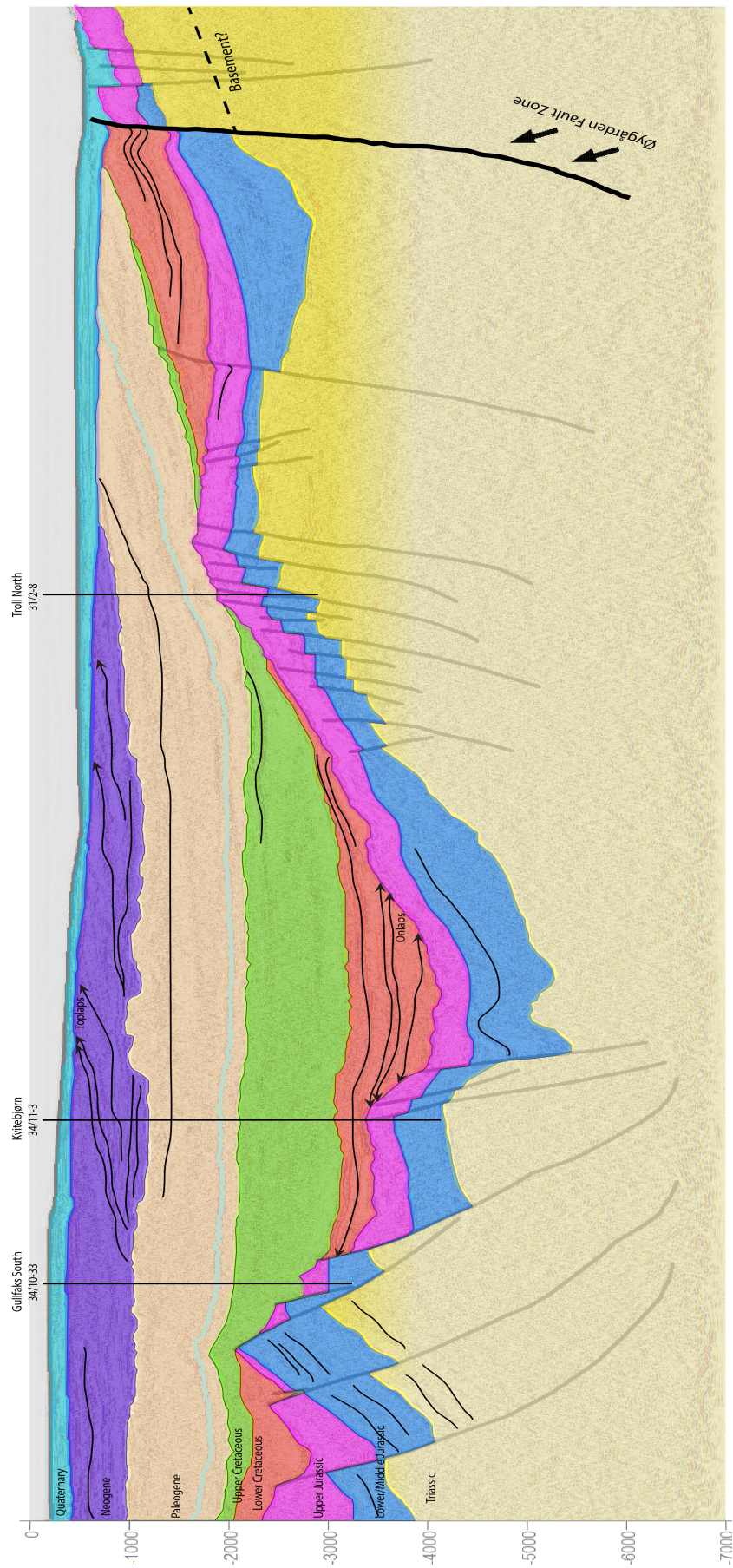


Figure 47: Model 2, based on interpretations of Line 7 (NVGTI92-101) in Fig. 35.

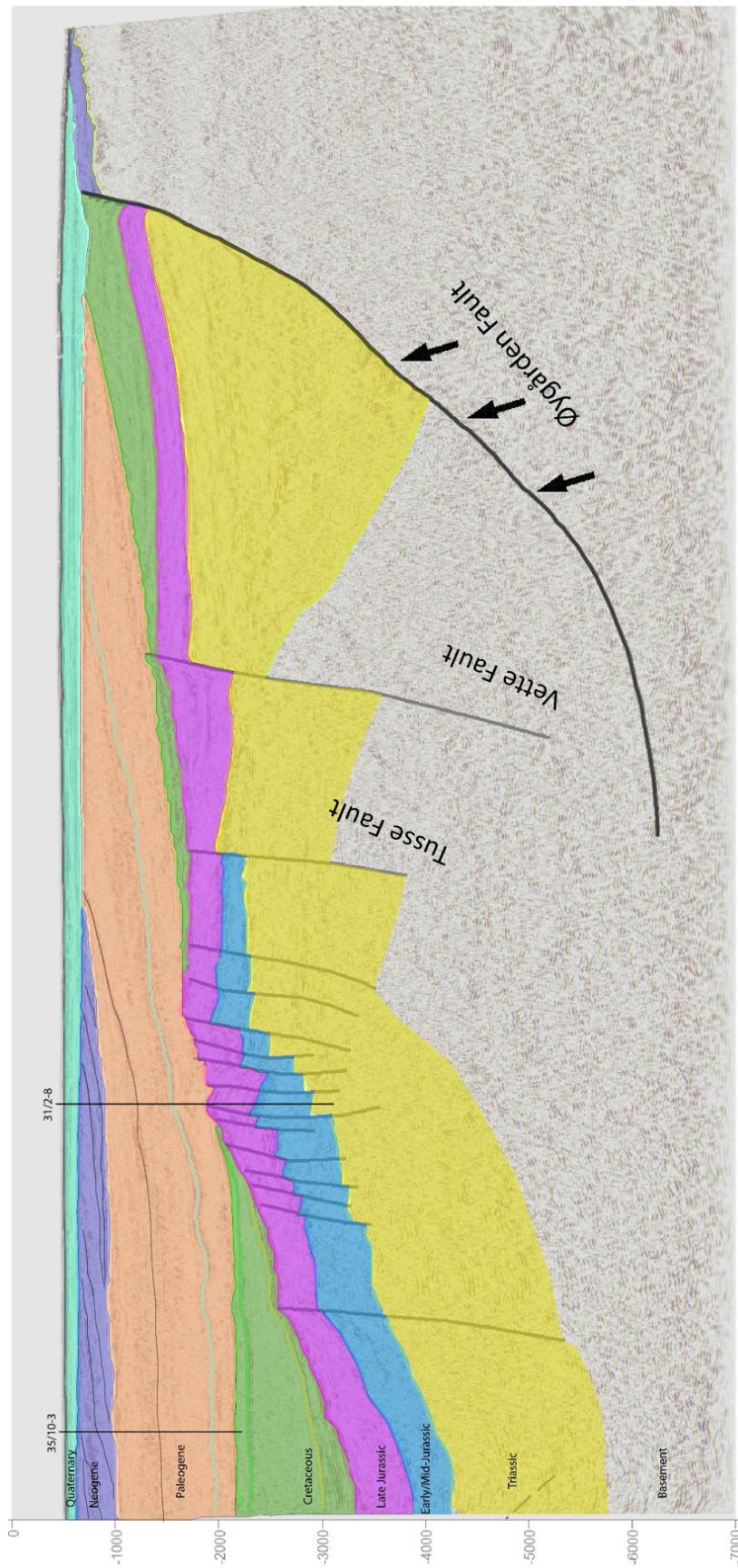


Figure 48: Model 3, based on interpretations of Line 14 (SG8043-REP91-403A) in Fig. 42.

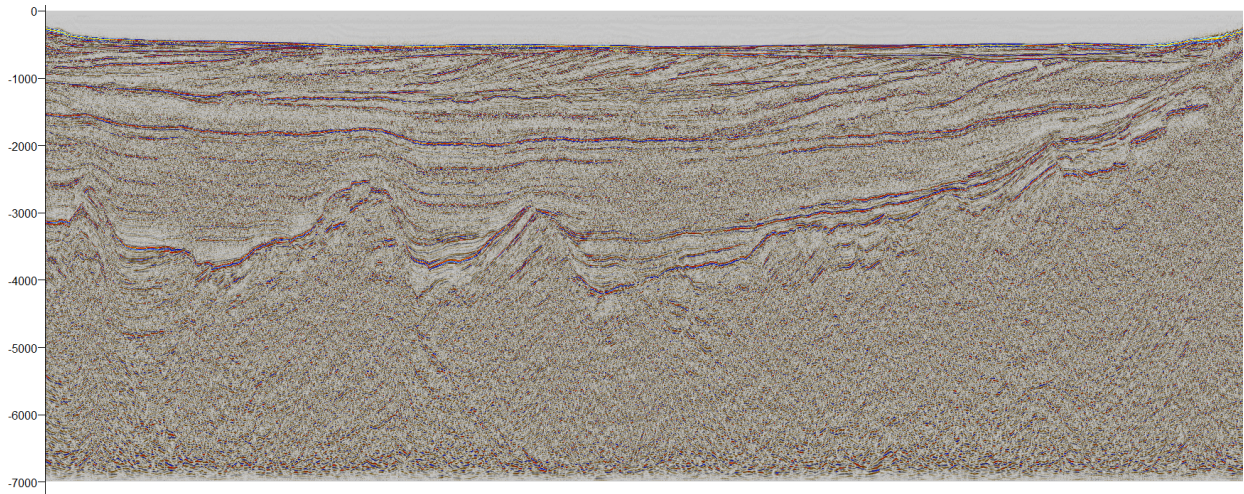


Figure 49: Uninterpreted line of Model 1

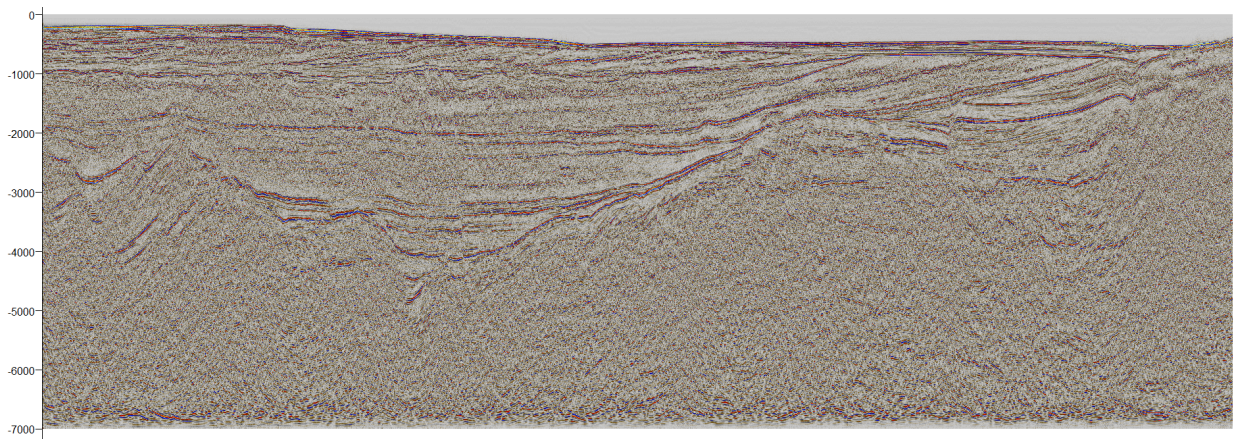


Figure 50: Uninterpreted line of Model 2

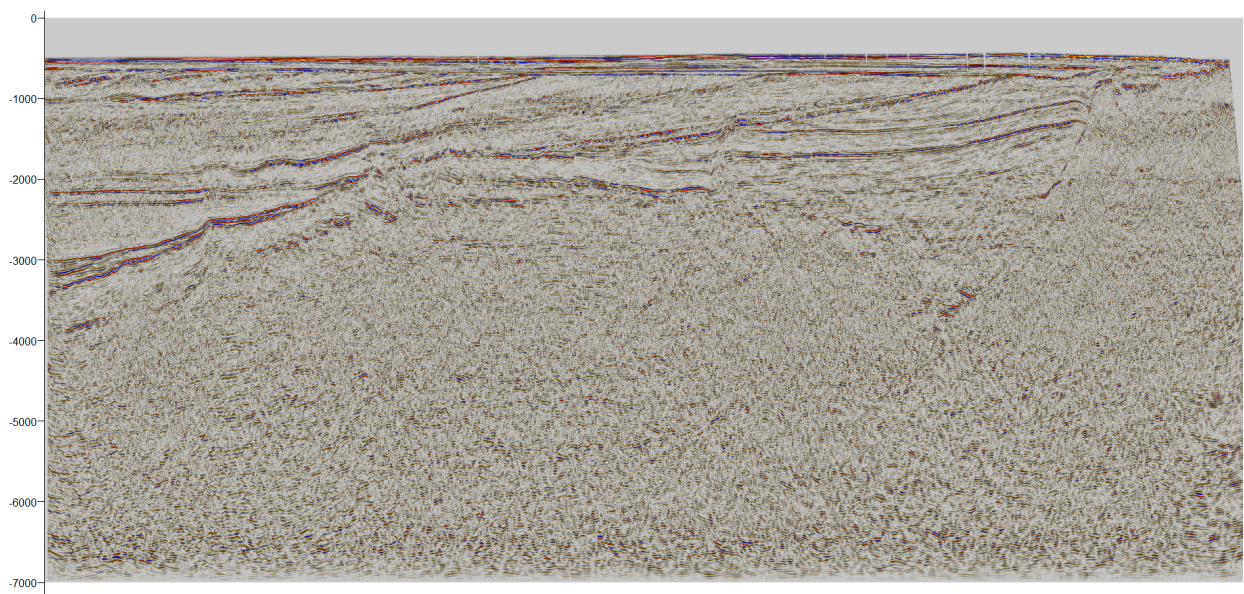


Figure 51: Uninterpreted line of Model 3

The decision was made to gradually fade out the color representing the Triassic deposits in model 1 and 2, due to the base of Triassic not being positively identified in wells. However, well 35/9-2 penetrates the basement, so the basement is interpreted in the surrounding area.

### 11.1 Evolutionary interpretation

The overall structure is believed to be a thinning of basement from the graben margins towards the rift axis, while the overlying sediment package thickens into the rift axis.

The thickness of the crust is not visible on shallow seismic, and any behaviour of the Moho can not be seen. This is unfortunate due to the proven importance of sub-crustal forces.

The clearest evidence for a Permo-Triassic rifting phase is found on the Horda Platform, where wedge-shaped **pre-Jurassic** packages can be seen overlying basement. This is most clearly seen in Line 9 east of the Troll field, where it is confirmed by a basement-penetrating well (Fig. 52a). If the same is found on the western margins of the graben, it can be concluded that the Late Jurassic rifting did not overprint the Permo-Triassic phase in the marginal areas and that the first rift phase affected a larger area than the latter, stretching from the Horda Platform, all through the Norwegian part of the North Sea and into the British side. In Model 3, differential tilting of the top basement can be seen at the Horda Platform, being indicative of basement-involved listric normal faulting. This is overlain by sequences of Late(?) Triassic to Mid Jurassic that exhibit basinward thickening, which was probably produced during a stage of post-rift thermal subsidence. Giltner (1987) found through subsidence modelling that a single Triassic event can explain almost all of the observed subsidence history of the Horda Platform, further supporting that Jurassic tectonism did not affect this area. There is no evidence for extensive uplift and erosion following the the Permo-Triassic rifting.

The models all display the basement-involved Øygården Fault Zone on the Horda Platform. It is the easternmost fault in a series a faults on the platform that also include the Tusse and Vette fault system. They are all N-S striking and dip westwards.

There is no basement penetrating wells in the central part of the Viking Graben, so any predictions of the graben axis during the Permo-Triassic rifting is difficult to make. It is believed that the most active faults were positioned at the eastern margin (Badley et al., 1988), and with the observable thickness distributions, where the post-rift deposits gradually increase in thickness towards the basin axis, and within individual faults, the early rift basin might have had an asymmetric shape.

Few indications of block tilting during the first stage of rifting is seen at the Horda Platform (Model 1, 3). This can mean that the faulting was associated with the thermal subsidence and not rifting

The **Late Triassic and Early Jurassic** deposits does not show the same syn-sedimentary traits. It is therefore concluded that the rifting ceased some time in the Triassic. The exact age of cessation of active extension is difficult to determine, due to lesser seismic quality at this depth. Following a rifting phase, thermal subsidence is assumed. **Triassic and Early-to-Mid Jurassic** deposits thickens towards the basin centre (See central parts of Line 2), indicating this.

It is interpreted that the Brent Group is the latest deposits before the onset of the next phase of rifting. The seismic configurations seen is commonly chaotic and subparallel to parallel in the group. Like the underlying groups it is highly faulted, indicating later rifting. The Brent Group is deposited in a deltaic environment, indicating a that the area was near sea-level at the onset of the second phase of rifting.

The overlying **Late Jurassic** is recognized by the Draupne Formation as the top. This also coincides with the Base Cretaceous Unconformity (BCU). The deposits are highly faulted and rotated, and often eroded at the uplifted fault blocks (See Fig. 59). A more detailed description of the BCU is given in chapter 11.2.1. The Late Jurassic deposits show wedge shaped geometries and the most common configurations are subparallel and parallel, that thicken towards syndepositional faults. The onset of the rifting can be recognized by the onlap syn rift deposits on tilted pre-Late Jurassic strata (represented by the blue line of the Brent Group in the results). The western part of the northern North Sea consists of a complex of differentially tilted fault blocks, reactivated from previous rifting. The syn-rift deposits are thickening down the slope of the tilted blocks. Erosion is seen on several fault blocks, particularly those close to the graben axis, indicating emergent footwalls during the early syn-rift phase. The axial graben area experienced rapid subsidence accompanied by block tilting and thick accumulation of sediments. East of the rift axis active block tilting occurred, and it is believed that many of the N-S trending faults were reactivated from the Permo-Triassic rifting phase. The fault pattern is more complex than what's observed on the western part (i.e. Line 7)

The deposits following the Late Jurassic rifting is defined by being deposited in the second thermal subsidence episode defining the development of the Viking Graben. During this stage, block rotation stopped. The **Lower Cretaceous** deposits are generally filling in the accommodation space resulting from the tilting of the underlying fault blocks. They are commonly restricted to the structural lows in the graben areas (See the red fill in Model 1 and 2). The Cromer Knoll Group of the Lower Cretaceous are thickest in the northernmost North Sea (See Line 1). The early post-rift strata onlaps the tilted fault blocks and creates an angular discordance that is easily recognized on seismic data. The seismic configurations are commonly parallel to subparallel, and the basal structure tends to follow the shape of the BCU. It is seen in Model 3, at the Horda Platform that

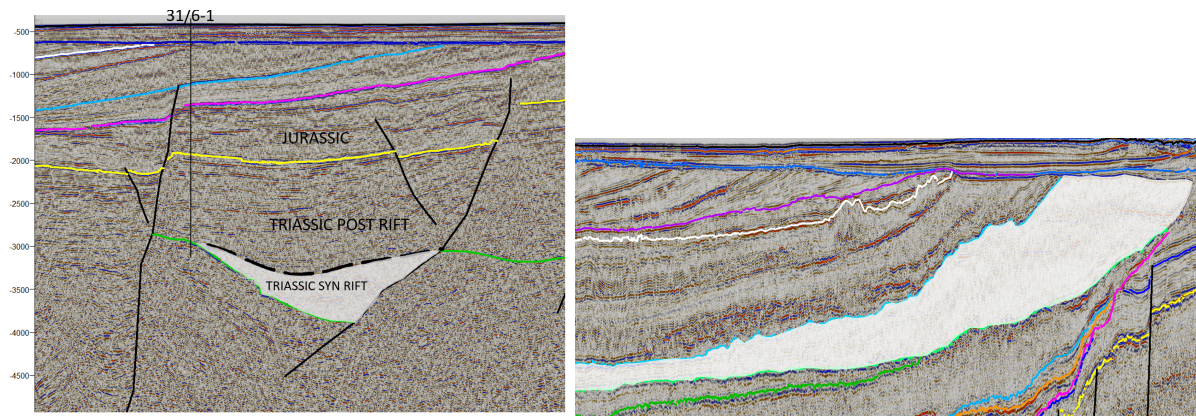
the Early Cretaceous deposits are slightly faulted, indicating prolonged non-rotational faulting at the Horda Platform, and that the rifting ceased here, later than further towards the graben proper.

The **Late Cretaceous** deposits are thick and generally chaotic to sub-parallel. The sediments fill the last of the accommodation space from the tilted underlying structure and drapes the whole graben area of thick sediment packages in a 'saucer-shape' with the thickest deposits accumulated at the basin centre. The Late Cretaceous formations show little change between each other, indicating little change of depositional environment other than continued subsidence.

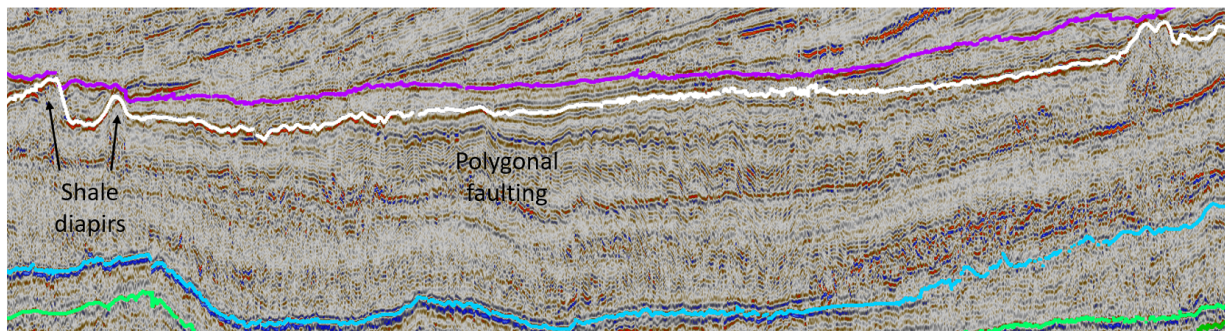
During the **Early Cenozoic**, the Viking Graben continued to be dominated by subsidence. From the results, it is concluded that the Horda Platform, and especially the northern part, was the last feature of the northern North Sea that became completely drowned (See Line 2, 3 and 4) and covered, first partially, by the Shetland Group and then later deposits. There are few signs of any faulting and is believed to be a relatively quiet tectonic period.

The **Paleogene** is characterized by continued sediment deposition and accumulation over the continuously subsiding graben. The main part of the Eocene succession is a slope/basin floor system downlapping and thinning towards the east in the northern North Sea. The eastward thinning indicate a near absence of sediment input from the eastern margin. The Balder Formation of **Late Paleocene/Early Eocene** is generally thin, and displays a parallel wavy pattern of the internal structure. The reflector show often low continuity, especially in the central part of the basin. Towards the east it thickens significantly. This can be seen on most lines in the results and is clearly outlined in Fig. 52b.

The **Eocene and Oligocene** deposits are largely represented by the Hordaland Group. The group displays a chaotic pattern. The horizons within the group were seemingly initially horizontal and parallel, but are frequently disrupted by small scale polygonal faulting (See Fig. 52c). The polygonal faulting occur over most of the group, but is strongest in the central parts of the graben. The faulting is believed to be due to post depositional processes, rather than external tectonic processes. The top of the group is highly irregular with mounds interpreted as shale diapirs overlapping onto the overlying layers (Fig. 52c). Diapirs are the result of density contrast between low density sediments moving vertically into higher density sediments, thus creating a buoyancy force that push the sediments upwards.



(a) Interpreted Triassic syn-rift deposits in Line 9 by well 31/6-1 (b) Vertically exaggerated. Showing how the Balder Formation thickens towards the east. From Line 3



(c) Vertically exaggerated. Shows how the Hordaland Group is influenced by polygonal faulting and shale diapirs. From Line 3.

Figure 52: Some features described in this chapter

The **Oligocene and Miocene** was characterized by tectonic quiescence in the North Sea. There is observed a regional unconformity in Miocene where the Utsira Formation is overlying the Hordaland Group. The Early Miocene deposits were dominated by accumulation of silt and clay. However, the lithology changes to sand with the deposition of the Utsira Formation consisting of marine sand.

The **Pliocene** deposits overly the Utsira Formation and is characterized by stacking of clinoforms, most clearly seen in Model 1. Sediments prograde towards the basin centre and form a succession of clinoforms from the Upper Pliocene. A cause for this can be the uplift of the Norwegian mainland and coast/near areas that force the sediments basinward. Stacking of clinoforms indicate very high sedimentation rates and can be due to the glaciation periods increasing the sediment supply to the continental shelf. The clinoforms are bounded by a surface of regional downlap at the base and the Base Quaternary Unconformity at the top.

Overlying the Pliocene clinoforms are the extensive flat lying, relatively uniform **Quaternary** deposits, separated by the Base Quaternary Unconformity. The internal reflections are strongly parallel, and generally thickens away from the graben axis. It is locally very thin and the Pliocene

clinoforms are sometimes interpreted to directly underlie the seabed (See for example Line 3). The seabed is recognized as the top of the Nordland Group.

## 11.2 Unconformities related to rifting

The transition from the synrift to the post-rift stage can be defined as the point where the amount of heat transported out of the system is larger than what is transported into the system from beneath (Kyrkjebø et al., 2003). The two phases are characterized by different tilting patterns. The synrift is associated with rotation of fault blocks during extension causing platform-directed synrift tilting, whereas the post-rift tilt of sedimentary strata typically is towards the basin axis. This is a result of thermal contraction and sediment compaction (Nøttvedt et al., 1995). This shift of direction from the synrift to the post-rift is connected to the production of a tectonically influenced onlap surface. The regional subsidence rate will decrease, although subsidence will occur over a wider area, eventually drowning and smoothing the relief of the late synrift stage (Prosser, 1993)

### 11.2.1 The Base Cretaceous Unconformity

The Base Cretaceous Unconformity (BCU) is the most easily identifiable surface of the Phanerozoic succession of the Norwegian continental shelf. It is almost always possible to map using seismic reflection data and well information. The BCU has its origin from the transition from the synrift to the post-rift stage of the Jurassic-Cretaceous basin development (Nøttvedt et al., 1995).

Even though the unconformity is easily recognizable and regional, is the reflection signature complex. The complexity is related to the previous rifting and influenced by the basin geometry, position within the basin, fault configuration, fault-related variations in subsidence pattern and possibly heat flow variations (Kyrkjebø et al., 2003). The BCU is commonly displayed in seismic reflection as a low-frequency, high-amplitude double reflection. However, due to the diversity of rocks present both above and under the unconformity the reflection signal varies in amplitude and change in polarity.

An analysis of the Base Cretaceous Unconformity can contribute to the understanding of the rifting that created the Viking Graben. Figure 53 below show different configurations of a rift-related unconformity and how an unconformity changes depending on the location within the basin, and how it related to the underlying rifted structure. In the following paragraphs it will be shown how the BCU is characterized at the axial parts of the graben, the graben margins and sub-platforms, at the platform areas and in the extra-marginal fault complex.



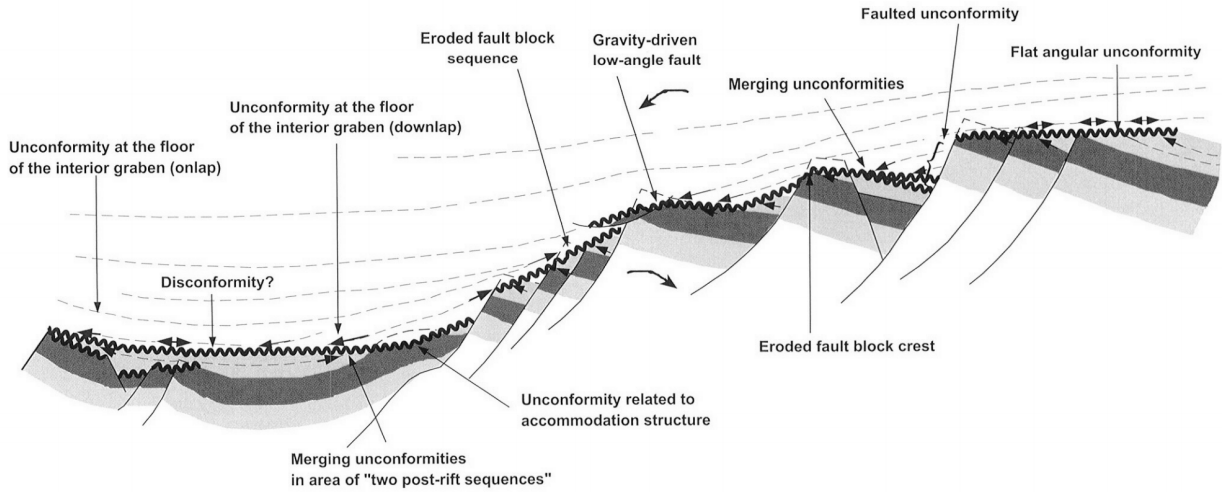


Figure 53: Sketch showing different configurations of the BCU, (Kyrkjebø et al., 2003)

1. Axial parts of the graben

The faulting here was less intense than on the margins. The BCU is characterized by a relatively simple geometric configuration in this area. The unconformity is generally developed as a disconformity with no significant angle between the over- and underlying layers (Fig. 54). In the Viking Graben the BCU is commonly a pronounced impedance contrast characterized by a clear and continuous reflection. Away from the basin centre post-rift sediments commonly onlap the unconformity, making it easier to distinguish. Rotated fault blocks are common beneath the BCU in the northern Viking Graben

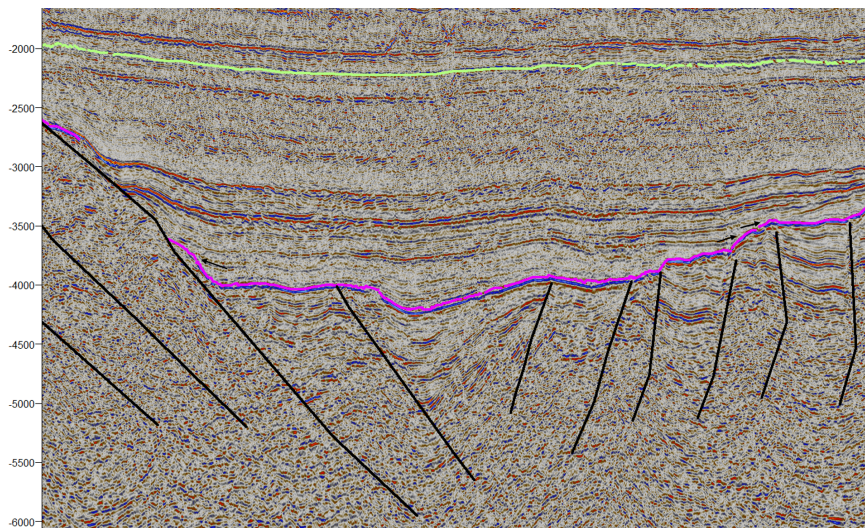


Figure 54: From Line 5 in the northern Viking Graben. Configuration of the BCU is relatively simple and geometric, represented by a continuous and clear reflection. Note the arrows representing onlap of post-rift strata at the basin margins. The green line represents the top Cretaceous.

## 2. Graben margins and sub-platforms

Sub-platforms are tectonic units situated in a structural position between the stable platforms and the basin interiors. The sub-platforms may have been a part of the platforms until the rift climax stage began and the master fault system separated them from the platform areas. At the uplifted crests of the sub-platforms the angular unconformity is shown as a horizontal, mainly unfaulted surface, or as a continuous curved surface (Fig. 55).

Sub-platform deformational style varies from cases where the throw is distributed among a few faults, so that throw is considerable on each fault (Fig. 56), to cases where the throw is distributed across a step-like fault system with minor throws at each fault (Fig. 57).

In the footwalls of larger, strongly rotated fault blocks (Fig. 58), the unconformity often consist of several separate unconformity surfaces that merge into one surface.

Gravity sliding and erosion affected the unconformity, demonstrating a clear time relation between the synrift and post-rift geometries (Fig. 59). Several surfaces existed as free surfaces exposed to late synrift erosion.

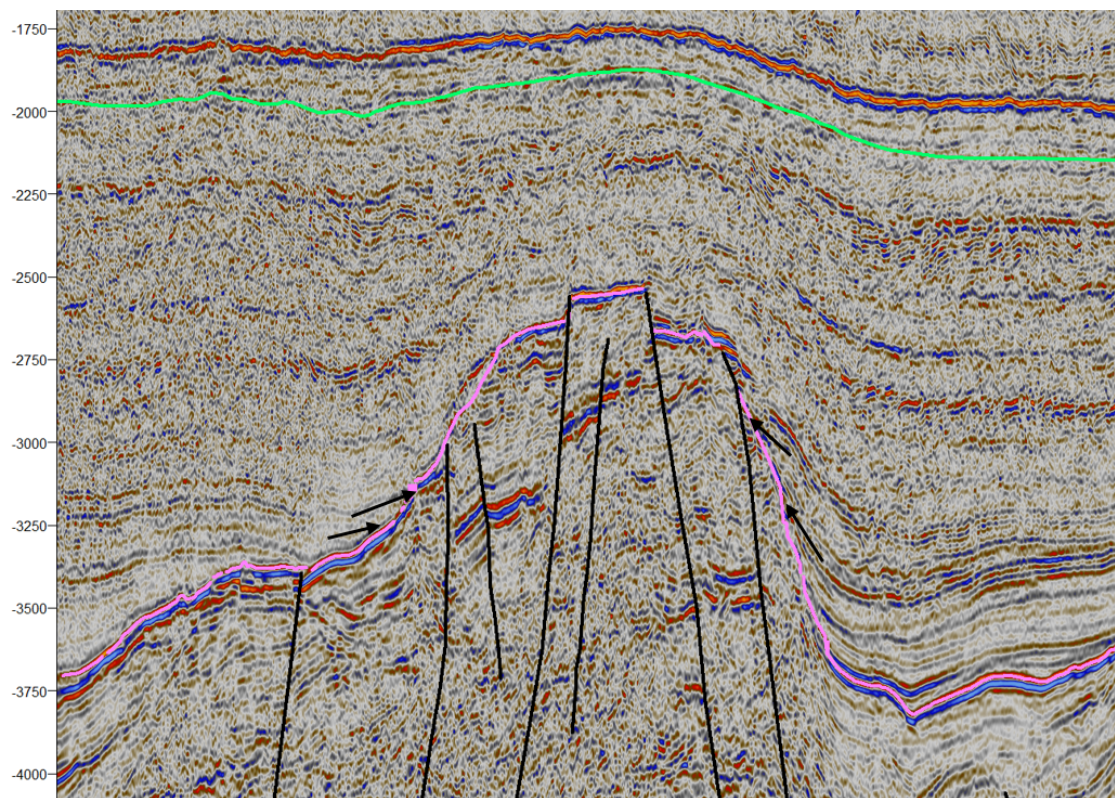


Figure 55: From Line 2 in the Viking Graben north of the Snorre Field. The BCU is faulted over the rotated fault block showing local angular unconformities, while being continuous on the side marked by onlaps on each side.

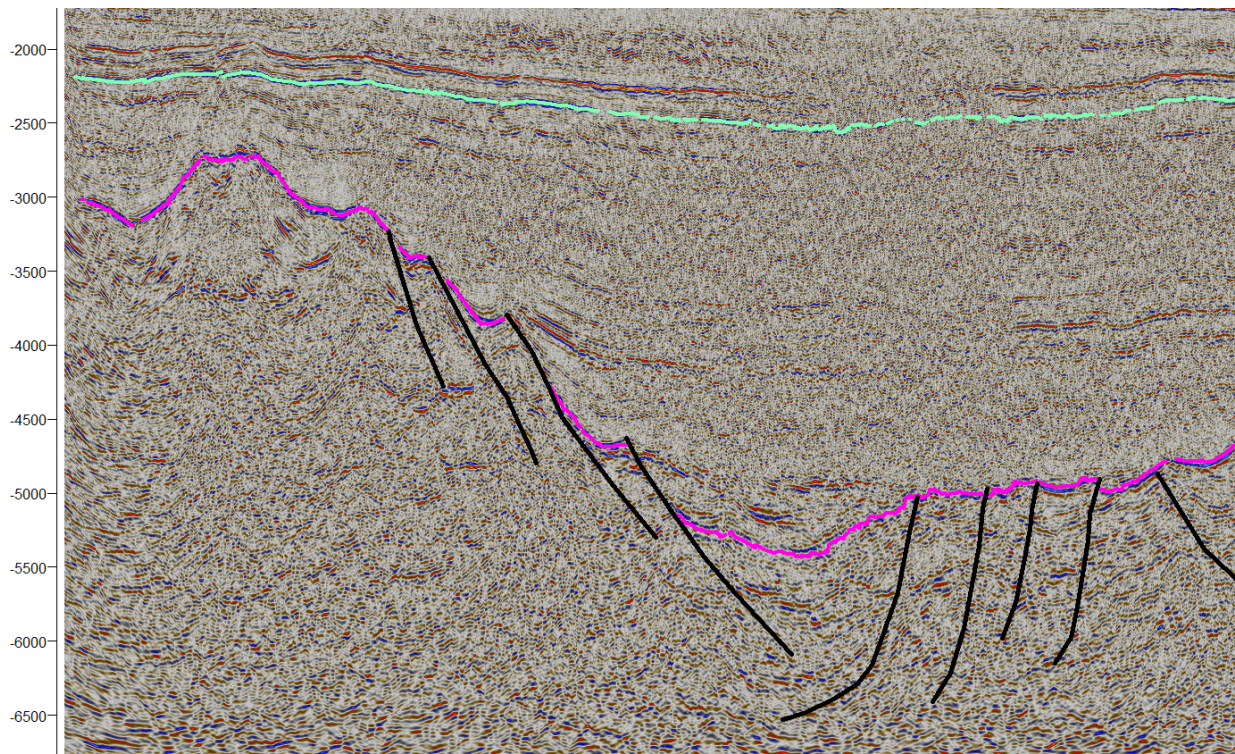


Figure 56: From Line 1 in the northernmost North Sea between the Magnus and Møre Basins. Configuration of the BCU being offset by faults with large vertical displacement.

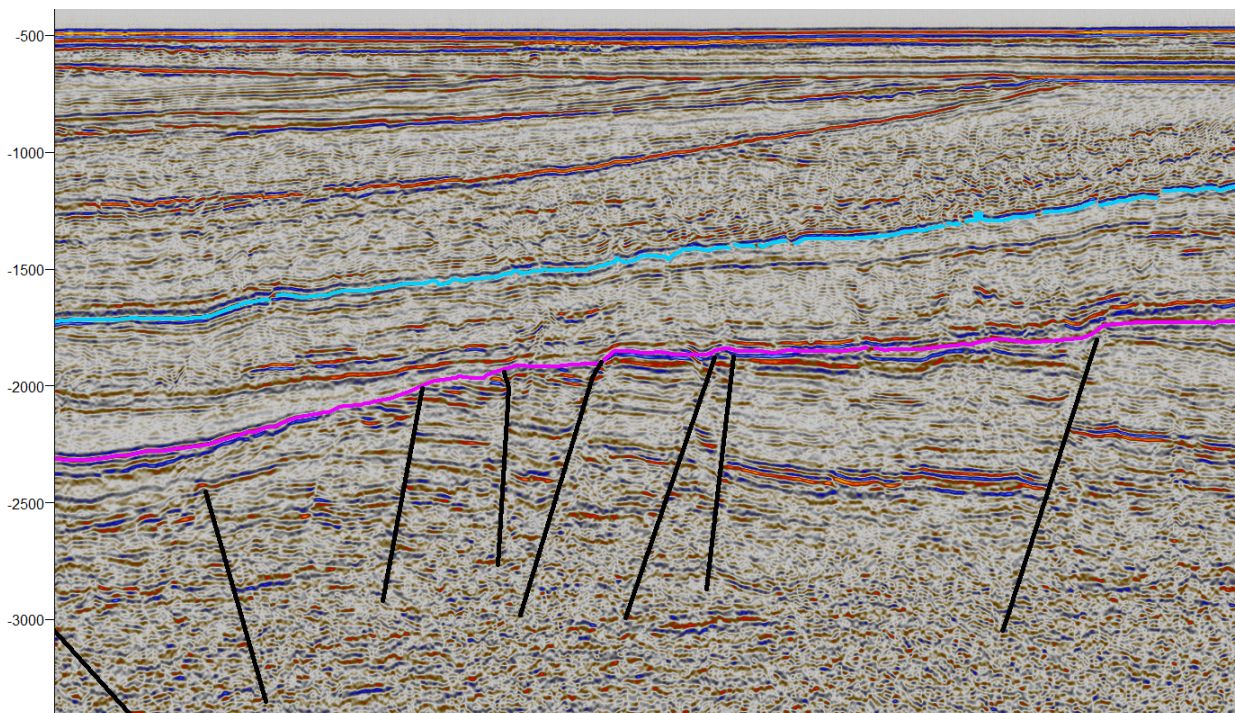


Figure 57: From Line 6 between the Viking Graben and the northwest of the Horda Platform, showing faults with minor throw. The blue line represents the Top Rogaland Group

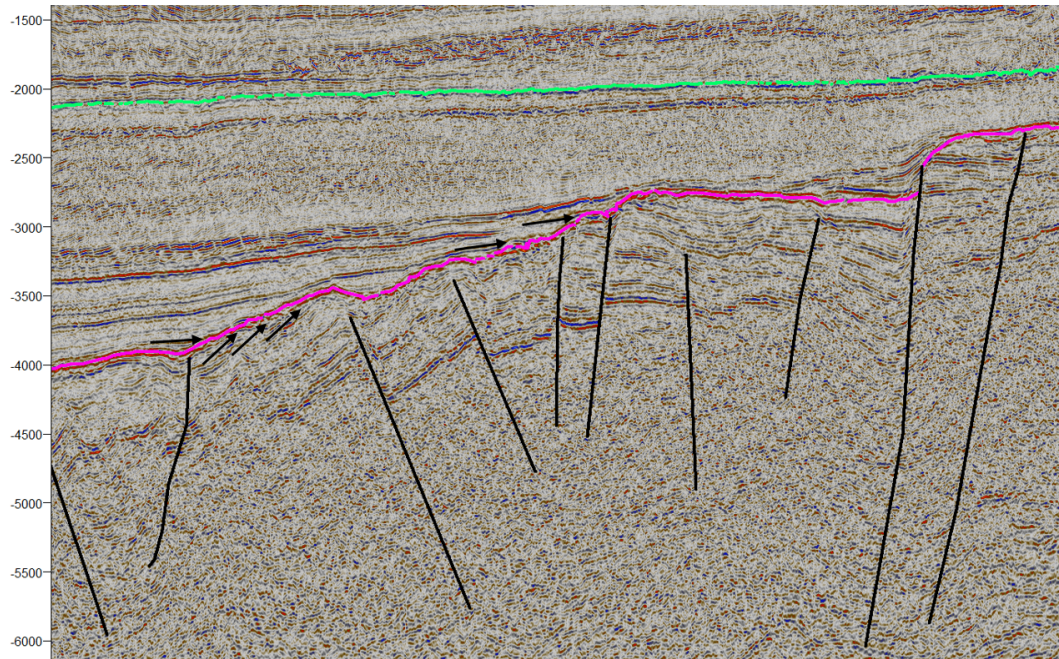


Figure 58: From Line 3, crossing the Vega Field in the northern North Sea. Highly faulted blocks underlay the uneven BCU at this location

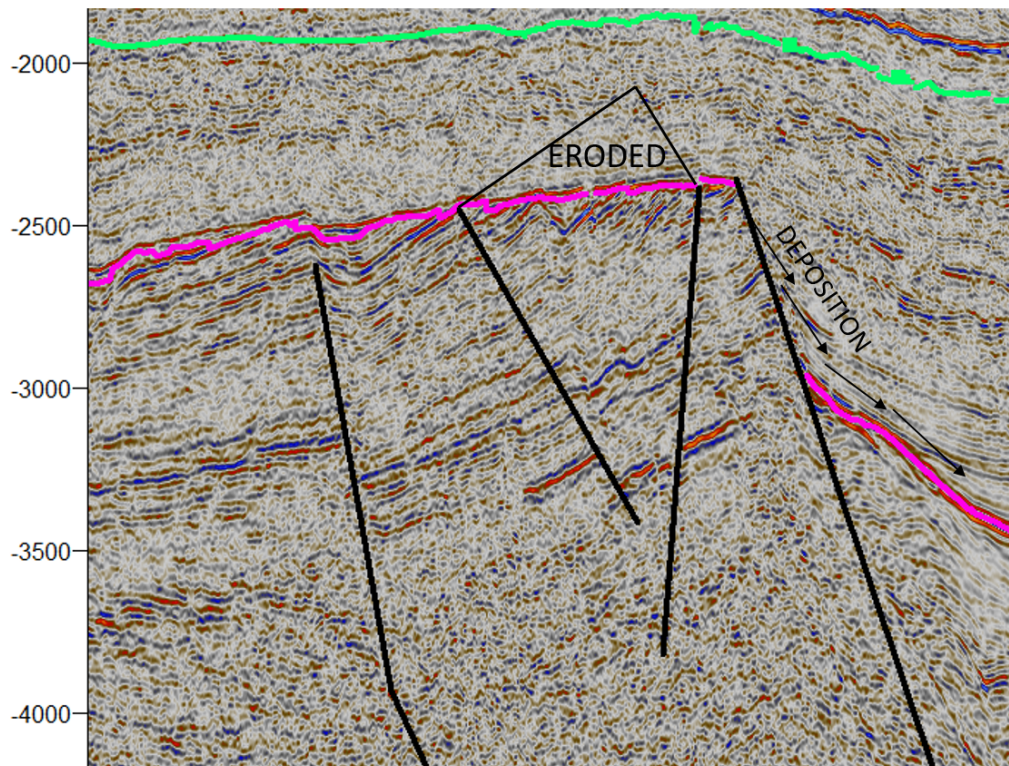


Figure 59: From Line 3, in the western margins of the northern Viking Graben, crossing the Statfjord Field. Showing a large part of the rotated fault block eroded and sediments deposited in the hangingwall low

### 3. The platform areas

The BCU is far simpler in the platform areas than at the basin margins and the sub-platforms, but there is still a variety of unconformity configurations in this setting (i.e. disconformity, local angular unconformity). This creates a complexity enhanced from the merging of several unconformities of Late Jurassic - Early Cretaceous to Early Tertiary age, creating a gap of stratigraphy that increase from the marginal fault complex to the uplifted marginal high of the platform. The interior platforms are commonly characterized by small dip gradients and modest fault-block rotation, where the BCU is displayed as a disconformity. Close to the marginal faults, the unconformity is characterized by downlap from above and top-lap from below. However, angular unconformities are commonly seen close to internal platform faults, and is even offset by faults in some places (Fig. 60).

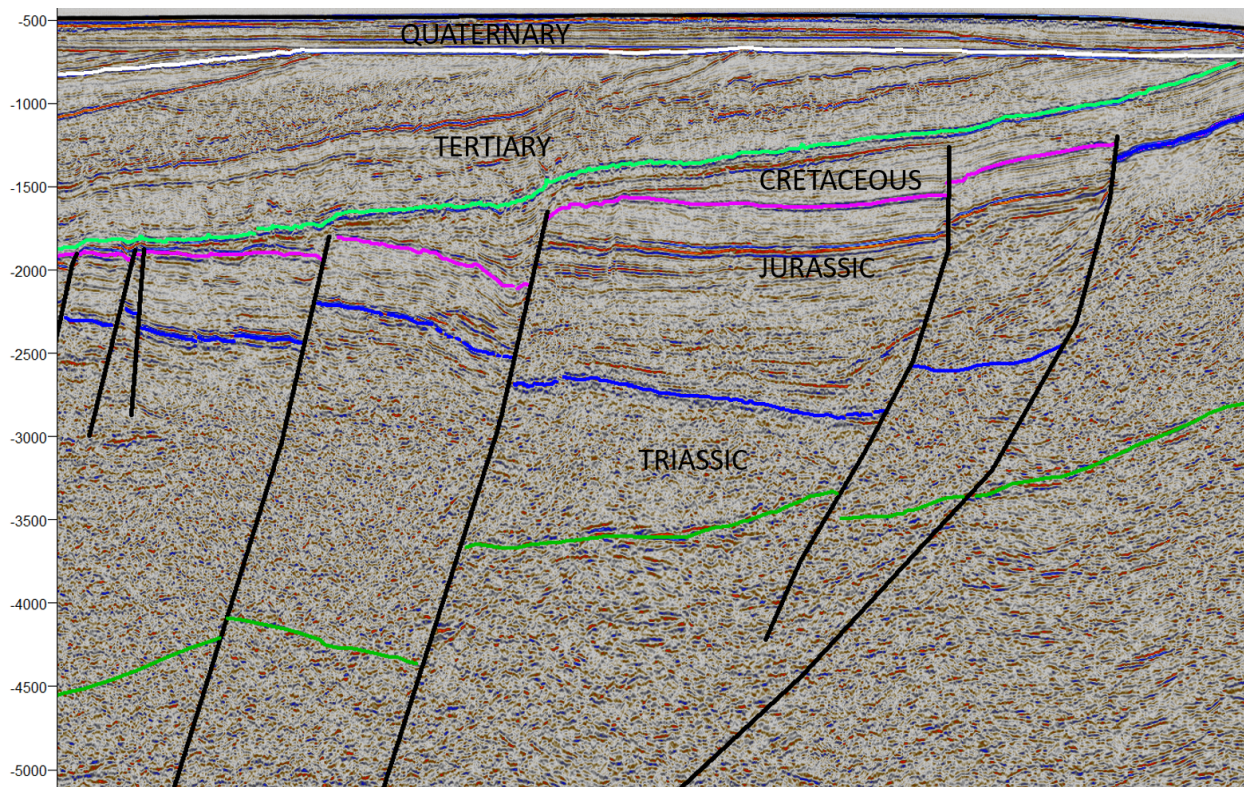


Figure 60: From line 6, on the Horda Platform east of the Troll Field. The BCU is in this location developed rather as a disconformity, with large offsets from faults

### 4. The extra-marginal fault complex

The extra-marginal fault complex is characterized by a series of medium-scale, mostly non-rotational fault blocks delineated by planar, steep faults defining a buried horst-and-graben relief. The Cretaceous and Tertiary sequences are locally completely eroded, and the Jurassic sediments onlap the basement (Fig. 61).

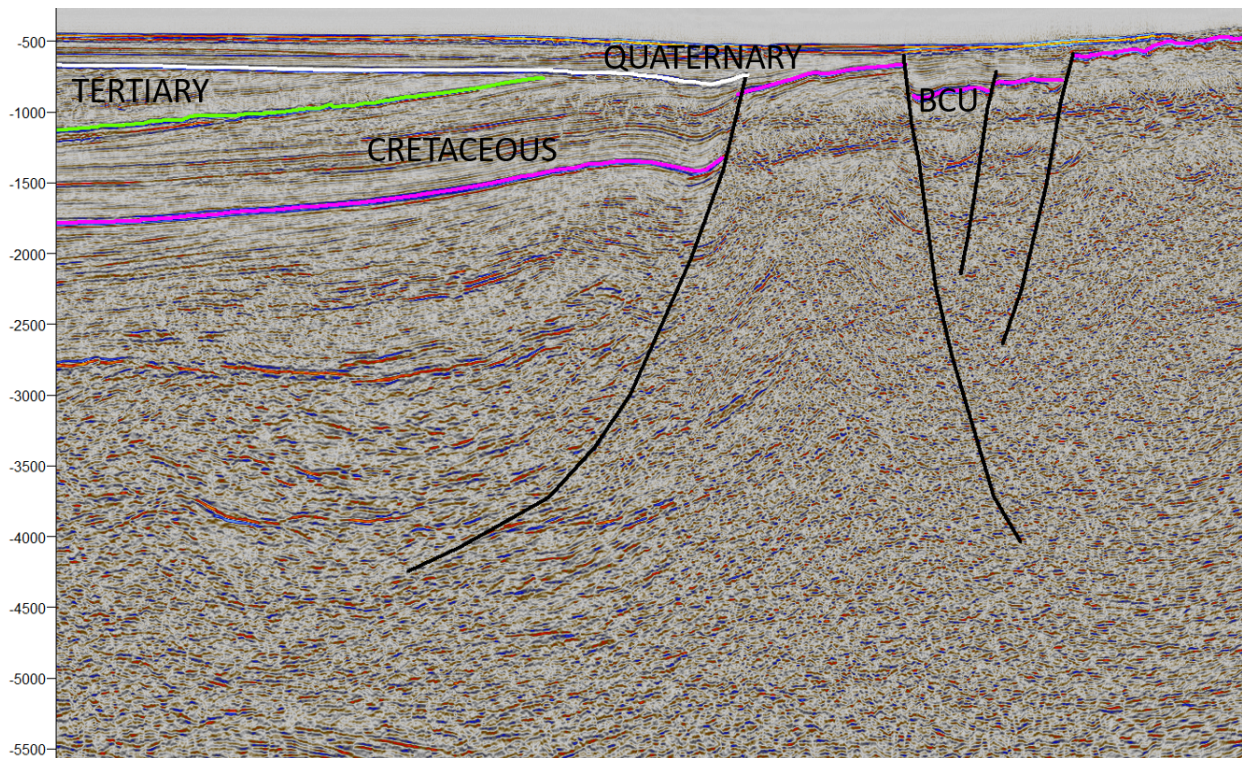


Figure 61: From line 7, close to the Norwegian coastline. Affected by a non-rotated horst-graben complex with significant relief, where several unconformities merge into one that lack Cretaceous and Tertiary sediments

### 11.3 Inherited basement structures of the northern North Sea

The geometry of rift systems that are superimposed on former mobile belts and follow their strike is generally strongly influenced by the pre-existing basement fabric. As mentioned, are the basins of the northern North Sea obliquely cross-cutting the Caledonides and are resting on a heterogeneous crust composed of structures stemming from the Caledonian orogeny and Devonian postorogenic extension. The rift system is made up of a combination of reactivated Caledonian and Devonian crustal discontinuities and new Mesozoic faults (Ziegler and Cloething, 2003). The Devonian strain and deformation was distributed throughout the Caledonian orogenic belt from central South Norway to the Shetland Platform, but most of the basins in the northern North Sea related to this extension were subsequently eroded away. However, this pre-existing framework exert a regional control onto which the later rifting events acted (Fazlikhani et al., 2017).

Doré et al. (1997) argue that the current dominance and visibility of the lineaments of Caledonian origin is because they were conveniently oriented to accommodate the extensional forces leading to the NE Atlantic break-up. Most prominently NE-SW shears, such as the Møre-Trøndelag Fault Zone (Noted MTFC in Fig. 15), which trends almost parallel to the continental margin.

Several shear and thrust zones affect large portions of the Caledonian crust and can be recognized with deep seismic data, and gravimetric and magnetic data. The seismic data interpreted in this thesis is of a maximum depth of 7s TWT and thus, generally too shallow to recognize many of the deeper structures of the study area. However, at the platform areas, there are some basement-penetrating wells. These areas experienced less post-rift thermal subsidence than the areas more proximal to the rift axis, making the post-rift sediment thickness significantly more shallow.

Fig. 62 shows a part of the Horda Platform east of the Troll Field with the well 32/4-1 penetrating the basement. The lower green line represents the upper basement and separates rift deposits from the underlying dipping reflections of the basement. The large rift is a part of the Øyegarden Fault Complex. The top of the basement is uneven and shallowing upwards towards the fault.

Due to the North Sea rift cross-cutting the orogenic fabric of the crust, it is not believed that many pre-Permian discontinuities are reactivated. New faults developed in the Permo-Triassic, that proceeded to be reactivated in the Late Jurassic rifting. However, the development of these faults is believed to be influenced by ancient fault zones such as the Caledonian Nordfjord-Sogn Detachment.

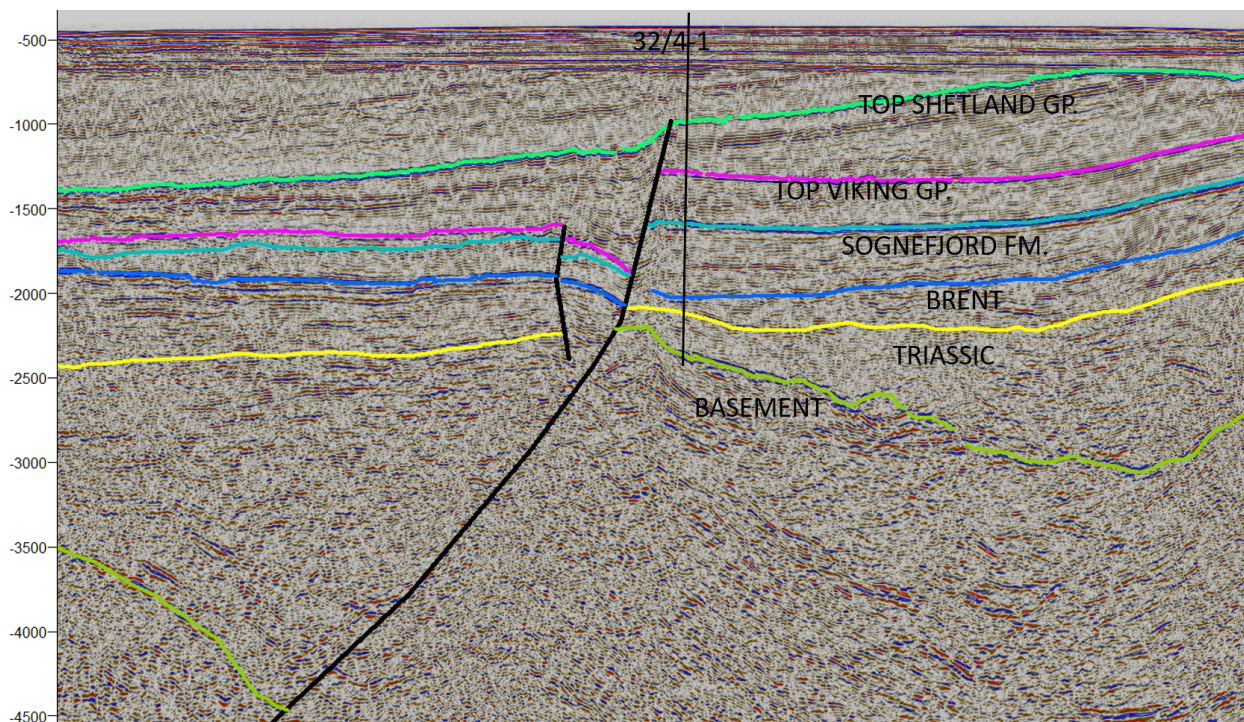


Figure 62: From Line 1. Showing well 32/4-1 penetrating the strata down to the basemen on the Horda Platform

## 11.4 Faults

Considering the northern North Sea basins are built on previously faulted basement and developed through several phases of rifting, interaction and linkage of reactivated and secondary faults is expected. The fault evolution in a multiphase basin is more complicated than the three-phase model of fault development described in chapter 4.3. Deng et al. (2017) created a discrete element model consisting of an upper brittle layer, a lower brittle layer and a lower crust. The model consider the behaviour of faults during increasing extension with pre-existing weaknesses in the lower brittle layer. It is indicated that early extension (10% extension) is characterized by reactivation of pre-existing weaknesses with very little throw, where approximately 80% of the pre-existing weaknesses reactivate. In the realm of 10-15% extension, the faults propagate from the pre-existing weakness and the displacements increase. There are also observed development of individual faults (mostly) perpendicular to the extension direction. There are not yet seen any displacement above the middle of the upper brittle layer. Further extension (20%) contribute to further lengthening and heightening of faults, both for the existing fault, and new faults, as well as increased interaction. At 25% extension there is continued upward propagation of the pre-existing fault and linkage of both pre-existing and newly formed faults. There is also a development of new faults parallel to the pre-existing fault, indicating its control on the orientation of new faults. Their results indicate that (i) pre-existing structures exert a control on the extending area by being a location of large displacements and linkage of new faults (ii) new faults with initially lesser displacement will develop perpendicular to the extension direction and (iii) new faults also develop parallel to the pre-existing fault. The behaviour and linkage of the faults are in agreement with the theory previously described. A conceptual model of the behaviour of both pre-existing and newly developed faults in a multiphase is seen in Fig. 63. It is clear how the pre-existing faults strongly influence the new faults through linkage, isolation, abutting, cross-cutting and otherwise interaction. Note also how the newer faults can influence the behaviour of the reactivated faults by relay interaction (the fault to the upper right corner).



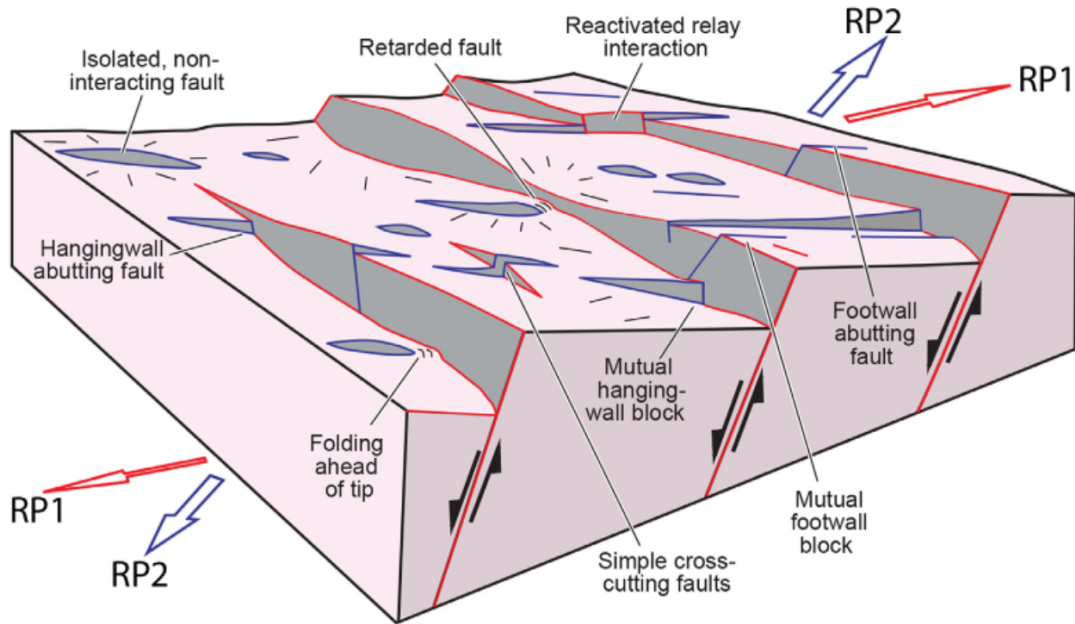


Figure 63: A fault model in a multiphase rift showing how faults (red) from rift phase 1 (RP1) is being reactivated, and crosscut and interacting with new faults (blue) from rift phase 2 (RP2).

Some new faults are being retarded and isolated by the pre-existing faults. From Duffy et al.

(2015)

An important question is whether or not the crustal fabric and pre-existing crustal weaknesses influenced the development of the North Sea basin and to what extent - could it have influenced the distribution of thermal subsidence as well as the geometry of the rift? The Permo-Triassic basin developed with predominantly N-S striking fault systems through an E-W extension direction. The extension direction during the second phase of rifting is believed to be slightly rotated in a NW-SE direction.

A study focusing on the fault growth and interactions of faults on the Horda Platform by Duffy et al. (2015) discuss how the Permo-Triassic faults on the platform dominate deformation also during the Late Jurassic rifting. New, smaller faults develop in a NW-SE direction and show varying degree of interaction and/or linkage with the pre-existing faults. They conclude that it is unlikely that structures or fabrics in the pre-Permian basement had any direct influence on the growth of the NW-SE striking faults, and that they developed due to the extension direction.

From these studies it seems likely that pre-existing faults become reactivated, and thus influence the rift geometry. Also, independent of pre-existing weakness zones, new faults will develop (near) perpendicular to the extension direction. Which faults that are most prominent will depend on the magnitude of extension during the phases of active extension. Considering that the Horda

Platform was significantly lesser involved in the Late Jurassic phase than the Permo-Triassic, it is natural that the dominating features are of Permo-Triassic age. Conclusively, pre-existing weakness zones exerted a control on the development of the Viking Graben and have to be considered when discussing the application of lithospheric extensional models.

#### 11.4.1 Øygarden Fault Zone

The Øygården Fault Zone (ØFZ) is found on the eastern margin of the interpreted lines 2, 3, 4, 6, 7 and 8, and particularly in line 14 (Model 3). It is a complex of linked or semi-linked faults. In accordance with the theory explained in chapter 4.3, the fault zone developed through linkage of smaller faults, with increasingly larger offset. It is clear from the results that generally, the largest offsets of the ØFZ are found in the lines that intersect the middle part of the fault zone, such as line 14, line 6 and line 7. This is in agreement with how the internal faults experience the largest displacement rate being frequently loaded by laterally adjacent segments.

It is also observed that the ØFZ follows the shape of the Norwegian coastline in a N-S direction, rather than the NE-SW direction of the late Jurassic development of the Viking Graben, indicating that it might be an inherited structure from the Permo-Triassic stretching. The Øygården Fault Zone bear no sign of being formed by reactivation of pre-existing structures

The coast-near side of the fault zone is characterized by little thinning of the lithosphere, leading to little accommodation space for sediments. Basement is often interpreted in shallow areas on this side of the fault zone. This is an indicator that the fault zone acted as the margin during the development of the Viking Graben and no rift-related thinning occurred to the east of this zone.

Extended or renewed tectonic activity of the Øygarden Fault Zone may be the reason for the polygonal faulting of the Hordaland Group.

## 12 Discussion

To be able assign the northern Viking Graben to a certain extensional stretching model, features that support or contradict the use of the different models must be observed. Such attributes are for example symmetric or asymmetric stretching, position of area of maximum thermal subsidence relative to the area of maximum crustal thinning, the existence of extensional detachment faults, the angle of faults, the role of upwelling asthenosphere during rifting and regional variations of stretching factors.

### 12.1 Application of models to the north Viking Graben

#### 12.1.1 Pure shear models

There has been made several estimation on the amount of extension in the northern North Sea (Ziegler, 1982; Beach et al., 1987; Badley et al., 1988; Marsden et al., 1991), and there is commonly a discrepancy between the observed and measured thinning, if the thinning was caused by stretching alone, which is assumed by the McKenzie model.  $\beta$  estimated from subsidence, by comparing pre- and post crustal thickness, is generally significantly higher than  $\beta$  measured from observed faulting. The seismic data presented in this thesis is limited to the Norwegian side of the North Sea, and is unable to display the western margin of the rift. This means that it is difficult to estimate the area of extension based on these data alone. However, Ziegler (1982) estimated, by measuring fault heaves, that the maximum extension of the northern North Sea rifting was 25 km. If stretching was the sole cause of the thinning of the crust, extensions must have been 75-100 km, to obtain the estimated  $\beta$  values. This means that in addition to extension, other factors must have contributed to the thinning of the Viking Graben.

It is possible that stretching-discrepancies can be explained by the Permo-Triassic faults not being imaged. If they are broken up and rotated by Late Jurassic faults, the measured fault extension will be lower than if estimated by subsidence calculations. Listric normal faults are observed during the syn-rift phase, while planar normal faulting associated with footwall uplift dominates during the thermal subsidence phase. The magnitude of footwall uplift is believed to be in agreement with the model of Jackson and McKenzie (1983) (Badley et al., 1988).

The McKenzie model correctly predicts the thermal subsidence in the deeper parts of the graben. One of the most important reasons the McKenzie model has been so widely used by the petroleum industry, is due to its ability to correctly predict the thermal subsidence. This is a key difference between the Wernicke and McKenzie model. The McKenzie model predicts that the area of largest

crustal thinning is below the area of largest thermal subsidence, and not offset a distance from it as the Wernicke model predicts. This is also the case in the Viking Graben. The margins consist mainly of thick, unthinned Caledonian crust, that experienced very little subsidence. It is estimated that the approximate basin depth of the deepest parts of the graben is approximately 12 km (Marsden et al., 1991), this is also the area of maximal thinning of the crust. A thinning of the crust to less than 10 km, will cause changes in the development of the rift (Peron-Pinvidic et al., 2013). If the crust is thinned to 10 km or less, the ductile part of the crust is completely removed, and the brittle upper crust is directly overlying the mantle. This can cause faults to propagate through the entire crust, down to the mantle, and cause exhumation of mantle, eventually causing a transition to a rifted margin. As the thinnest region of pre-Mesozoic crust in the Viking Graben is about 12 km, this indicate that the Viking Graben got far in the thinning coupling phase, but ceased its extension before the hyperextension exhumation phase. The phases are described in chapter 3.7.

While a uniform extensional model can predict the basin subsidence, this is not the case with the graben flanks. The eastern flank of the graben does not show subsidence during Late Jurassic/Early Cretaceous times as predicted by the model (Giltner, 1987).

There is observed uplift of the graben flanks in the Viking Graben during the first rifting phase. Most explanations of this phenomenon involve a non-uniform depth dependent stretching model where the lower lithosphere is stretched more than the upper crust (Fig. 4c). This type of model allow more heat from upwelling asthenosphere to interact with the basin. The lower lithosphere beneath the graben flanks will be thermally expanded, and thus counteract the initial subsidence due to crustal thinning. Similarly, Neugbauer (1983) explained uplift of the flanks to be caused by passive upwelling of asthenospheric material to the moho during rifting. Badley et al. (1988) argue that the uplift of basin margins during stretching can be explained with the uniform stretching model (McKenzie model), through lateral heat flow into the mantle lithosphere beneath the unthinned margin crust. The crustal composition can also affect the subsidence. If the crustal material of the graben flanks is abnormally light, it can inhibit subsidence. Other explanation for uplifted flanks are presented in Chapter 3.

The discrepancy between stretching factors calculated from different methods, can possibly be explained by a system composed of a strike-slip pull apart basin, where strain is distributed, but does not contribute to basin formation. However, this would propose problems when explaining the seemingly laterally consistent subsidence rates. It is therefore most likely that a model of non-uniform depth dependent stretching, as explained by Royden and Keen (1980) (Fig. 7b), with greater stretching of the mantle lithosphere than the crust, can best explain the discrepancy of

calculated stretching factors. Greater stretching in the mantle than in the crust would produce a lower subsidence rate during the thermal subsidence phase. The uplift of the basin margin could also be explained by the thinning of the mantle lithosphere beneath the rift edges.

A further argument for a pure shear model, is that the North Sea rift developed by cross-cutting the crustal fabric, thus developing new faults and the deformation is likely to follow the theory as described by McKenzie (1978).

### 12.1.2 Simple shear models

Simple shear models generally predicts wider rifts than models incorporating pure shear. The Wernicke model was initially applied to the Basin and Range Province, which is a wide extensional system, the North Sea rift is classified as a narrow system. It will also predict an asymmetric graben structure, something that is observed in some parts of the Viking Graben. As mentioned, the Permo-Triassic phase affected a wider area than the Late Jurassic rifting. This could indicate, but not prove, that a simple shear model may be more accurate for describing the first phase of rifting, than the latter.

The simple shear model assumes that the extension is accommodated mainly along one master fault that cuts across the whole lithosphere. In this case, it would be expected to be observed low-angle faults that could be explained as faults bounding extensional allochthons overlying an exhumed detachment fault. The detachment fault itself would correspond with the top of the basement. This is not observed. The faults observed have commonly a steeper angle than what the Wernicke model predicts.

Commonly, the thickest part of a deposit is overlain or underlain by the thickest part of other packages. For example, the thickest part of the syn rift phase is directly overlain by the thickest packages of deposits during the thermal subsidence (see for example Line 7). This indicate that the relative amount of subsidence remained similar throughout the stages of basin development. A Wernicke model can not confidently explain this. It will predict that the area of maximum subsidence during extension will be laterally offset from the area of maximum thermal post-rift subsidence.

In regards to uplift of the graben flanks, a Wernicke model does not fit as good as the pure shear models, due to the geographical offset between the stretching and the subsidence. It will predict a significantly higher uplift of the Horda Platform in the second extension phase, than what did occur.

Another problem that needs to be adressed when applying the models, is the fact that there was

two main extensional periods and two episodes of thermal subsidence. If there was a low-dipping shear zone of the second phase, it would have to cut through and displace the steeply-dipping fault zones of the early rift phase, which is not observed. Faulting during thermal subsidence could indicate a mechanically weak lithosphere, and faults associated with the subsidence would probably penetrate to the mantle and offset any dipping shear.

The McKenzie model generally predicts development of high angle normal faults in a rift-basin, while the Wernicke model predicts faults with lower angle, related to the lithospheric low angle shear zone. From the results, it is concluded that high angle normal faults dominate, but listric faults can also be seen. Referring to Fig. 64, the type of faults outlined in the square in the pure shear model is the dominating type of fault in the Viking Graben, especially on the western side of the graben axis. The eastern side show generally a more complex fault geometry, and is stronger faulted. The figure also clearly show how differently the sub-crustal behaviour of the two models are. This can not be observed in the results of this thesis.

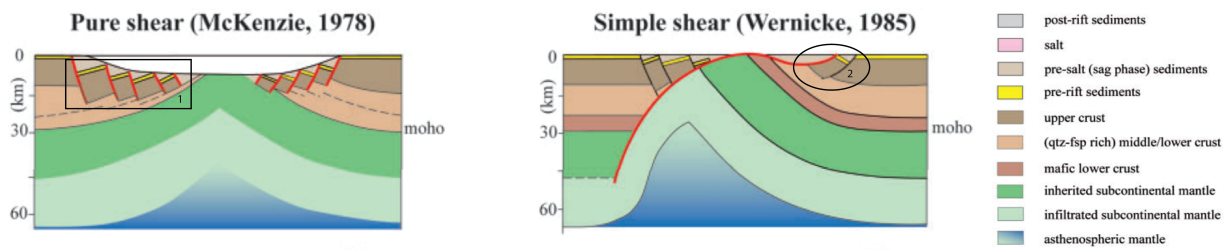


Figure 64: The domino-style normal faults seen in rectangle 1, has a striking resemblance to the faults on the western side of the graben axis in Model 2 (from the Gullfaks South and westwards).

Whereas the type of faults in ellipse 2 under the simple shear model is not observed. (Modified from Unternehr et al. (2010))

The McKenzie model assumes a symmetric rift as the result and the Wernicke model an asymmetric rift. The Viking Graben is both. It changes from being asymmetric in the northern parts, to symmetric at around  $60.5^{\circ}\text{N}$ , and back to asymmetric at  $60^{\circ}\text{N}$ . This indicate that a prediction of the shape of the rift is not easily done using any of the models. A reason for the change in symmetry can be pre-existing crustal discontinuities asserting a control on the development of the shape of the graben. This can play a significant role in the distribution of strain, and thus, the formation and behaviour of internal structures of the graben. This has previously been discussed and is believed to contribute significantly to the geometry of the Viking Graben

### 12.1.3 Other models

The flexural cantilever model will yield a more localized rift than what is described by pure shear stretching models, it will also produce a deeper rift, due to the assumption of a finite flexural strength for the lithosphere. This model can explain the footwall uplift and hanging wall collapse. It also predicts the domino-style block rotation of multiple fault systems as observed on the western side of the Viking Graben. The amount of stretching such a model will predict, is largely based on adjustments of parameters, such as the chosen necking depth.

It is unlikely that a model relying on an active mantle plume as the primary extension mechanism will be appropriate for the Viking Graben. However, this may be the case for the Central Graben south of the Viking Graben, where a volcanic center was located during the late Jurassic rifting. The timing of the volcanism relative to the Late Jurassic rifting is consistent with a model of active rifting associated with a mantle plume.

The determination of appropriate models have been closely linked to the development of increasingly higher quality seismic data. As more, and deeper, structures can be seen, better models can be developed. The models discussed in this thesis largely comprises older models, that paved way for our understanding of rifts and extensional tectonics. While they are still relevant, numerical models are today the way of modelling the development of extensional structures. With such models, detailed experiments with numerous parameters can be completed, that elevates the models to another level of individuality that is out of reach of the models considered in this thesis.

## 13 Conclusions

It is concluded that it is difficult to directly apply a pre-existing lithospheric extensional model, to explain the entire development of the Viking Graben. Regarding the post-rift subsidence, a pure shear model is preferred, due to no observed discrepancy between the area of largest subsidence and area of largest crustal thinning. Pure shear models can also best explain the type of faults observed in the Viking Graben. The asymmetry occasionally observed, is believed to be due to pre-existing inhomogeneous weaknesses, rather than extension following the Wernicke-model. A non-uniform depth dependent model can explain many observed features and is deemed the best model for explaining the development of the Viking Graben. However, it does not consider the possible influence of an active thermal mechanism accompanying the far-field forces. To discuss this, data reaching deeper depths are needed.

Re-activation of basement structures exerts a dominating control on the graben. It especially influences the width, and internal fault-structure of the graben, as well as the length. However, the behaviour of upwelling asthenosphere can also impact this. The cessation of rifting of the Viking Graben is believed to be attributed to de-localization of strain, meaning the strain became redirected before sea-floor spreading could commence. From the observed thickness of the crust, it is interpreted that the Viking Graben got far in the rifting-process, but ceased before the start of sea-floor spreading.

Deeper seismic is crucial to obtain a clearer understanding of how the rift developed. It will give a better picture of the behaviour of the sub-crustal processes involved during rifting. With this, it will be easier to discuss and apply models. Also, numerical models that can be specified to the Viking Graben, is preferred to general theoretical lithospheric extension models.



## References

- Allemand, P. and Brun, J.-P. (1989). Width of continental rifts and rheological layering of the lithosphere. *Tectonophysics*.
- Allen, P. A. and Allen, J. R. (1990). *Basin Analysis, Principles and Application to Petroleum Play Assessment*. Wiley-Blackwell, 3 edition.
- Badley, M., Price, J., Dahl, C. R., and Agdestein, T. (1988). The structural evolution of the northern viking graben and its bearing upon extensional modes of basin formation. *Journal of the Geological Society*.
- Barbier, F., Duvergé, J., and la Pichon, X. (1986). Structure profonde de la marge nord-gascogne. implications sur le mécanisme de rifting et de formation de la marge continentale. *Bull. Centres Rech. Explor.*
- Barnard, P. C. and Bastow, M. A. (1991). Hydrocarbon generation, migration, alteration, entrapment and mixing in the central and northern north sea. *Petroleum Migration*.
- Beach, A., Bird, T., and Gibbs, A. (1987). Extensional tectonics and crustal structure: deep seismic reflection data from the northern north sea viking graben. *Continental extensional tectonics*.
- Beaumont, C., Keen, C. E., and Boutilier, R. (1981). On the evolution of rifted continental margins: comparison of models and observations for the nova scotia margin. *Journal of Geophysical Research*.
- Boggs, S. (2010). *Principles of Sedimentology and Stratigraphy*. Pearson Educational International, 4 edition.
- Braun, J. and Ceaumont, C. (1989). A physical explanation of the relation between flank uplifts and the breakup unconformity at rifted continental margins. *Geology*.
- Buiter, S. and Torsvik, T. (2014). A review of wilson cycle plate margins: A role for mantle plumes in continental break-up along sutures? *Gondwana Research*.
- Catuneanu, O. (2002). Sequence stratigraphy of clastic systems: concepts, merits, and pitfalls. *Journal of African Earth Sciences*, (35).
- Childs, C., Holdsworth, R., Jackson, C., Manzocchi, T., Walsh, J., and Yielding, G. (2017). Introduction to the geometry and growth of normal faults. *Geological Society, London*.
- Coward, M. P. (1986). Heterogeneous stretching, simple shear and basin development. *Earth and Planetary Science Letters*.

- Deng, C., Gawthorpe, R., Finch, E., and Fossen, H. (2017). Influence of a pre-existing basement weakness on normal fault growth during oblique extension: Insights from discrete element modeling. *Journal of Structural Geology*.
- Doré, A., Lundin, E., Fichler, C., and Olesen, O. (1997). Patterns of basement structure and reactivation along the ne atlantic margin. *Journal of the Geological Society*.
- Duffy, O., Bell, R., Jackson, C., Gawthorpe, R., and Whipp, P. (2015). Fault growth and interactions in a multiphase rift fault network: horda platform, norwegian north sea. *Journal of Structural Geology*.
- Etheridge, M. (1986). On the reactivation of extensional fault systems. *Philosophical Transactions of the Royal Society of London*.
- Faleide, J. I., Bjørlykke, K., and Gabrielsen, R. H. (2010). *Petroleum Geoscience: From Sedimentary Environments to Rock Physics*, pages 467–483. Springer.
- Fazlikhani, H., Fossen, H., Gawthorpe, R., Faleide, J., and Bell, R. (2017). Basement structure and its influence on the structural configuration of the northern north sea. *AGU Publications*.
- Fichler, C. and Hospers, J. (1989). Deep crustal structure of the northern north sea viking graben: results from deep reflection seismic and gravity data. *Tectonophysics*.
- Fjeldskaar, W., ter Voorde, M., Johansen, H., Christiansson, P., Faleide, J., and Cloetingh, S. (2004). Numerical simulation of rifting in the northern viking graben: the mutual effect of modelling parameters. *Tectonophysics*.
- Fossen, H. and Hurich, C. (2005). The hardangerfjord shear zone in sw norway and the north sea: a large-scale low-angle shear zone in the caledonian crust. *Journal of the Geological Society of London*.
- Færseth, R. B. (1996). Interaction of permo-triassic and jurassic extensional fault-blocks during the development of the northern north sea. *Journal of the Geological Society*.
- Færseth, R. B., Gabrielsen, R. H., and Hurich, C. A. (1995). Influence of basement in structuring of the north sea basin, offshore southwest norway. *Norsk Geologisk Tidsskrift*.
- Gautier, D. L. (2005). Kimmeridgian shales total petroleum system of the north sea graben province. *U.S. Geological Survey*.
- Gawthorpe, R. and Leedert, M. (2000). Tectono-sedimentary evolution of active extensional basins. *Basin Research*.
- Gibbs, A. (1990). Linked fault families in basin formation. *Journal of Structural Geology*.

- Giltner, J. P. (1987). Application of extensional models to the northern viking graben. *Norsk Geologisk Tidsskrift*.
- Gupta, S., Cowie, P., Dawers, N., and Underhill, J. (1998). A mechanism to explain rift-basin subsidence and stratigraphic patterns through fault-array evolution. *Geology*.
- Halland, E. K., Ine Tørneng Gjeldvik and, W. T. J., Magnus, C., Meling, I. M., Pedersen, S., Riis, F., Solbakk, T., and Tappel, I. (2011). *CO2 Atlas For The Norwegian Continental Shelf*, page 30. NPD, 2 edition.
- Hellinger, S. and Sclater, J. (1983). Some comments on two-layer extensional models for the evolution of sedimentary basins. *Journal of Geophysical Research*.
- Houseman, G., McKenzie, D., and Molnar, P. (1981). Convective instability of a thickened boundary layer and its relevance for the thermal evolution of continental convergent belts. *Journal of Geophysical Research*.
- Huisman, R., Podladchikov, Y., and Cloetingh, S. (2001). Transition from passive to active rifting: Relative importance of asthenospheric doming and passive extension of the lithosphere. *Journal of Geophysical Research*.
- Jackson, J. (1998). Fault death: a perspective from actively deforming regions. *Journal of Structural Geology*.
- Jackson, J. and McKenzie, D. (1983). The geometrical evolution of normal fault systems. *Journal of Structural Geology*.
- Johnson, H., Leslie, A. B., Wilson, C. K., Andrews, I. J., and Cooper, R. M. (2005). Middle jurassic, upper jurassic and lower cretaceous of the uk central and northern north sea. *British Geological Survey*.
- Konstantinovskaya, E., Harris, L., Poulin, J., and Ivanov, G. (2007). Transfer zones and fault reactivation in inverted rift basins: Insights from physical modelling. *Tectonophysics*.
- Koopman, A., Speksnijder, A., and Horsfield, W. (1987). Sandbox model studies of inversion tectonics. *Tectonophysics*.
- Koptev, A., Calais, E., Gurov, E., Leroy, S., and Gerya, T. (2018). Along-axis variations of rift width in a coupled lithosphere-mantle system, application to east africa. *AGU, Geophysical Research Letters*.
- Kusznir, N., Karner, G., and Egan, S. (1987). Geometric, thermal and isostatic consequences of

- detachments in continental lithosphere extension and basin formation. *Sedimentary Basins and Basin-forming mechanisms*.
- Kusznir, N., Marsden, G., and Egan, S. (1991). A flexural cantilever simple-shear/pure-shear model of continental extension. *Geological Society of London*.
- Kusznir, N. and Ziegler, P. (1992). The mechanics of continental extension and sedimentary basin formation: A simple-shear/ pure-shear flexural cantilever model. *Tectonophysics*.
- Kyrkjebø, R., Gabrielsen, R. H., and Faleide, J. (2003). Unconformities related to the jurassic-cretaceous synrift-post-rift transition of the northern north sea. *Journal of the Geological Society*.
- Lyngsie, S. and Thybo, H. (2006). A new tectonic model for the laurentia-avalonia-baltica sutures in the north sea: A case study along mona lisa profile 3. *Tectonophysics*.
- Mandl, G. (2000). Faulting in brittle rocks: an introduction to the mechanics of tectonic faults. *Springer-Verlag*.
- Marsden, G., Yielding, G., Roberts, A., and Kusznir, N. (1991). Application of a flexural cantilever simple-shear/pure-shear model of continental lithosphere extension to the formation of the north sea basin. *Geological Society London Special*, (2).
- McKenzie, D. (1978). Some remarks on the development of sedimentary basins. *Earth and Planetary Science Letters*.
- Mitchum, R., Vail, P., and Sangree, J. (1977). Seismic stratigraphy and global changes of sea level, part 6: Stratigraphic interpretation of seismic reflection patterns in depositional sequences. *Payton*.
- Naliboff, J., Buitter, S., Péron-Pinvidic, G., Osmundsen, P. T., and Tetreault, J. (2017). Complex fault interaction controls continental rifting. *Nature Communications*.
- Neugbauer, H. J. (1983). Mechanical aspects of continental rifting. *Tectonophysics*.
- Norton, M. G. (1987). The nordfjord-sogn detachment, w. norway. *Norsk Geologisk Tidsskrift*, (67):93–106.
- Nøttvedt, A., Gabrielsen, R., and Steel, R. J. (1995). Tectonostratigraphy and sedimentary architecture of rift basins, with reference to the northern north sea). *Marine and Petroleum Geology*.
- Peron-Pinvidic, G., Manatschal, G., and Osmundsen, P. (2013). Structural comparison of archetypal atlantic rifted margins: A review of observations and concepts. *Marine and Petroleum Geology*.

- Prosser, S. (1993). Rift-related linked depositional systems and their seismic expression. *Tectonics and Seismic Sequence Stratigraphy*.
- Ramberg, I. B., Bryhni, Nøttvedt, and Rangers (2013a). *Landet Blir Til, Norges Geologi*, pages 335–357. 2 edition.
- Ramberg, I. B., Bryhni, Nøttvedt, and Rangers (2013b). *Landet Blir Til, Norges Geologi*, pages 361–385. 2 edition.
- Reston, T. and Pérez-Gussinyé, M. (2007). Lithospheric extension from rifting to continental breakup at magma-poor margins: rheology, serpentinisation and symmetry. *International Journal of Earth Sciences*.
- Rowley, D. and Sahagian, D. (1986). Depth-dependent stretching: A different approach. *Geology*.
- Royden, L. and Keen, C. (1980). Rifting process and thermal evolution of the continental margin of eastern Canada determined from subsidence curves. *Earth and Planetary Science Letters*.
- Simm, R. and White, R. (2002). Phase, polarity and the interpreter's wavelet. *First Break*.
- Unternehm, P., Péron-Pinvidic, G., Manatschal, G., and Sutra, E. (2010). Hyper-extended crust in the south Atlantic: in search of a model. *Petroleum Geoscience*.
- Wernicke, B. (1981). Low-angle normal faults in the basin and range province: nappe tectonics in an extending orogen. *Nature*.
- Wernicke, B. (1985). Uniform sense simple shear of the continental lithosphere. *Can J Earth Science*.
- Ziegler, P. A. (1982). Faulting and graben formation in western and central Europe. *Philosophical transactions of the royal society*.
- Ziegler, P. A. (1990). *Geological Atlas of Western and Central Europe*. Shell Internationale Petroleum Maatschappij BV, 2 edition.
- Ziegler, P. A. and Cloetingh, S. (2003). Dynamic processes controlling evolution of rifted basins. *Earth Science Reviews*.
- Ziegler, P. A., van Wees, J.-D., and Cloetingh, S. (1998). Mechanical controls on collision-related compressional intraplate deformation. *Tectonophysics*.

